THE MICROWAVE SPECTRA OF CARBONYL SULFIDE AND CYANOGEN CHLORIDE IN THE 8 mm. REGION

by

J.F. Mathison, B.A.

A thesis submitted to the Faculty of Graduate Studies and Research of McGill University in partial fulfilment of the requirements for the degree of Doctor of Philosophy

Radiation Laboratory
Department of Physics

April, 1956

TABLE OF CONTENTS

SUMMARY

The construction of a microwave spectroscope is described and the results of the first investigations using this instrument given. Details of a frequency standard for operation in the 40,000 mc/s region are included. Carbonyl sulfide has been studied to gain familiarity with and confidence in the instrument as well as to resolve minor disagreements. The magnitude of the Fermi resonance and the vibration-rotation interaction constants have been determined. The spectrum of cyanogen chloride is somewhat complicated by nuclear electric quadrupole-quadrupole interactions as well as Fermi resonance. A decrease in the quadrupole coupling constant with vibrational excitation, in both first and second excited degenerate bending mode vibrations, has been observed for the first time in any linear molecule, so far as is known. The magnitude of the Fermi perturbation is tentatively given. Two of the rarer isotopic species of cyanogen chloride have been observed for the first time.

ACKNOWLEDGEMENT

The help of many friends and associates is acknowledged. Among these are Mr. Robert Lorimer for his glass work; Mr. K. Heinstein for assistance in construction of electronic equipment in the latter phase of this work; Dr. H. Sheffer, Ottawa, for his courtesy in providing the sample of cyanogen chloride, and Mr. George Cruickshank for his drawings of the energy level diagrams and spectra. Professor J.D. Jackson has assisted the writer greatly, especially in the more formal aspects of two-quadrupole theory. Dr. G. Herzberg and Dr. C.C. Costain have kindly offered helpful criticism, which is deemed most valuable. The conclusions reached in the present work are the writer's alone, however, Indeed the final arguments have not been discussed before. To Professor J.S. Foster, F.R.S., Director of the Radiation Laboratory, especial thanks are due for his constant interest in this work and his keen sense of understanding which has provided stimulation and encouragement. Assistance from the Defence Research Board, Ottawa, in the form of a grant, is hereby gratefully acknowledged.

THE MICROWAVE SPECTRA OF CARBONYL SULFIDE AND CYANOGEN CHLORIDE IN THE 8 mm. REGION

I. INTRODUCTION

1) Historical Background

a) General Remarks (the influence of Fermi resonance)

i) The microwave spectra of less than a dozen linear molecules[1,2] has been studied within the past decade. Of this number not more than four* have been investigated for the effect of Fermi resonance perturbation, (Section III), on the rotation-vibration interaction constant α_1. Even within this smaller group in only one case[7] has the investigation been carried out for more than one isotopic species of the molecule. Thus, with few exceptions, the α_1 values listed in tables[8,9,10] in the literature are the perturbed, or uncorrected, α_1 although this is not always clearly indicated.

ii) Perhaps the most studied molecule of the entire microwave spectrum is carbonyl sulfide. This is a non-symmetric linear, triatomic molecule. Due, initially, to the preponderance of the second world war surplus in radar equipment operating in the 12.5 mm. region, most of the early microwave investigations in molecular spectroscopy were carried out in the 24,000 mc/s region. For SCO this corresponds to the $J = 2 \leftarrow 1$ rotational transition. Because of certain restrictions in the selection rules governing the absorption of radiation, (Section III), an unperturbed companion line (02^20) to a Fermi perturbed line (02^00) does not appear for this transition. Thus it is not possible in the $J = 2 \leftarrow 1$

---

*These are:
1) $S^{32}CO$: references 3, 4, 5, 6.
2) $Se^{80}CO$: references 3,5.
3) ICN : references 3,5.
4) $Br^{79}CN$, $Br^{81}CN$: reference 7.

transition to measure the magnitude of the Fermi perturbation directly and apply it as a correction in getting the unperturbed α_1.

For the $J = 3 \leftarrow 2$ and higher transitions a direct determination of all pertinent data is possible. It is with this transition in carbonyl sulfide that the first part of this investigation is concerned.

iii) Strandberg, Wentink and Kyhl[11] reported a single line in the 36,000 mc/s region due to the $J = 3 \leftarrow 2$ ground state transition for the principal isotopic species $S^{32}C^{12}O^{16}$. Low[5] reported four additional lines in the $J = 3 \leftarrow 2$ transition due to the same isotope. These lines arise from the first and second excited states of the doubly degenerate bending mode vibration. The magnitude of the resonance was observed directly for the first time, but the unperturbed α_1 could still not be obtained directly because the $(10^{\circ}0)$ line, due to the symmetrical stretching vibration interaction, was not observed. The problem was resolved by making use of additional data obtained in the $J = 2 \leftarrow 1$ transition from several sources.

The first complete analysis of Fermi resonance in SCO, in which all the lines required for the analysis and arising within a single rotational transition in both the ground and excited vibration states were observed, was carried out by Tetenbaum[4] for the $J = 4 \leftarrow 3$ transition.

Generally the purely microwave aspect of the work of Low and Tetenbaum is in accord. The principal differences appear to arise from their selection and subsequent treatment of the infra-red data. This point will be discussed in a later section.

The microwave spectrum of carbonyl sulfide provides a convenient point at which to begin this work. Many of the results can be compared directly with those of other workers, and thus it lends confidence to the analysis of the much more complicated spectrum which forms the second, and main part of this investigation.

b) General Remarks (quadrupole-quadrupole interaction)

i) If any nucleus within a molecule possesses a nuclear spin angular momentum greater than $1/2 \frac{h}{2\pi}$ then each rotation line in the absorption spectrum is split into a number of components dependent upon the vector sum of the rotation and spin angular momenta. Such hyperfine structure is well known.

The more complex case of two interacting nuclear spins has been considered by Bardeen and Townes[12], and the microwave spectra of a number of linear XYZ molecules, including this category, investigated by Townes, Holden and Merritt[13]. This work represents one of the monumental papers in the literature of microwave spectroscopy.

To-date only four linear, triatomic molecules each possessing two spins, (Cl CN, Br CN, ICN and NNO), have been investigated by the methods of microwave spectroscopy.

ii) For the N_2O molecule very little microwave information[4] is at hand because the rather small electric dipole moment results in only a weak absorption. This molecule has been investigated in the infra-red[14], however, and found to possess an appreciable Fermi resonance.

iii) The cyanohalogens were investigated originally by Townes, Holden and Merritt[13]. In none of these molecules, because of insufficient data, were the effects of Fermi resonance perturbations taken into account. For ICN, $Br^{79}CN$ and $Br^{81}CN$ the rotation-vibration constants α_1 (perturbed), α_2 and the ℓ-doubling constant q_ℓ were determined. In addition the quadrupole coupling constants were determined for the halogen and, in the case of BrCN, for N^{14} as well. For ClCN, ($J = 2 \leftarrow 1$ transition), the investigation was less extensive. Only for the most abundant isotopic species, $Cl^{35}CN$, were the investigations sufficiently detailed to permit evaluation of α_2 and q_ℓ. Again, the

quadrupole constants were determined for chlorine in $Cl^{35}CN$ and $Cl^{37}CN$, (ground vibrational state), and for N^{14} in $Cl^{35}CN$.

iv) At almost the same time as the above work of Townes et al. was in progress Smith, Ring, Smith and Gordy[15] published a paper on the interatomic distances and nuclear quadrupole couplings in ClCN, BrCN and ICN. Ground state transitions only were observed. The quadrupole coupling constants derived from this work are in very close agreement with those of Townes, Holden and Merritt. A somewhat earlier publication by the same authors[16] includes a determination of the quadrupole coupling constant for N^{14} in ICN.

v) In 1955 Low[5] published the results of investigations in the Fermi resonance of linear XYZ molecules carried out in 1949 at Columbia[3]. Specifically, this paper deals with SCO, SeCO and ICN. The now somewhat obsolete Molecular Microwave Spectra Tables[10], N.B.S. Circular 518, (1952), list the various lines accredited to Low for each of these molecules. In all cases these include the two most essential lines, $02^{0}0$ and $02^{2}0$, required for the study of the perturbation problem. For ICN Low's analysis yields the result $W_{10^{0}0;\ 02^{0}0} = 3\ cm^{-1}$ for the interaction constant.

In their recent book[1] on microwave spectroscopy Townes and Schawlow make no reference to the above work of Low, nor are his conclusions regarding SCO, SeCO and ICN included in their table of molecular constants. The same data, as used by Low for SCO, has apparently been reanalysed and while the conclusions in the two cases are close they are not quite identical.

vi) In 1952 Tetenbaum, with an unpublished analysis of Fermi resonance in linear triatomic molecules made available to him

by Professor C.H. Townes, investigated the microwave spectra of BrCN[7], SCO and N_2O[4]. These two latter molecules are referred to above. BrCN was investigated by Tetenbaum for the $J = 6 \leftarrow 5$ transition in the 49,000 mc/s region, (second harmonic of K-band). Because the intensity of absorption in a linear molecule goes up as the cube of the frequency, it was to be expected that many lines unavailable to Townes, Holden and Merritt in their original investigation, especially those arising from excited vibration states, would show up clearly. This indeed proved to be the case, and it may be said that BrCN is the first example of a linear, triatomic molecule containing two nuclear spins whose microwave spectrum has been fairly comprehensively worked out. The vibration-rotation interaction constants, the Fermi resonance perturbation and the perturbation interaction constant, and the quadrupole coupling constant in both the ground and the first excited bending vibration states were determined. Both principal isotopic species, $Br^{79}CN$ and $Br^{81}CN$, were investigated.

The significant results of the above analysis are two fold: a) the Fermi resonance perturbation is fairly large yielding an interaction constant $W_{10^00;\ 02^00} = 61.5\ cm^{-1}$; b) the quadrupole coupling constant is slightly smaller in the first excited degenerate bending mode vibration state than in the ground vibration state. This effect is observed for both isotopic species.

II. STATEMENT OF PROBLEM

With the concepts of the foregoing section in mind it was decided:

1) to investigate the microwave spectrum of carbonyl sulfide for the $J = 3 \leftarrow 2$ transition, with particular regard for the effects of Fermi resonance on the vibration-rotation interaction constants.

2) To investigate the microwave spectrum of cyanogen chloride for the $J = 3 \leftarrow 2$ transition; to evaluate the nuclear electric quadrupole coupling constant and to note its variation as a function of excited vibration state; to study the effect of the Fermi resonance perturbation on the vibration-rotation interaction constants, and to evaluate these constants as a function of vibration state.

III. SPECTRUM OF A LINEAR TRIATOMIC MOLECULE

1) Pure Rotation Spectrum

The pure rotation frequency of a diatomic or linear polyatomic molecule is given by:

$$\nu = 2B\,(J + 1)\ \text{mc/s} \qquad \text{(III-1)}$$

where

$$B = \frac{h}{8\pi^2 I_B} \qquad \text{(III-2)}$$

is the rotational constant, J is the quantum number of total angular momentum and I_B the moment of inertia about an axis perpendicular to the figure axis of the molecule and passing through the center of mass. In addition, the selection rule

$$\Delta J = +1 \qquad \text{(III-3)}$$

for absorption, applies.

According to (III-1) the molecular rotation spectrum should consist of a number of lines* of equal spacing separated by a distance 2B.

---

* In the far infra-red region such lines give rise to the familiar band spectrum. In the microwave region, on the other hand, the line separation is frequently so large that only a single transition can be seen within the entire working range of any given spectrometer. For example, for SCO the $J = 2 \leftarrow 1$ and $J = 3 \leftarrow 2$ transitions are separated by about 12,000 mc/s. This generally requires two instruments for adequate frequency coverage. Since line widths of less than one mc/s are common the microwave spectrometer might be expected to have a resolution far higher than any infra-red spectrometer. According to Professor C.H. Townes[17] this difference in resolution is approximately a factor of 10,000.

2) Rotation-Vibration Interaction

a) The Interaction Constants, α_i

If the effects of hyperfine structure and Fermi resonance are neglected the rotation frequency of a linear triatomic molecule in any vibration state is given by[18]:

$$\nu = \left[2B_v \pm q_o (v_2 + 1)\right] (J + 1) - 4D_v \left[(J + 1)^3 - (J + 1)\ell^2\right] \text{ mc/s} \qquad \text{(III-4)}$$

where $\Delta J = +1$ for absorption, and where:

$$B_v = B_e - \alpha_1 (v_1 + 1/2) - \alpha_2(v_2 + 1) - \alpha_3(v_3 + 1/2) \qquad \text{(III-5)}$$

B_e is the equilibrium rotation constant in the vibrationless state; B_v and D_v are the rotation constant and the centrifugal distortion constant, respectively, in any vibration state v. The α_i are coefficients measuring the interaction of vibration upon rotation. Thus it may be seen that even in the vibrationless state B_v and B_e are not equal. In other words, the zero-point vibration within the molecule makes evaluation of B_e impossible unless the α_i can be evaluated. So far this has been done for only one linear molecule[19] investigated by the methods of microwave spectroscopy, viz. the 32-12-16 isotopic species of SCO.

b) The ℓ-Doubling Constant, q

Of the three possible normal vibrations in a linear triatomic molecule, excitation of the doubly degenerate bending mode results im an "induced" angular momentum, ℓ, about the internuclear axis such that:

$$|\ell| = v_2,\ v_2 - 2,\ v_2 - 4,\ \ldots\ldots\ 0 \text{ or } 1 \qquad \text{(III-6)}$$

The total angular momentum, of course, cannot be less than the angular momentum ℓ, so that

$$J \geq |\ell| \qquad \text{(III-7)}$$

Thus the levels J = 0, 1, 2, ..., (ℓ - 1) do not occur[21]*. The rotation-vibration interaction, as pointed out by Herzberg[22], splits the degenerate components because of perturbing elements linking the two states ℓ = +1 and ℓ = -1, resulting in the so-called ℓ-doublets. Physically these perturbing terms can be attributed in part[20,23,24,25,26] to Coriolis forces** acting on the atoms vibrating in a rotating coordinate system.

The ℓ-splitting is symmetrical about the unperturbed position. It has been predicted from theory[20,25], for the state ℓ = 1, to be:

$$\Delta\nu = 2q\,(J + 1)\ \text{mc/s} \qquad \text{(III-8)}$$

where

$$q = q_o(v_2 + 1)\ \text{mc/s} \qquad \text{(III-9)}$$

Here $\Delta\nu$ is the frequency interval between the ℓ-doublets; q is the ℓ-doubling constant which, according to (III-9), is a function of v_2. For the most commonly encountered case in microwave spectroscopy v_2 = 1, hence $q = 2q_o$. This quantity is designated as q_ℓ by some microwave spectroscopists and referred to simply as the ℓ-doubling constant.

The ℓ-splitting has been shown theoretically to be appreciable only for the state $|\ell| = 1$ except at very high J where it has not yet been observed. For $|\ell| \geq 2$ the splitting is of the order $B(\frac{B}{\omega 2})^{|\ell|}$[27], where ω_2 is the fundamental frequency for the doubly degenerate bending mode.

c) The Centrifugal Distortion Constant, D

The centrifugal distortion term in (III-4) must now be considered. Because of the influence of vibration on rotation D_v, strictly, should be used instead of D; however $D \ll B$ so that its dependence upon v can

---

* For this reason, for example, the 02^20 line does not occur for the J = 2 ← 1 transition, (see Section I).

** According to Ta-You Wu[31], Teller was the first to suggest the concept of Coriolis perturbation in rotation-vibration interaction, in an application to the anomalous spacings in the Q-branches of Axially Symmetrical molecules.

be entirely neglected. Indeed the entire second term* is frequently neglected, especially for low-J transitions.

3) Fermi Resonance Perturbation

a) Appearance, Discovery and Preliminary Considerations

This form of perturbation shows itself in the microwave spectrum in the apparently anomalous positions of particular rotation-vibration lines.

The explanation lies in the fact that, for polyatomic molecules, the anharmonic terms in the vibration potential function are sufficient to produce perturbations when certain levels happen to lie very close together[28].

It may happen that two normal vibrational frequencies, or one normal frequency and a harmonic of a second nearly coincide. If, in addition, the two states have the same symmetry, that is belong to the same electronic state and carry the same angular momentum l, they will perturb each other. This effect was first recognized by Fermi[29] in the Raman spectrum of carbon dioxide with the appearance of two almost equally intense lines in the place of the usual single Stokes' line.

According to Fermi, the perturbation interaction results in a mutual sharing of the wave functions of the states concerned. This concept has yielded quantitative results in agreement with experiment and is the explanation for the appearance of two Stokes' lines in the Raman spectrum of CO_2. Such a system may be described by the quantum mechanics of

---

*For example, for SCO in the $J = 3 \leftarrow 2$ ground state transition, the second term in (III-4) is equal to (-)108D or 141 Kc/s. Thus the center of gravity of the absorption line is shifted toward lower frequencies by this amount. Since the accuracy of our measuring equipment is better than this by a factor of at least several times, this correction cannot be neglected here.

perturbation theory for degenerate systems. Herzberg[30] has given an outline of this perturbation theory and discussed it in relation to the Fermi resonance problem[28].

b) Vibrational Levels Affected by Perturbation

Figure (III-1) is a sketch of the vibrational energy level diagram for SCO, (not to scale), illustrating the effect of the perturbation repulsion between neighboring levels of the same symmetry. In the case where only two levels perturb each other the vibration quantum numbers are $(v_1, v_2^{|l|}, v_3)$ and $(v_1 - 1, v_2 + 2^{|l|}, v_3)$ so that, for example, the first perturbation occurs between the $10^0 0$ and $02^0 0$ levels.

The symmetrical stretching vibration ν_1 and the antisymmetrical stretching vibration ν_3 carry out vibrations along the internuclear axis, and so do not contribute an angular momentum component about this axis. Therefore $l = 0$ for all v_1 and v_3 quantum states and, by analogy with atomic spectra, these states are designated as Σ states.

The degenerate bending vibration ν_2 has associated with each of its vibrational states v_2, the quantum number l. For a two-quantum excitation, for example, the resultant angular momentum of the final state about the inter-nuclear axis is determined by the various possible orientations of the unit l-angular momenta vectors, i.e.

$$\Leftarrow \quad \text{or} \quad \Rightarrow \quad \text{or} \quad \leftrightarrows$$

Resultant l = 2 , 2 , 0

Hence a Σ and a Δ state arise. The Δ state is doubly degenerate because of the equivalence of the two directions for the resultant angular momentum.

c) First Fermi Resonance Spectrum

Figure (III-2) is a plot of the microwave spectrum up to and including the first Fermi resonance perturbation for the $J = 3 \leftarrow 2$ transition in SCO. The magnitude and direction of the Fermi perturbations are shown by arrows. That the Fermi resonance perturbation depends upon the symmetry of the state and is not due to the accidental coincidence of energy alone is shown in the observed spectrum where the $10^{0}0$ and $02^{0}0$ states perturb only each other. The $02^{2}0$ state remains unperturbed. Neglecting the small second-order corrections due to centrifugal distortion, therefore, the magnitude of the perturbation, F_1, is obtained by measuring the interval between the $02^{2}0$ and $02^{0}0$ lines.

If the $10^{0}0$ level was unperturbed its distance from the ground state, 000, level would be $6\alpha_1$ for the $J = 3 \leftarrow 2$ transition. Because of Fermi resonance perturbation the measured distance will, instead, be $(6\alpha_1 - F_1)$. Since F_1 is known, (above), the unperturbed value of α_1 is immediately obtained.

d) More General Perturbation Spectrum

Figure (III-3) is a plot of the $J = 3 \leftarrow 2$ transition in SCO showing additional structure and new resonance systems, (see also Figure (III-1)). Resonating pairs are joined. These lines have not been observed since they are appreciably weaker than the resonating pair shown in Figure (III-2).

e) Fermi Resonance Theory

i) We shall here attempt only an outline of the more formal theory of Fermi resonance.

The fact that certain lines cannot be predicted from Equation (III-4) becomes understandable when the influence of the potential function of the molecule on its vibrational levels is examined in greater

detail*.

When the anharmonic terms in the vibrational potential function are introduced into the Schrodinger wave equation the resultant energy is no longer the sum of independent terms corresponding to the different normal vibrations, but contains cross-terms containing the quantum numbers of two or more normal vibrations. For example, for the linear triatomic molecule the vibrational energies[33] are:

$$\begin{aligned} G(v_1,v_2,v_3,\ell_2) = {} & \omega_1(v_1 + 1/2) + \omega_2(v_2 + 1) + \omega_3(v_3 + 1/2) \\ & + x_{11}(v_1 + 1/2)^2 + x_{22}(v_2+1)^2 + x_{33}(v_3 + 1/2)^2 \\ & + x_{12}(v_1 + 1/2)(v_2 + 1) + x_{13}(v_1 + 1/2)(v_3 + 1/2) \\ & + x_{23}(v_2 + 1)(v_3 + 1/2) + g_{22}\ell_2^2 + \ldots \end{aligned} \qquad \text{(III-10)}$$

The ω_i are the frequencies for infinitesimal amplitudes of the normal vibrations (i.e. the zero-order frequencies); the $x_{ik} \ll \omega_i$ are anharmonic coefficients; the v_i are the quantum numbers of normal vibrations; the $g_{ik} \sim x_{ik}$ and give a number of different sublevels when the degenerate vibration γ_2 is excited. Terms such as $x_{12}(v_1 + 1/2)(v_2 + 1)$ result from coupling between the normal vibrational modes and are the direct result of the anharmonicity of the potential function.

ii) If the levels lie very close together the magnitude of the shift is obtained from first order perturbation theory by solving the secular determinant:[34]

$$\begin{vmatrix} E_n^o - E & W_{ni} \\ W_{in} & E_i^o - E \end{vmatrix} = 0 \qquad \text{(III-11)}$$

*Generally the treatment of much of this section follows Herzberg[32]. In what follows, however, only those concepts immediately pertinent to the Fermi theory are introduced. The result is that the organization of the material presented is often quite different from Herzberg, as is perhaps to be expected where the principal ideas are abstracted from a work so comprehensive. For example, some of the equations are written in a way possibly more applicable to the analysis to be considered in later section s of this thesis. Equations (III-23) and (III-24) do not appear in Herzberg, for instance.

where E_n^o and E_i^o are the unperturbed energies; E is the perturbation energy and W_{ni}, the interaction energy, is the matrix element of the perturbation function W, that is[35]:

$$W_{ni} = \int \Psi_n^o \, W \, \Psi_i^{o*} \, d\tau \qquad \text{(III-12)}$$

where W is essentially given by the anharmonic term in the potential energy. Ψ_n^o and Ψ_i^o are the zero approximation eigenfunctions of the two vibrational levels that perturb each other.

The condition that $W_{ni} \neq 0$ gives the selection rules for the perturbed transitions in so far as they are determined by the quantum numbers and symmetry of the two states concerned. Note that the perturbations are due to the same anharmonic terms in the potential energy that cause the cross-terms in the energy formula (III-10).

The most effective perturbations are between levels of the type $(v_1, v_2^{|l|}, v_3)$ and $(v_1 - 1, v_2 + 2^{|l|}, v_3)$. Indicating these states by the subscripts 1 and 2 respectively, then[36]:

$$\begin{vmatrix} E_1^o - E & W_{12} \\ W_{21} & E_2^o - E \end{vmatrix} = 0 \qquad \text{(III-13)}$$

where E_1^o and E_2^o are the unperturbed energies and W_{12} the interaction energy. Hence the perturbation energy, E, is found[37]:

$$E = 1/2(E_1^o + E_2^o) \pm 1/2 \left[4 \left| W_{12} \right|^2 + (E_1^o - E_2^o) \right]^{1/2} \qquad \text{(III-14)}$$

For convenience let:

$$\delta \equiv (E_1^o - E_2^o) = \text{the unperturbed energy difference} \qquad \text{(III-15)}$$

$$\epsilon \equiv \left[4 \left| W_{12} \right|^2 + \delta^2 \right]^{1/2} = \text{the perturbed energy}^{\bigstar} \text{ difference} \qquad \text{(III-16)}$$

$\bigstar$ Since we are dealing here with energy differences between vibrational states the quantity ϵ is directly observed from the near infra-red spectrum.

$$\bar{E}_{12} \equiv 1/2(E_1^o + E_2^o) = \text{the mean energy} \qquad \text{(III-17)}$$

$$\text{then } E = \bar{E}_{12} \pm \epsilon/2 \qquad \text{(III-18)}$$

These relationships are shown in Figure (III-4). Note that as $\delta \to 0$,

$$E \to (\bar{E}_{12} \pm W_{12}) \qquad \text{(III-19)}$$

that is, the maximum perturbed shift comes when E_1^o and E_2^o coincide.

iii) From perturbation methods the eigenfunctions of the two resulting (i.e. perturbed) states can be shown to be composed of mixtures of the zero order approximation (i.e. unperturbed) eigenfunctions ψ_1^o and ψ_2^o, that is[38]:

$$\psi_1 = a\,\psi_1^o - b\,\psi_2^o$$
$$\psi_2 = b\,\psi_1^o + a\,\psi_2^o \qquad \text{(III-20)}$$

where

$$a^2 = \frac{\epsilon + \delta}{2\epsilon}$$
$$b^2 = \frac{\epsilon - \delta}{2\epsilon} \qquad \text{(III-21)}$$

$$\text{and } a^2 + b^2 = 1 \qquad \text{(III-22)}$$

The significance of a^2 and b^2 will be apparent upon examination of Figure (III-4). The ϵ in the denominator of (III-21) is a normalizing factor so that a^2 and b^2 are dimensionless quantities, and in this case obviously their sum must be unity.

From (III-21):

$$\delta = (a^2 - b^2)\epsilon = (1 - 2b^2)\epsilon \qquad \text{(III-23)}$$

From (III-16) and (III-21):

$$W_{12} = \left(\frac{ab}{a^2 - b^2}\right)\delta = (ab)\epsilon \qquad \text{(III-24)}$$

Equations (III-23) and (III-24) permit us to solve for δ, the unperturbed separation of the energy levels, and for W_{12} the interaction energy. But before, (this point is further considered in subsection (e-vi) below), this can be done a^2 and b^2 must be evaluated. For this we turn to the microwave spectrum.

iv) Consider the microwave rotation-vibration spectrum. Through rotation-vibration interaction a given $J' \leftarrow J''$ transition, (' indicates upper, " lower state), will consist of not just a single absorption line due to the pure rotation, (000) line, but also a number of other lines arising from the interaction process. For the symmetrical stretching mode vibration ν_1 the average moment of inertia of the molecule is increased slightly. As a result of this somewhat slower molecular rotation a new line, $(10^{0}0)$, appears on the low-frequency side of the (000) line, (Figure (III-2)). For the degenerate bending mode vibration, the "scissors-like" configuration of the molecule decreases* its average moment of inertia slightly, resulting in the $(01^{1}0)$ doublet appearing on the high frequency side of the (000) line. Thus a definite, yet slightly different moment of inertia of the molecule is associated with each new rotation-vibration line.

A rotating-vibrating molecule in which Fermi interaction occurs will, in general, exhibit a change in the effective B values of the two interacting levels. According to Adel and Dennison[39] the actual, (i.e. perturbed), B-values of the resonating levels 1 and 2 are:

$$B_1 = a^2 B_1^{\,o} + b^2 B_2^{\,o}$$
$$B_2 = b^2 B_1^{\,o} + a^2 B_2^{\,o} \qquad \text{(III-25)}$$

* Theoretically this is not necessarily true, but it has been found to be true in all observed cases. That is, α_2 is negative[40,41].

with $a^2 + b^2 = 1$* and B_1^o, B_2^o are the unperturbed values.

Hence:

$$B_1 + B_2 = B_1^o + B_2^o \qquad \text{(III-26)}$$

That is, the centers of gravity of the perturbed and unperturbed levels coincide. Also:

$$b^2 = \frac{B_1 - B_1^o}{B_2^o - B_1^o} \qquad \text{(III-27)}$$

Equations (III-26) and (III-27) permit the immediate evaluation of b^2 from the microwave data. For example, (refer to Figure (III-2), since the 10^o0 and 02^o0 lines (perturbed), and the 02^20 line (unperturbed) are the <u>observed</u> lines, we calculate their B-values, and let:

$$\begin{aligned} B_1 &= B_{10^o0} \\ B_2 &= B_{02^o0} \\ B_2^o &= B_{02^20} \end{aligned} \qquad \text{(III-28)}$$

from which B_1^o and b^2 are to be evaluated. Since ϵ, the <u>observed</u> perturbed infra-red separation of the 10^o0 and 02^o0 states in this example, is also known, then (III-23) and (III-24) give directly the unperturbed separation δ, and the interaction energy W_{12}.

---

*In equations (III-20) and (III-25) the constants a^2 and b^2 are sometimes referred to as the "mixing constants". Historically this mixing was first observed in the Raman spectrum of CO_2, (Section II-3a). Since this molecule is linear and symmetrical it possesses no permanent electric dipole moment. The symmetrical stretching vibration is, therefore, infra-red inactive. In the Raman spectrum however ν_1 should appear as a single line; instead two lines appear with an intensity ratio of almost (1:0.59)[42]. The explanation, according to Fermi, lies in the resonance between ν_1 and $2\nu_2^o$ resulting in a mutual sharing of the wave functions of the two states so that two lines appear instead of one. Because of the presence of the wave function ψ_1^o, (Equation III-20), two Raman lines whose intensities are in the ratio of the squares of the matrix elements of the induced electric moment[43] result. When δ is very small $a^2 \rightarrow b^2 \rightarrow 1/2$, (Equation III-21). This is the case for CO_2, where the two lines have comparable intensities. Thus we can no longer say that one line is ν_1 and the other $2\nu_2^o$, but rather that they are a mixture[42] of both ν_1 and $2\nu_2^o$.

v) The above example is the simplest case for Fermi resonance. Perturbations occur between any sets of levels satisfying the relationship $(v_1, v_2{}^{|l|}, v_3)$ and $(v_1 - 1, v_2 + 2^{|l|}, v_3)$. For example, the (11^10) and (03^10) levels comprise the next group, (Figure (III-3). Fortunately the magnitude of the perturbation in all other levels may be predicted[44] from a knowledge of the (10^00) and (02^00) level data.

The general expression for the interaction energy[45] is:

$$W(v_1, v_2{}^{|l|}, v_3;\ v_1-1, v_2+2^{|l|}, v_3) = \frac{-h^{3/2}}{16\sqrt{2}\,\pi^3 c^{3/2}\,\omega_1{}^{1/2}\,\omega_2}\,\alpha_{122} v_1{}^{1/2}\left[(v_2+2)^2 - l^2\right]^{1/2} \qquad \text{(III-29)}$$

where the ω_i are the fundamental frequencies and α_{122} [44] is an anharmonic potential constant involving the normal coordinates $q_1 q_2{}^2$ only, that is, none of the other cubic terms gives any contribution.

From (III-29) the resonating pairs $(10^00;\ 02^00)$, $(11^10;\ 03^10)$, $(12^20:\ 04^20)$, etc., are perturbed in the ratios* $1: \sqrt{2} : \sqrt{3}$: etc.... Thus all resonating levels differ from $(10^00;\ 02^00)$ only by a constant factor. Therefore all perturbed levels may be described in terms of δ and $W_{10^00;\ 02^00}$. These two constants are required in addition to the three ω_i, the six x_{ik} and the g_{22} of Equation (III-10) for a complete description of the vibrational energies of the linear molecule considered above.

vi) Because δ may be very small, especially in molecules exhibiting a large perturbation, solution of the determinant in twelve unknowns, aside from the enormous amount of numerical labour involved, appears impractical. The reason is that even very small changes in determining the positions of the energy levels can cause large changes

---

* For CO_2 the observed[46] separations are 97.7, 144.0 and 188 cm^{-1}, respectively.

in δ, even allowing it to become imaginary[47]. It is therefore necessary to find an alternative method for the evaluation of δ, and to use instead only eleven of the most accurately observed bands to set up the determinant.

Historically Adel and Dennison proposed the methods of a) intensity ratios in the Raman doublet[47], (e.g. recall the historical discovery of this effect in CO_2) and b) the convergence of the band lines arising from vibration rotation interaction[48]. Other methods are known[49].

A third method, capable of considerable accuracy, provided the $02^{0}0$ and $10^{0}0$ vibration levels are known* from infra-red or Raman spectra, is the method of microwave spectroscopy outlined above. While this method has been used for a small number of molecules, as discussed in Section I, the reason for its use has not been pointed out in a single publication on microwave spectroscopy with which the writer is familiar.

---

* Whether the infra-red or Raman data is known or not, of course, does not prevent determination of b^2 and a^2 from the microwave data. This is a point of fundamental significance.

IV. MICROWAVE SPECTROSCOPE

1) Hughes-Wilson Stark-Modulated Microwave Spectroscope

a) Introduction

A Hughes-Wilson[50] type, Stark-modulated, microwave spectroscope, Figure (IV-1), built in this laboratory by the writer, has served in the present investigations. This instrument operates in the (7.5 - 9.0) mm. region, corresponding to a frequency range (40,000 - 33,000) mc/s. From the observed signal-to-noise ratios of a number of absorption lines due to lesser abundant isotopic species of SCO and ClCN, and from lines in vibrationally excited states, it is estimated that the sensitivity of the present instrument is of the order of 1×10^{-8} cm^{-1}.

The above frequency region has been chosen for a number of reasons: i) the possibility of investigating a greater variety of molecules; ii) higher rotational transitions can be observed where centrifugal distortions may be studied; iii) while the available power output from the higher frequency Klystrons is low, the sharp increase in the absorption of radiation with increasing frequency, (for a linear molecule as ν^3), to some extent compensates for this decrease.

b) Principle

In the presence of an external electric field (Stark effect) the molecular absorption frequencies are changed. If the external field is caused to vary, the absorption line will be modulated at the frequency of the external field.

c) Operation

i) In practice an electric square wave (Stark field) rising from zero to a maximum, at a frequency of 100 Kc/s, is applied to a plane electrode, centrally located between the broad faces in a waveguide

absorption cell. The amplitude of the square wave may be varied. At the same time a Klystron oscillator is slowly, (about 2 c/s), swept over a small frequency interval about some mean frequency. A sample of gas at a few microns pressure is admitted to the cell whose ends are thin mica "windows", about 0.001 inch thick. The mica windows permit the passage of microwave radiation, at the same time allowing the cell to be evacuated and filled as required. The Klystron oscillator is now slowly tuned so that the mean frequency changes. If the instantaneous Klystron frequency passes through a rotational frequency of some molecule within the gas, then the microwave energy, at this frequency, which reaches the crystal detector is decreased. Because the Stark modulation frequency is very much greater than the frequency at which the Klystron is swept, the decrease in crystal current associated with the absorption is "chopped" at the Stark modulation frequency. That is, the presence of the electric field changes the absorption frequency, so that the line is alternately at the field-free frequency and then at some other frequency dependent upon the amplitude of the Stark modulation. If the splitting is not too large, both the field-free line and its associated Stark components appear. In passing the detected signal through the chain of amplifiers following crystal detection, it is customary to phase-detect just before the signal is displayed upon an oscilloscope or recorded. One reason for this is that while the crystal detector passes the molecular absorption line, chopped at the Stark modulation frequency, the phase-detector passes only the envelope of the spectral line and its Stark components. Thus the actual contour of the absorption is displayed upon the screen of a cathode ray oscilloscope whose sweep is synchronized with the Klystron sweep frequency. Another very important reason is that the phase

detector rejects a considerable portion of all out-of-phase with signal components, such as noise, so that a very marked increase in sensitivity results. Because of the effectively very narrow band pass in such a system, (relatively long time-constant filter), it is necessary to use slow sweep rates to avoid distortion of the true line shape, and to prevent an actual shift in the measured frequency of the line.

ii) So far only the detection process has been described. To determine the frequency of the spectral line a specially constructed secondary frequency standard is used. In principle, this device generates a series of harmonic markers in the microwave region whose positions are known absolutely to within one part in 10^7.

Such a system of markers constitutes a microwave "harmonic spectrum" whose purpose is the analogue of the well known optical "comparison spectrum". A most important advantage which the former enjoys, however, is the fact that the position of a marker may be shifted at will while still maintaining the overall absolute accuracy. Thus, identification of a spectral line consists of bringing a marker into coincidence with that spectral line.

d) Advantages

The Stark modulation method holds many advantages. Perhaps the most striking is the reduction in noise as compared with earlier methods. Spurious signals arising from impedance mismatches in the microwave system are largely eliminated, since only the molecular absorption line is modulated and no signal, except that which is modulated at the correct frequency, can pass through the highly selective amplifiers following the crystal diode detector. Much of the low frequency Klystron noise

and detector crystal noise is also eliminated by selection of a modulation frequency of about 100 Kc/s. At higher modulation frequencies the impedance of the cell becomes so low that it is difficult to obtain sufficient amplitude of modulation to permit a proper examination of second order Stark effects. For a typical (1 x 0.5) inch cross section wave guide cell, the first order Stark effects appear at from (1 to 10) volts, while the second order effects may require from (50 to 1500) volts amplitude of the square wave. A further disadvantage to still higher frequency square wave modulation is that it distorts the true line shape[51]. The Stark patterns, while adding to the complexity of the analysis, do give additional information, for example, in identifying an unknown transition and in evaluating the dipole moment of the molecule.

2) Instrumentation

a) Commentary (design and construction; original work)

A detailed description of the instrumentation of this spectroscope is beyond the scope of this thesis. The writer has spent a great deal of time and effort, completely alone, in the construction and, in many places, the original design of this equipment. Even where the result is not necessarily new it frequently had to be worked out from first principles.

This is especially the case for the high frequency units (810 and 4860 mc/s) on the frequency standard, and the method of mixing frequencies at the microwave harmonic generator. To his knowledge this work on the frequency standard is original.

Acknowledgement must be given to the vast bulk of the literature on the subject and, especially at this phase, to those publications dealing

with the instrument as a whole[52,53,54,55,56]. Where it has been found convenient to do so, circuitry from various of these sources has been adapted for use on the present instrument, for which no apology is offered.

The general features of such a spectroscope are well known, therefore only those units or components which merit special mention will be discussed in any detail. Circuit diagrams for the entire instrument, however, are given.

b) Electronic Equipment

The following is a list of the major equipment constructed by the writer:

A) Frequency Standard

i) 5 mc/s Butler Cathode-Coupled Crystal Oscillator; Buffer; Power Amplifier

ii) (5-10-30) mc/s Multipliers

iii) (30-90-270) mc/s Multipliers

iv) (270-810) mc/s Multiplier

v) (810 mc/s - 40,000 mc/s region) - general circuitry for harmonic generator.

B) Stark Cell Modulator (100 Kc/s square wave generator)

i) 100 Kc/s Crystal Oscillator

ii) Triggered Multivibrator and Amplifier

iii) Triggered Blocking Oscillator

iv) Pulse Driver-Amplifier

v) High Voltage Square Wave "Switch"

vi) Complete Power Supply

C) Microwave Detector Amplifiers

i) 100 Kc/s Cascode-Coupled Preamplifier

ii) 100 Kc/s Tuned Amplifier

iii) 100 Kc/s Phase-Sensitive Detector

D) Klystron Power Supply

i) Unregulated High Voltage Beam Power Supply

ii) Electronically Regulated Grid-Reflector, and Beam Supplies

E) Voltage Standing Wave Ratio Components

i) VSWR Modulator, (500 c/s - 5 Kc/s)

ii) VSWR Detector and Amplifier, (500 c/s - 5 Kc/s)

c) Frequency Standard

A block diagram of the complete standard is shown in Figure (IV-2). The standard has run many thousands of hours without trouble. It is stable and the microwave harmonic spectrum clean without a trace of subharmonics.

This stability is attributed to the nature of the circuit here used as the oscillator.

5 mc/s Oscillator, Figure (IV-3): This is a cathode-coupled[57,58] oscillator, comprising essentially a grounded grid amplifier with a feedback loop through a cathode follower. A quartz crystal operating in the series mode forms the frequency determining element. The stability of the oscillator is high because i) the crystal is operated in the series mode where the effect of stray shunting capacitances is small, ii) the true tune position is apparently for minimum anode current whereas for many crystal oscillators this is the least stable position.

It is unusual for the present frequency standard to be off-frequency by more than one or two cycles per second for random frequency comparisons with WWV, the National Bureau of Standards transmitter in Washington, D.C. More usual is for the standard to be on-frequency to within one-half cycle per second for many hours.

The frequency of the Butler oscillator is independent of the tube[57], and new tubes, as observed by the writer, generally oscillate within one or two cycles of the former frequency without adjustment of any kind.

Multipliers (5-10-30),(30-90-270) mc/s, Figures (IV-4), (IV-5):

The grid-to-ground capacitances in the first of these units is exactly balanced by the use of Johnson ultra-midget differential capacitors[59]. In this case the presence of related harmonics is negligible. In principle, if all the multiplier stages are exactly balanced, only the 810 mc/s primary markers should result in the microwave spectrum. This is precisely what is observed. (All 30 mc/s harmonics completely disappear when additional sideband excitation is removed from the harmonic generator crystal; the 810 mc/s markers, only, remain.)

Multiplier (270-810) mc/s, Figure (IV-6):

This is a push-pull circuit of quite unusual design and employing two 2C43 lighthouse triodes. The successful construction of this basically simple circuit has brought a great deal of personal satisfaction to the writer. To understand more fully what is involved a discussion follows.

Very-high frequency amplifiers or oscillators may be broadly classified into three groups according to frequency: a) below 500 mc/s

b) above 1000 mc/s

c) intermediate (500-1000) mc/s.

Below 500 mc/s amplifiers generally employ parallel-wire resonant lines as tank circuit elements. Transit-time effects in the tube are small. Efficiencies of operation are good, and ordinary precautions in construction are sufficient to give satisfactory performance.

In the higher frequency regions both output and efficiency fall-off, and eventually reach zero at some frequency which depends upon the tube. For lighthouse tubes this is generally above 3000 mc/s. Co-axial line resonant cavities are used almost exclusively. Since much greater care is necessary to guard against radiation losses, and the effects of circuit shielding are much more pronounced because of the danger of excessive feedback, co-axial cavities are ideal. In addition they possess very high Q's, and are very stable in operation.

In the intermediate frequency region, (500-1000) mc/s, (the present case), parallel wire resonant lines become so short as to be impractical. Resonant cavities, on the other hand, may become so large that they are impractical. Their size may be reduced by deliberately designing the characteristic impedance of the cavity to such a value that the cavity wavelength becomes much less than the free-space wavelength, but such an impedance will not generally represent the optimum value for the lighthouse triode to work into, and while the cavity may operate it will certainly do so only under very much reduced efficiency.

Examination of available tubes leads ultimately to the conclusion that by far the best amplifier tube for this frequency region is the lighthouse triode. Quite a number of tubes qualify as oscillators, but here the problem is much simpler. They are good oscillators simply because they cannot do anything else, since the ratio of input to output capacities is in the vicinity of unity. Among such tubes are the 955 acorn triode (up

to 500 mc/s), the 6J4 and the 703-A "doorknob" triodes (up to 1000 mc/s). In not a single instance to which the writer's attention has been called have these tubes been used as amplifiers in this frequency region. For a good amplifier the input to output capacity ratio must be much greater than unity. For the 2C43 this ratio is 58 : 1.

Accordingly it was decided to start with a 2C43 lighthouse triode, and to build some form of circuit, (not a co-axial cavity), around it. The circuit ultimately worked out is a hybrid, but it works beautifully as a tripler from 270 to 810 mc/s, and there is not a trace of self-excited oscillation in it. Briefly, this circuit consists of parallel-wire resonant lines for the 270 mc input. These are of large dimension so that one 2C43 triode plugs co-axially into the end of each line. Specially designed disc-to-cylinder sections fit over the triode, and electrically join the cathode to the end of the line. In this manner the entire metallic base, (cathode), of the lighthouse tube becomes an integral part of the parallel line, and the standing voltage-wave can be tuned right up to the tip of the cathode inside the tube. Another advantage of this arrangement of the input circuit is that all leads to the base pins of the triodes are contained inside the resonant-lines in an r.f. field-free region. They are brought out for connection to the power-supply at the point where the short-circuit tuning connection is made, i.e. at a point where no r.f. voltage field exists.

The grids are grounded through multi-fingered phosphor-bronze disc seals 0.009 in. thick to assure good springiness of contact. The ground plane through the grids forms the natural partition shielding the plate from the cathode circuits.

The plate circuit is a modified butterfly-tuner, joined directly to both anode caps, at points 180° apart on the butterfly-tuner.

The entire assembly is silver-plated, and completely shielded. The variation in output power with anode voltage is shown in the accompanying table. These values are conservative since no estimate of losses* in the indicator have been taken into account.

2C43 anode (Volts)	810 mc/s Output (milliwatts)
250	--
325	275
350	400
400	665
450	920

The frequency has been measured using a General Radio Ultra-High Frequency Wavemeter, type 1140-A. Simple lecher wire measurements over six half-wave lengths gave the preliminary result 805 mc/s, which is actually somewhat better than the wavemeter. Since this first determination a General Radio Line-Stretcher of 50 cm length, has confirmed the operating frequency to within 2 mc/s. Second (540 mc/s) and fourth (1080 mc/s) harmonics are almost entirely absent as judged by the type 1140-A wavemeter.

Multiplier (810 - 4860) mc/s, refer to Figure (IV-2):

So far as is known, this is the first application of such a high frequency multiplier unit to any microwave frequency standard used for microwave spectroscopy. The reason is simple: the present spectroscope is operating at fundamental frequencies in the (33-40) Kmc/s region, whereas many existing instruments operate in the 24 Kmc/s region

* These values have since been found to be low by at least 50%. This unit is actually operated at only 250 volts, (13 m.a. total anode current), where the output power is more than adequate for driving the following multiplier.

(K-band) and go to higher frequencies by "doubling" the microwave frequency itself. Thus the frequency standards for these "harmonic" spectroscopes need be designed to operate only in the relatively lower frequency microwave region; higher frequency readings are taken by multiplying the frequency standard reading by the harmonic number. For example, at 48,000 mc/s a factor two is used. (The interpolation error is also multiplied by two.)

Because the present instrument starts at a much higher frequency, existing type standards are not too satisfactory, since it would appear that many of these do not adequately cover the 40,000 mc/s region. On the other hand the present standard is operating with very great efficiency indeed at 40,000 mc/s.

Considerable time and effort was spent in an unsuccessful search for high order, (about 50X), 810 mc/s harmonics in an effort to avoid the use of the relatively expensive Klystron frequency multiplier. This result, while disappointing, was not entirely unexpected. Professor J.S. Foster therefore suggested that the Sperry SMC-11-L be procured. This is an experimental tube with the following frequency characteristics:

input: 810 $\pm$ 2.5 mc/s

output: 4860 $\pm$ 15 mc/s

The ($\pm$) signs indicate the possible spread in tuning. The multiplication is, of course, always exactly six times. For a crystal controlled 810 mc/s input, such as is available with the existing frequency standard, the output frequency of the Klystron is rigidly controlled. It now forms the penultimate link in a chain of multipliers starting at 5 mc/s. The final link is the crystal harmonic-generator-mixer.

In practice the SMC-11-L is operated at 300 volts (10 milliwatts output power), with a 20 db. flap attenuator* in the output. A double-stub co-axial tuner assures proper impedance matching of this 6 cm. radiation into the crystal harmonic-generator-mixer unit.

Harmonic-Generator-Mixer Unit 4860 mc/s to 40,000 mc/s region.

Figure (IV-7)a illustrates the principle of harmonic production and subsequent detection.

Figure (IV-7)b elaborates upon this principle and illustrates the need for two additional components shown in blocks A and B, without which the microwave frequency standard will not work.

Consider Figure (IV-7)a: then obviously the standard frequency may go not only to the crystal generator but it will also short-circuit itself in the low impedance detector (antenna coil of National HRO receiver). In addition, harmonics arising within the crystal as the result of rectification of the standard frequency, may go not only to the receiver but may be short circuited in the extremely low impedance output loop of the standard frequency generator.

As a consequence of the above, between S and X, Figure (IV-7)b, a series resonant circuit is required so that the standard high frequency will go to the crystal, but the lower frequency beats will go the detector. Accordingly a "short-circuit" at 4860 mc/s was designed, Figure (IV-8), which is actually an integral part of the co-axial line system at this frequency.

---

* This apparently curious mixture of a single waveguide component with co-axial units comes about from availability of units, not choice. The flap attenuator is ideally suited for controlling the output to the harmonic generator, however. It is also less expensive than the equivalent co-axial unit.

To prevent the standard from short-circuiting itself through the detector, the distance XD, Figure (IV-7)b, is made some odd quarter wave length of the standard frequency. The detector is thereby transformed into an infinite impedance at this frequency, so that only the much lower frequency beats can arrive at the detector.

Figure (IV-7)c illustrates the actual arrangement shown in Figure (IV-2).

In addition to the matching requirements for proper power transfer to the harmonic-mixer crystal, and the conditions A and B given above, a new set of conditions is imposed.

Take each frequency standard multiplier unit in turn, separately, and match it to the crystal at X. Now impose conditions A and B. Then, in addition the line lengths S_1X, S_2X, S_3X must be so selected that each generator does not "know" the other is in parallel with it, for otherwise the generators will mutually short-circuit.

Therefore S_3X must be an odd multiple of the quarter wave lengths of both 4860 and 810 mc/s. This is impossible since 4860 mc/s is the sixth harmonic of 810 mc/s. But it is not, in practice, "absolutely impossible". For, if the line is exactly an odd multiple of quarter waves for 4860 mc/s, it can be within "one-sixth of a quarter-wave" for 810 mc/s.

Similar arguments hold for S_1X and S_2X as well as XD.

A word about A_1, A_2, A_3.

A_1 is the co-axial short circuit at 4860 mc/s mentioned above, and described below.

A_2 is a 10 mmf. ceramic capacitor, although 5 mmf. would certainly be adequate. This is the simplest practical arrangement.

A_3 cannot be a condenser because of the low value of this frequency. Instead a 30 mc/s series resonant circuit is used, to act as a low impedance "gate" at this frequency only. The beat-frequencies of interest cannot get beyond this circuit element hence go to the receiver.

It comes about in practice that the 810 and 4860 mc/s generators are so nicely paralleled that removing the 810 mc/s excitation from the crystal altogether, by disconnecting S_2X at the crystal, does not cause the monitored 810 mc/s input to the SMC-11-L cavity to change in any perceptible way.

The entire Frequency Standard set-up is extremely convenient in operation. What at first appears as rather combersome, - three generators in parallel, - is a blessing in disguise. Removal of 30 mc/s excitation, e.g. causes all harmonics to drop-out except the 270 mc/s intervals, thereby providing, if necessary, an unambiguous check on the exact position of a particular 30 mc/s harmonic. If need be the 30 mc/s harmonic intervals can simply be counted from one 270 mc/s point to the other. Under these conditions the wavemeter resolution need not be very high.

4860 mc/s Co-axial Series Resonant Circuit: Reference to Figure (IV-8) will show that this unit is simply a series resonant circuit, or "short-circuit". The co-axial line center conductor was machined to the dimensions given, and the two sections press-fitted together with a teflon dielectric spacer to maintain the alignment.

Since the slot length is a half-wave length at 4860 mc/s, waves of this frequency will "see" a short circuit at the outer gap, and hence proceed without reflection or attenuation.

Since the slot length is one half wavelength, current maxima are at the ends, and no current flows at the center. Therefore the center conductor of the co-axial element is made open-circuit at this point. No low frequency phenomena can now cross the gap since the effective capacitance between sections is of the order of 3 mmf., (540 ohms at 100 mc/s), and the d.c. component from crystal rectification of the standard frequency is forced into the beat detector circuit.

Sperry Model 350 Wavemeter Calibration: One of the first and most useful tasks which the standard made possible was the accurate calibration of the Sperry Model 350 search type wavemeter. The purpose of this meter is to identify the harmonic number of a given marker.

Illustration: (Figure IV-9) illustrates the principal features of the harmonic spectrum. For simplicity and clarity not all harmonic lines are shown.

Figure (IV-10) illustrates the formation of a particular harmonic pattern in the 38,880 mc/s region. In actual operation, of course, only a small part of the mode is swept over at any one time. The operating point of the Klystron is kept near the mode center.

d) Stark Modulator (100 Kc/s square wave generator)

Refer to Figures (IV-11) to (IV-16) inclusive.

This unit is essentially a single-pole double-throw switch through which, first, a high voltage d.c. source charges a pure capacitance (the capacity of the Stark septum to the walls of the waveguide) and, second, the capacitative lead is discharged when the switch is reversed.

The circuits (IV-15) and (IV-16) are due to Sharbough[55], except that in (IV-15) the bias arrangement on the upper switch tube, S_1, has

been considerably modified to prevent ringing on the rising edge of the square wave. In addition the non-inductive resistor, R_d, has been added in the discharge circuit, only, as a critical damping resistor. The interlocks in (IV-16) are the writer's.

As the unit stands a maximum square wave amplitude of about 800 volts, working into a capacitative load (500 - 2000) $\mu\mu$f, 0.125 microseconds rise-time, 0.150 microseconds fall-time, maximum droop less than 2%, is obtained.

e) Microwave Detector Amplifiers

Refer to Figures (IV-17), (IV-18), (IV-19).

This cascode preamplifier is due to Good[60]. It is an extremely low noise circuit widely used as a microwave-detector preamplifier. In actual practice the second stage is deleted, and has been replaced by a cathode-follower for increased stability at high gain.

Circuits (IV-18) and (IV-19) are due to Gordy et al[56].

f) Klystron Power Supply

Refer to Figures (IV-20), (IV-21), (IV-22).

The beam regulator is an extremely simple, effective unit, the basic principle of which is illustrated in Figure (IV-20). It will be seen that the reference voltage for the beam regulator is itself an electronically stabilized voltage. This circuit is patterned after the Polytechnic Research and Development Co., (Brooklyn, New York), universal Klystron power supply. The circuit has been modified to suit present requirements.

As adjusted in this laboratory, the beam regulator has a ripple of not more than 3 m.v. rms at 2,500 volts, 15 ma. load. The use of separate transformers, (uneconomical commercially), and extremely careful shielding has helped in obtaining this low figure. For the

reflector supply the ripple is not more than 1 m.v. at 900 volts, 27 ma. internal load.

g) Voltage Standing Wave Ratio Components

Refer to Figures (IV-23), (IV-24), (IV-25).

The modulator in (IV-23) is due, basically, to the Polytechnic Research and Development Co., (Brooklyn, New York).

Frequency: (500 - 5000) c/s

Amplitude: (0 - 162 volts peak-to-peak.

The detector unit in (IV-24) is the well known M.I.T. Radiation Laboratory Twin-T Amplifier[60], except that the transformer input and bolometer supplies have been considerably changed.

g) Absorption Cell

The absorption cell consists, essentially, of a length of "oversize" waveguide. Running along the entire length, parallel to the broad faces of the guide and centered between them, is a thin metallic septum. The septum is supported by two continuous teflon tapes slotted along their centers. A Stark voltage can, therefore, be applied between the septum and the walls of the absorption cell. To ensure a uniform electric field it is necessary to maintain the center electrode-to-cell wall spacing to quite close tolerances. Tapered transition sections join the cell to the smaller, normal waveguide and components at each end.

The design of the cell follows:

Klystron waveguide: RG-96/U, silver, (0.280 x 0.140 x 0.040) in I.D.

Absorption cell waveguide RG-52/U, brass, (0.900 x 0.400 x 0.50) in I.D.
8 feet long

Tapered transition sections one at each end, 5 in. long

Windows: mica 0.001 inch thickness, located at small end of taper section.

Stark electrode	Silver strip 8 feet long, mirror-like finish. width: 0.843 ± 0.005 in. thickness: 0.032 ± 0.001 in. (max).
Stark electrode insulator	Teflon tape running along entire length of side-walls of waveguide cell. nominal thickness: 0.050 in. width: 0.400 ± 0.001 in. slot depth: 0.023 ± 0.001 in. slot width: 0.032 ± 0.001 in.
Vacuum inlet	located extreme end of cell, consists of 1/32 in. slot milled exactly in center of broad face of waveguide. Length of slot: 3.5 inches.
Stark lead inlet	located adjacent to vacuum inlet but in narrow face of waveguide. A 1/4 in. hole in the center of the face to carry lead-in connector to septum. A Kovar seal with a teflon sleeve, and fitted with a small O-ring so that the entire assembly is removable, serves as the insulated lead-in support for the square-wave Stark modulating voltage. The entire assembly is housed in a rectangular brass block, fitted with a type HN connector, which serves to relieve mechanical stress on the Kovar seal, as well as to shield the input.

As indicated above the absorption cell is a length of "oversize" waveguide. There are a number of reasons for this.

Weak absorption lines require relatively higher microwave powers for their detection. This at once leads to several undesirable effects the most significant of which is line-broadening. At higher microwave powers transitions among molecular states are induced at a rate not negligible compared with the collision rate, thermal equilibrium does not exist, and broadening results from a frequency dependent alteration of energy-level populations.

A cell of large cross-section may, therefore, be employed with advantage. It decreases the microwave energy density, while permitting more power to be delivered to the crystal detector without disturbing the population of rotational energy levels in the gas. As a consequence:

i - Power saturation broadening is decreased

ii - Collision broadening is decreased, as well, since the mean-free-path is greater

iii - The resolving power of the instrument is increased since line broadening generally is reduced

iv - The sensitivity is increased since more power can be used in the search for weak lines

v - The microwave attenuation is less

vi - Mechanically it is much easier to machine to close tolerances.

i) Commercial Components

i) Microwave Components:

Klystron: Raytheon QK142 or QK292.

All other items are either Sperry or Polytechnic Standard units.

ii) Cathode Ray Oscilloscope

Tektronix 535 with dual-beam pre-amplifier and long persistence screen. The absorption signal is fed into one channel and either the frequency standard or the Klystron mode-monitor, at the detector end, fed into the other channel. All spectra observed at from (0.6 to 2.0) c/s sweep repetition rate.

iii) Communications-Type Radio Receiver

National HRO-50-T1, extensively calibrated against a BC-221-AK crystal calibrator on all bands from 180 Kc/s to 35 mc/s. This is a remarkably stable receiver. No drifts greater than 3 Kc/s at the highest frequencies, nor greater than 1 Kc/s below 5 mc/s, have ever been observed. In use all plug-in coils are pre-warmed to approximately the equilibrium temperature of a coil in the receiver, although this precaution is probably not absolutely necessary. In addition, especially above 10 mc/s, the BC-221-AK is frequently brought into use to pin-point more exactly the position of a line.

V. CARBONYL SULFIDE

1) The Observed Spectrum

The observed spectrum is given in Table I. The molecular constants derived from this spectrum are listed in Table II.

a) Intensities

In column four, Table I, the absolute intensity has been calculated using the relationship:

$$\gamma_{max} = 5.48 \times 10^{-17} \mu^2 \nu_o^3 \left(\frac{f_v}{\Delta\nu}\right) \text{ cm}^{-1} \qquad \text{(V-1)}$$

where:

μ is the electric dipole moment in Debye units, or 10^{-18} e.s.u.

ν_o is the frequency of the center of gravity of the line.

$\Delta\nu$ is the line-breadth parameter, the one-half (not the whole) width at one-half maximum intensity. It is usually given in mc/s at 1 mm. Hg. (This is because the maximum intensity is sensibly constant from about 1 to 10^5 microns.) In the absence of exact data it is commonly assumed to be 25 mc/s at 1 mm. Hg since this value is reasonably close for many gases.

f_v is the fraction of molecules in the vibrational state under consideration. For the ground vibration state $f_v = 1$, that is no molecules are in excited vibration states, and the transition is said to be one for pure rotation.

TABLE I

$J = 3 \leftarrow 2$ Rotational Spectrum of SCO

Isotopic Species S C O	Absolute Abundance %	Vibrational state (v_1, v_2, ℓ, v_3)	Calculated Intensity 300°K, in 10^{-6} cm^{-1}	Observed Frequency mc/s	Previously observed Frequency mc/s	Reference
32-12-16	93.81%	000	176×10^{-6} cm^{-1}	36,488.858 ± 0.006	36,488.82	11
		$01^{1}_{1}0$	12.7	36,533.218 ± 0.010	36,532.47	5
		$01^{1}_{2}0$	12.7	36,571.509 ± 0.005	36,570.83	5
		$02^{0}0$	1.2	36,601.141 ± 0.066	36,600.81	5
		$02^{2}0$	1.3	36,615.216 ± 0.016	36,615.3	5
		$10^{0}0$	2.8	36,380.032 ± 0.064	---	
32-13-16	1.06	000	2.0	36,371.502 ± 0.006	---	
33-12-16	0.73	000	(1.4 total)			
$(F' \leftarrow F'') =$		$3/2 \leftarrow 1/2$, $5/2 \leftarrow 3/2$	0.33	36,027.820 ± 0.012	---	
		$7/2 \leftarrow 5/2$, $9/2 \leftarrow 7/2$	0.83	36,029.688 ± 0.003	---	
34-12-16	4.16	000	8.6	35,596.905 ± 0.005		
		$01^{1}_{1}0$	0.62	35,641.028 ± 0.023	---	
		$01^{1}_{2}0$	0.62	35,677.225 ± 0.032	---	

TABLE II

Rotational Constants for SCO
(all units mc/s)

	This Work	Others	Reference
32 12 16 S C O			
B_{000}	6081.500 ± 0.001*	6081.490	8
		6081.453	10
		6081.466 ± 0.013	4
$\alpha_2(01^10)$	-10.584 ± 0.003	-10.594 ± 0.022	4
		-10.61 ± 0.01	11
		-10.59 ± 0.02	13
$\alpha_2(02^20)$	-10.530 ± 0.007	-10.533 ± 0.009	4
$\alpha_1(10^00)$	20.473 ± 0.024	20.56 ± 0.04	4
		(20.49$_0$ calc. for $\alpha_2(02^20)$ by J.F.M.)	4
		20.55	3
		20.5	5
$q_\ell = 2q_o$	6.382 ± 0.003	6.344 ± 0.018	4
		6.34 ± 0.01	11
		6.393 ± 0.013	13
32 13 16 S C O			
B_{000}	6061.940 ± 0.001*	6061.923 ± 0.015	13
		6061.886 ± 0.013	4
$S^{33}C^{12}O^{16}$			
B_{000}	6004.912 ± 0.001*	6004.899 ± 0.007	4
		6004.905	8
$S^{34}C^{12}O^{16}$			
B_{000}	5932.841 ± 0.001*	5932.843 ± 0.01	13
		5932.816 ± 0.013	4
$\alpha_2(01^10)$	-10.35 ± 0.01	-10.37 ± 0.06	64
$q_\ell = 2q_o$	6.03 ± 0.01	6.07 ± 0.06	64

* Assuming D = 1.310 x 10^{-3} mc/s,[62,63].

For example, for $S^{32}C^{12}O^{16}$ we have taken:

μ = 0.709 Debye

ν_o = 36.5 Kmc/s, (J = 3 ← 2)

$\Delta\nu$ = 6 mc/s at 1 mm Hg.

isotopic abundance = 93.8%

f_v = 83%

In order to evaluate f_v the vibrational partition function may be used[66]. In practice it is often more convenient to evaluate f_v for several vibration states and simply add up the individual fractions. To do this we go to the infra-red spectrum and take, for SCO[67]:

ν_1 = 859 cm^{-1} , ($10^00 \leftarrow 000$) vibration transition
ν_2 = 524 cm^{-1} , ($01^10 \leftarrow 000$) " "
$2\nu_2^0$ = 1048 cm^{-1}, ($02^00 \leftarrow 000$) " "

Then it may be shown that the ratio of molecules in any vibration state to the ground vibration state[66] is the Boltzmann factor for that state multiplied by the statistical weight of the state, i.e.

$$\text{Ratio}\left(\frac{v = v}{v = 0}\right) = (v_2 + 1)\, e^{-E/kT} = (v_2 + 1)\, e^{-G_o(v)\,\frac{hc}{kT}} \qquad \text{(V-2)}$$

where v_2 is the quantum number of the doubly degenerate bending vibration, and $(v_2 + 1)$ is the statistical weight[68] for such a vibration.

E is the energy in cm^{-1}

$G_o(v)$ is the vibrational energy measured above the ground vibration state, that is, it is the observed energy, in cm^{-1}

h, c, k, and T have their usual significance. Equation (V-2) may be written:

$$\text{Ratio}\left(\frac{v = v}{v = 0}\right) = (v_2 + 1)\, e^{-\nu/0.6952\,T} \qquad \text{(V-3)}$$

where ν is the observed vibrational energy in cm^{-1}.

Equation (V-3) is not quite complete. For all states in which $l \neq 0$ the molecule acts like a slightly symmetric top[69] *, that is in all doubly degenerate bending vibrations for which $|l| > 0$ the molecule can no longer be considered strictly linear. We therefore introduce for these states only the correction factor:

$$1 - \frac{l^2}{(J+1)^2} \qquad \text{(V-4)}$$

Making use of the above equations and infra-red information the absolute intensities in Table I were calculated.

b) Fermi Resonance Perturbation Correction

In the absence of Fermi resonance the $(02^0 0)$ and $(02^2 0)$ states should coincide, aside from a very small factor, (Equation III-4) due to the slightly different centrifugal distortion corrections for these lines. Table I shows that the $02^0 0$ line is perturbed from the $02^2 0$ position by about 14 mc/s. We take the magnitude of this perturbation and apply it as a correction to the $(10^0 0)$ line, since the magnitudes of the perturbations for $(02^0 0)$ and $(10^0 0)$ are equal and opposite. Therefore $F_1 = 14.012 \pm 0.082$ mc/s. from the observed microwave spectrum, where F_1 is the magnitude of the first resonance perturbation. From the observed $(02^2 0)$, $(02^0 0)$ and $(10^0 0)$ lines we calculate, first the unperturbed $(10^0 0)$ position, (Equation III-26), and then the "mixing constant" b^2, (Equation III-27).

Taking into account the effect of centrifugal distortion for all lines, then:

$$b^2 = \left(\frac{\text{magnitude of perturbation}}{\text{total separation between unperturbed states}}\right) = \frac{14.012 \text{ mc/s}}{249.133 \text{ mc/s}} = 0.0562$$

*Strictly, a slightly asymmetric top, but the amount of asymmetry is extremely small.

This result may be compared with that from the infra-red work of Bartunek and Barker[70], and Callomon, McKean and Thompson[67].

	B.B.	C.M.T.	
	(observed)		
ν_1	= 859.2	859	cm^{-1}
$2\nu_2^0$	=1047.4	1048	
ν_2^2	= 521.5	524	
$(02^00 \leftarrow 01^10)$	= 526.6	530	
$(02^20 \leftarrow 01^10)$	= 514.3	517	
	(derived) by J.F.M.		
ϵ	= 188.2	188	cm^{-1}
δ	= 163.6	162	cm^{-1}
b^2	= 0.065	0.069	

Taking an average of the results of (B.B.) and (C.M.T.) we calculate, according to Equation (III-24), and the infra-red b^2 and ϵ :

$W_{12} = (ab)\epsilon = (0.250)(188.1) = 47.0\ cm^{-1}$, the interaction energy.

From the microwave value of b^2 and the average ϵ above:

$W_{12} = (0.231)(188.1) = 43.5\ cm^{-1}$.

c) Discussion

i) First, the section immediately above is considered. The microwave and infra-red determinations for b^2 appear to show small but persistent differences.

Examination of the infra-red data shows that errors as large as almost 4 cm^{-1} are not uncommon, which percentage-wise is a relatively large error. The microwave data on the other hand yields highly consistent results. Results from these two sources are compared below:

Microwave	b^2	
0.0562	Present work	
0.0566	Low[5]	
0.0564	Tetenbaum[4], (calc. by J.F.M. for α_2 from 02^20 only).	
0.056	Townes and Schawlow[6]	
Infra-red	b^2	
0.065	Bartunek and Barker[70]	
0.069	Callomon, McKean and Thompson[67]	

ii) The results of the present research on SCO are in close agreement generally with previous work. On the whole the B-values appear to favor the early results of Townes, Holden and Merrit[13], while Tetenbaum's[4] results appear slightly low.

The α_2 values from the first and second excited bending vibration states are in close accord with those of Tetenbaum[4], and confirm the small but definite decrease in α_2 as the excitation energy rises.

The q_ℓ result for $S^{32}C^{12}O^{16}$ appears strongly to favor the work of Townes[13], et al., and again suggests that Tetenbaum's[4] result is slightly low.

For α_1 the present result appears slightly low with respect to the published values; however, evaluation of this constant from Tetenbaum's[4] data, (for α_2 from the 02^20 state only), yields a value in very close agreement indeed.

The only serious disagreement in the observed data, with respect to external comparison, will be noted in the (01^1_10), (01^1_20), (02^00) lines of $S^{32}C^{12}O^{16}$. These lines have been observed in only one[5] other investigation. The differences are so large, (0.75, 0.68 and 0.33 mc/s respectively), as to represent a distinct error. The constants derived from these lines, in the present work, however, are in excellent agreement with those from many other investigators.

iii) It will have been noted above that we have compared the microwave and infra-red data through the evaluation of the mixing-constant b^2. This procedure is believed by the writer to be the only legitimate comparison, since only the mixing constants a^2 and b^2 can be evaluated <u>entirely</u> by microwave or <u>entirely</u> by infra-red data.

Unfortunately most microwave spectroscopists appear to favor comparison of their work through evaluation of the interaction constant $W_{12}=W_{10^{o}0;02^{o}0}$, and in one paper at least the mixing constants do not even appear but must be derived for purposes of comparison. The difficulty here is that W_{12} depends upon the perturbed separation, ϵ, observed in the infra-red, so that comparison of W_{12} values involves a second comparison of the various possible infra-red ϵ-values. This in itself is not serious since generally only one or two infra-red works will be used in any case. What is serious is that frequently the infra-red data is so meagre that it does not permit the evaluation of ϵ. For example, for the cyanohalogens, until very recently the only information available was from the Raman work of West and Farnsworth[71] who give only ν_1, ν_2 and ν_3, the fundamental observed vibration frequencies. From this information alone it is not possible to evaluate ϵ, the perturbed separation between $(10^{o}0)$ and $(02^{o}0)$ states, since the $(02^{o}0)$ state is not observed. What has been done under this circumstance by some microwave workers is to assume that $\epsilon = (2\nu_2 - \nu_1)$ or, with equal frequency, that $\delta = (2\nu_2 - \nu_1)$. It is obvious, (refer to Figure III-4), that such assumptions may lead to results of little value especially when the interaction energy is large. Somewhat regretably the symbols ω_i appear to be widely used instead of ν_i, although in fact it is the ν_i which are used. The CO_2 molecule is a good choice for illustrating the above argument:

$\nu_1 = 1388.1\ cm^{-1}$

$\nu_2 = 667.3\ cm^{-1}$

Then for the assumption that ϵ, (or δ), $= 2\nu_2 - \nu_1$

ϵ, (or δ) $= 53.5\ cm^{-1}$ which is nonsense.

For the correct solution of ϵ, or δ, more information is needed from the infra-red or Raman Spectra. For CO_2 this additional information is furnished by observation of the transition $(02^{0}0 \leftarrow 000) = 2\nu_2^{o}$, and the known potential constants, the ω_i, x_{ik} and g_{22}, (Section III-3). Thus:

$$\epsilon = 102.3 \text{ cm}^{-1}$$

$$\delta = 16.65 \text{ cm}^{-1}$$

d) Errors

The errors quoted beside observed frequencies are the statistical errors of a set of observations for that frequency. The more significant absolute error is difficult to evaluate precisely. In the present case it may arise from two principal causes: a) the frequency standard and associated components, b) the Stark square wave modulator.

For the frequency standard, (see Section IV-2C), a maximum error of 1 c/s would give an error of $\pm$ 0.008 mc/s. The National HRO receiver is so well calibrated that it is believed to be within $\pm$ 0.01 mc/s for all frequencies below 10 mc/s, and not more than $\pm$ 0.05 mc/s above this frequency. For this reason it was customary to check higher frequency intervals with the BC-221-AK calibrator directly. An overall error of $\pm$ 0.02 mc/s would seem very liberal here.

The square wave generator is rigidly clamped to ground by three General Electric germanium diodes, (IN-158), whose internal resistance is far lower than any vacuum tube. No detectable "lift" of the waveform from 0 d.c. can be noticed with d.c. coupling to the Tektronix 535 oscilloscope. In addition the measured frequencies, (see also ClCN), seem close where an opportunity for comparison does exist. (Note: the IN 158 diodes are located in the vacuum tube voltmeter, not shown in IV-11 to 16).

VI. CYANOGEN CHLORIDE

1) Nuclear Quadrupole Interactions

a) Introduction

The magnetic field arising from the atomic electrons and interacting with the nuclear magnetic moment gives rise to the familiar hyperfine structure of atomic spectra.

In molecules, on the other hand, the magnetic field is usually exceedingly small because of electron pairing. This comes about from the manner in which a molecule is formed since the chemical bond results from each atom sharing its unpaired electrons. As a result molecules usually do not exhibit the "atomic" type of hyperfine structure. A new phenomenon manifests itself: the nuclear electric quadrupole moment, giving rise to a corresponding hyperfine structure of the rotational lines in the microwave spectrum. This effect was discovered by Good[72] in 1946 in the microwave spectrum of ammonia.

The nuclear electric quadrupole moment may be considered as arising from the non-spherical distribution of the electric charges within the atomic nucleus. The result is that small deviations from Coulomb's law occur, that is the nuclear electric field is no longer spherically symmetrical but possesses a definite axis of polarization. The molecular electric field, as well, is not spherically symmetrical, and therefore the interaction between the two results in small but distinct changes in the energy with nuclear spin orientation. These changes are evident when molecular spectra are examined under the high resolution afforded by microwave spectroscopy.

b) Spin in a Single Nucleus

Where a single nucleus has a non-zero quadrupole moment a molecular

hyperfine structure results. The quadrupole interaction in this case, for a linear or symmetric-top molecule, has been given by Casimir[73] and Van Vleck[74]. The hyperfine energies are:

$$E_Q = (eqQ) \left[\frac{3K^2}{J(J+1)} - 1\right] \left[\frac{3/4\ C\ (C+1) - I\ (I+1)\ J\ (J+1)}{2(2J+3)(2J-1)\ I\ (2I-1)}\right] \qquad \text{(VI-1)}$$

where:

$C = F(F + 1) - I\ (I + 1) - J(J + 1)$

$F = J + 1,\ J + I - 1,\ \ldots .\ ,\ |J - I|$

(eqQ) is the quadrupole coupling constant. (For simplicity, the words "nuclear electric" are frequently dropped since no confusion is apt to result.)

e is the protonic charge

$q = \frac{\partial^2 V}{\partial z^2}$ is the gradient of the molecular electric field at the nucleus in question, arising from all extra-nuclear charges, and taken along the direction, z, of the molecular symmetry axis.

Q is the nuclear electric quadrupole moment

K is the projection of J on the internuclear (symmetry) axis. For a linear molecule in an excited vibrational state $|K| = |\ell|$

For the ground vibration state $K = \ell = 0$

The second term in square brackets is usually written f(I,J,F), and is known as the Casimir function. It has been tabulated[75]. For a linear molecule in the ground vibration state Equation (VI-1) simplifies to:

$$E_Q = (-)\ (eqQ)\ f\ (I,J,F) \qquad \text{(VI-2)}$$

c) Quadrupole-Quadrupole Interaction

i) For the case in which two nuclei within a single molecule possess spin greater than one-half, quadrupole-quadrupole interactions result. The theory for this somewhat more complicated

case has been given by Bardeen and Townes[12]. Only a resume of this theory, illustrating those steps essential to the derivation of the energy levels in a molecule whose rotation lines are split by h.f.s. - h.f.s. structure, will be given.

For the specific case of ClCN both the chlorine and the nitrogen nuclei possess spin. The extent to which these effects are coupled into the molecule is quite different for the chlorine and the nitrogen nuclei. For chlorine the nuclear coupling is much larger than for nitrogen, being in the ratio of about 20:1. This fortunate circumstance permits us to simplify the following theory.

ii) Let the subscripts 1 and 2 refer to the chlorine and nitrogen nuclei, respectively. Then the nuclear spin $\vec{I}_1$ adds vectorially to the molecular angular momentum $\vec{J}$ to give the resultant angular momentum $\vec{F}_1$. Spin $\vec{I}_2$ is much more weakly coupled and adds vectorially to $\vec{F}_1$ to give the total angular momentum, $\vec{F}$, of the molecule. Therefore:

$$\vec{F}_1 = \vec{I}_1 + \vec{J} \qquad \text{(VI-3)}$$

$$\vec{F} = \vec{I}_2 + \vec{F}_1 \qquad \text{(VI-4)}$$

Under these conditions $\vec{I}_1$ and $\vec{J}$ precess so much more rapidly about $\vec{F}_1$ than $\vec{F}_1$ and $\vec{I}_2$ precess about $\vec{F}$, that $\vec{F}_1$ and $\vec{I}_2$ may be regarded as stationary during one complete rotation of $\vec{I}_1$ and $\vec{J}$. Therefore the $(\vec{I}_2,\vec{J})$ interaction is averaged over this motion. For the quadrupole interaction, under the above circumstance, this is proportional to $\cos^2(\hat{\vec{I}_2\vec{J}})$, and thus a more formal description from quantum mechanics must be used to evaluate this interaction[76].

iii) Consider the wave functions describing Equations (VI-3) and (VI-4). The Hamiltonian for these interactions is:

$$H = H_1(\vec{I}_1,\vec{J}) + H_2(\vec{I}_2,\vec{J}) \qquad \text{(VI-5)}$$

Now consider the wave functions describing the following relationships:

$$\vec{F}_2 = \vec{I}_2 + \vec{J} \qquad \text{(VI-6)}$$

$$\vec{F} = \vec{I}_1 + \vec{F}_2 \qquad \text{(VI-7)}$$

The number of wave functions with the same $\vec{F}$ is the same in the two cases.

In case H_1 and H_2 are appreciable the resultant eigenfunctions are not given by either of the above sets of wave functions but by linear combinations of either set. For a specific F value:

$$\sum_{F_1'} \left[H_{F_1F_1'} - E\,\delta_{F_1F_1'} \right] a(F_1') = 0 \qquad \text{(VI-8)}$$

where

$$H_{F_1F_1'} = \sum_{F_2} C\,(F_1F_2)\; C\,(F_1'F_2)\; E_2(F_2) \qquad \text{(VI-9)}$$

and where the $E_2(F_2)$ are the eigenvalues of $H_2(\vec{I}_2, \vec{J})$

Expand (VI-8), therefore:

$$(H_{F_1F_1} - E)\; a\,(F_1) + \sum_{F_1' \neq F_1} H_{F_1F_1'}\; a\,(F_1') = 0 \qquad \text{(VI-10)}$$

Substitute (VI-9) into (VI-10), hence:

$$\left[\sum_{F_2} \left[C\,(F_1F_2) \right]^2 E_2(F_2) + E_1(F_1) - E_Q \right] a\,(F_1)$$

$$+ \left[\sum_{F_1' \neq F_1} \sum_{F_2} C(F_1F_2)\; C\,(F_1'F_2)\; E_2(F_2) \right] a(F_1') = 0 \qquad \text{(VI-11)}$$

where $E = E_Q - E_1(F_1)$, and E_Q is the total quadrupole energy of the system. Two cases will be distinguished: a) <u>when there is an appreciable interaction</u>, so that H_2 and H_1 may have comparable magnitudes. In this case, for Equations (VI-10) or (VI-11) to have a solution the determinant of the coefficients must be zero.

b) when $H_2 \ll H_1$, as is true in the present case where the coupling of the nitrogen spin to the molecule is much less than the coupling of the chlorine spin. In this case the off-diagonal terms, (second terms), in Equations (VI-10) or (VI-11) can be neglected.

a) When $H_2 \ll H_1$:

$$\begin{vmatrix} (H_{F_1F_1} - E) & (H_{F,F_1-1} - E) \\ (H_{F_1-1,F_1} - E) & (H_{F_1-1,\,F_1-1} - E) \\ \cdots & \cdots \end{vmatrix} = 0 \qquad \text{(VI-12)}$$

b) When $H_2 \ll H_1$:

$$(H_{F_1F_1} - E) = 0 \qquad \text{(VI-13)}$$

or

$$\sum_{F_2} \left[C(F_1F_2)\right]^2 E_2(F_2) + E_1(F_1) - E_Q = 0 \qquad \text{(VI-14)}$$

This equation immensely simplifies the solution. It is the basic working equation for all subsequent calculations. Since E_Q is the total quadrupole energy, this equation may be further simplified by writing it as:

$$E_Q = E_{Q_1} + E_{Q_2} \qquad \text{(VI-15)}$$

where E_{Q_2} is the first, and E_{Q_1} the second term, respectively, in Equation (VI-14). E_{Q_1} is taken directly from Equations (VI-1) or (VI-2). Assuming the ground vibrational state:

$$E_{Q_1} = (-)\ (eqQ)_1\ f\ (I_1, J, F_1) \qquad \text{(VI-16)}$$

Similarly:

$$E_{Q_2} = (-)\ (eqQ)_2 \sum_{F_2} \left[C(F_1F_2)\right]^2 f(I_2, J, F_2) \qquad \text{(VI-17)}$$

The $C(F_1F_2)$ are the Bardeen-Townes[12] transformation coefficients. They are very tedious to evaluate numerically. They are related to the Racah[77] coefficients:

$$C(F_1F_2) = (-1)^{F + J - I_1 - I_2} \left[(2F_1+1)(2F_2+1)\right]^{1/2} W(JF_1F_2F;\ I_1I_2) \quad \text{(VI-18)}$$

in which the W-term is the Racah[77] coefficient. Fortunately, tables[78] of these coefficients have now appeared.

Note: The development of Equations (VI-8) to (VI-14), above, differs in a number of details from the outline of Bardeen and Townes or Townes and Schawlow. Our E is related to their E by the equation:

$$E_{\text{(this work)}} = E_{\text{(Townes-Schawlow)}} - E_1(F_1)$$

This has been done in order to preserve simplicity in the writing of equations (VI-8) and (VI-12), and also because they then appear in possibly somewhat more standard form. Another very practical reason will be obvious in Section (VI-2). It will be noted that Townes E is simply E_Q, the total quadrupole energy of the system.

---

d) Second-Order Quadrupole Effects

The above theory, Section (VI-1b), has assumed that the hyperfine splitting is small in comparison with the frequency of the rotational transition. This is usually the case, but in the class of molecules, (cyanohalogens), with which this investigation is concerned this is not always true. For ICN errors as large as 6.3 mc/s can occur for the $J = 4 \leftarrow 3$ transition. Fortunately, for ClCN such effects are very small, being of the order of the accuracy of measurement in a few cases and less in all other cases.

This theory has been given by Bardeen and Townes[79]. It will not be developed here. Strictly, we should write Equation (VI-15), for example, as

$$E_Q^{(1)} = E_{Q_1}^{(1)} + E_{Q_2}^{(1)} \quad \text{(VI-19)}$$

where the superscript refers to first order theory. Then:

$$E_Q = E_Q^{(1)} + E_Q^{(2)} \qquad \text{(VI-20)}$$

where

$$E_Q^{(2)} \text{ is proportional to } \frac{(eqQ)^2}{B_o} \qquad \text{(VI-21)}$$

The constant of proportionality depends upon the J,K,I and F for the transition in question, and is given in Townes and Schawlow[80].

2) Calculation for J = (3 ← 2) Transition in ClCN

The procedure used by the writer for evaluating the theoretical equations will be given in brief outline, but details of calculation omitted except for illustration only.

a) Recall Equations (VI-3 and 4), (VI-6 and 7), and set up the following table for:

$J = 3$, (upper level)

$I_1 = 3/2$, (chlorine)

$I_2 = 1$, (nitrogen)

Then $\vec{F}_1 = \vec{J} + \vec{I}_1$ may go from 9/2 to 3/2

$\vec{F}_2 = \vec{J} + \vec{I}_2$ may go from 4 to 2

$\vec{F} = \vec{F}_1 + \vec{I}_2 = \vec{F}_2 + \vec{I}_1$ may go from 11/2 to 1/2

F =	+ F_1	9/2	7/2	5/2	3/2
	I_2	1	1	1	1
F_2 + I_1					
4 3/2		11/2	9/2	7/2	5/2
3 3/2		9/2	7/2	5/2	3/2
2 3/2		7/2	5/2	3/2	1/2

Therefore the J = 3 rotation level is split into six F-sublevels, (diagonals), and these sublevels are in turn split into various numbers of sublevels. The total of all sublevels is twelve.

b) Take a particular sublevel, say F = 7/2. Then from Equation (VI-13) and the above table:

$$(H_{9/2\ 9/2} - E) = 0$$

$$(H_{7/2\ 7/2} - E) = 0$$

$$(H_{5/2\ 5/2} - E) = 0$$

c) Each of these equations is now expanded in the form of Equation (VI-14), e.g.:

$$(H_{9/2\ 9/2} - E) = \left[C(9/2,\ 4)^2\ E_2(4) + C(9/2,\ 3)^2\ E_2(3) + C(9/2,\ 2)^2\ E_2(2)\right] + E_1(9/2) - E_Q = 0$$

d) The Bardeen-Townes transformation coefficients are expressed in terms of the Racah coefficients, and numerically evaluated, e.g.

$$C(9/2,\ 4) = (+)\ \sqrt{10 \times 9}\ \ W(3\ 9/2\ 4\ 7/2;\ 3/2\ 1) = \left(\frac{1}{336}\right)^{1/2}$$

e) The complete set of equations arising in b), above, is evaluated as illustrated. As a check on the correctness of the work after this has been done the sum of the coefficients in any one equation must equal unity. This is the "horizontal" sum, for F_1 = constant. Similarly the "vertical" sum, for F_2 = constant, must be unity.

f) The $E_2(F_2)$ are evaluated in d), e.g.

$$E_2(4) = f(1,\ 3,\ 4) = 0.083333$$

from tables for the Casimir function.

g) This process is repeated for all equations in b).

h) Now recall the relationship between Equations (VI-16), (VI-17) and (VI-14), and take $(eqQ)_1 = -83.33$ mc/s; $(eqQ)_2 = -3.63$ mc/s as preliminary values. Then the energy equation in d), above, becomes

$$E_Q = (6.945 + 0.554)\ \text{mc/s}$$

The larger splitting is due to chlorine, the smaller to nitrogen. This is one of twelve sublevels for the $J = 3$ rotational level evaluated on the assumption that $H_2 \ll H_1$ and that second order quadrupole effects can be neglected.

i) The complete $J = 3$ and $J = 2$ rotational levels are evaluated as above. A total of 78 terms is involved.

j) With the above information the energy levels are constructed, Figure (VI-1). Then for $\Delta J = +1$; $\Delta F_1 = 0, \pm 1$; $\Delta F = 0, \pm 1$, the transition frequencies for the ground vibration state are calculated. It should be noted that since $(eqQ)_1 \gg (eqQ)_2$ the nitrogen h.f.s. levels cluster about each chlorine h.f.s. level. Under low resolution we may say that the chlorine levels are only broadened by the presence of the nitrogen quadrupole.

k) For the excited vibration-rotation levels a new energy-level diagram must be constructed. For these states $|\ell| > 0$ so that the first square bracket in Equation (VI-1) provides a scale- and sometimes an inversion-factor by which the various excited vibrational states are adjusted. The result is shown in Figure (VI-2), in which (for practical reasons) the effect of the nitrogen spin is neglected. That this step is justified will be apparent in what follows.

3) Intensities

For the calculation of intensities reference is made to White[81]. This process is straight-forward except for the following simple substitution:

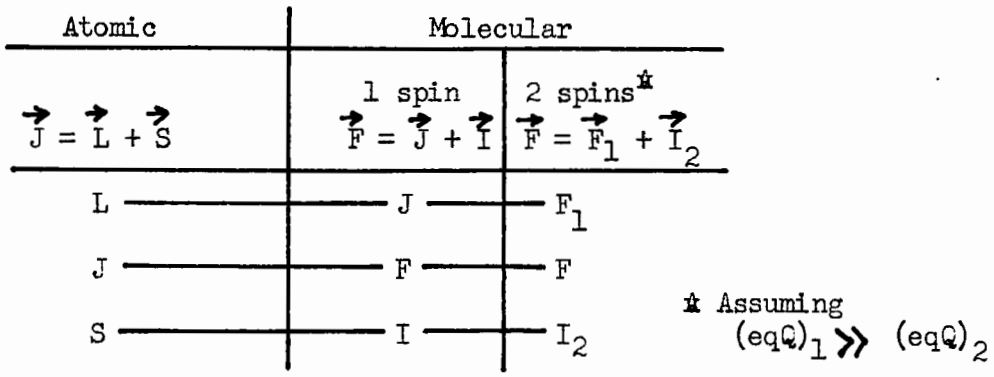

4) Calculated Spectra

The calculated h.f.s. spectra in the ground and excited vibration states is shown in Figures (VI-3) to (VI-7) inclusive.

5) Observed Spectra and Discussion

i) Tables (IV to VII) inclusive list the observed spectra.

Table III summarizes the above work in the sense that it lists for each isotopic species the "hypothetical" frequency of the center-of-gravity, ν_0, for the pure rotational transition of the ground vibrational state. It is this frequency which must be used in the determination of the majority of molecular parameters.

Table VIII summarizes the evaluation of molecular constants from the microwave spectra. Where comparisons are possible it is felt that the results exhibit generally good agreement.

The (35-12-15) and (37-12-15) relatively rare N^{15} isotopes are here reported for the first time. $Cl^{37}C^{12}N^{15}$ exists in nature in 0.089% abundance. It is estimated that, without increasing sensitivity, an isotopic abundance of only 0.02% could be detected in this gas.

The α_2 values in the second excited degenerate bending mode are reported for the first time. The very small but definite decrease with excitation is to be noted, e.g. compare with SCO.

ii) Table IX summarizes what is perhaps the most interesting observation in this gas, viz. the variation (decrease) in the nuclear electric quadrupole coupling constant with excited vibration state. To the writer's knowledge this is the first observation of this effect in any molecule in the $v_2 = 2$ state. It has been observed here for both principal isotopic species of cyanogen chloride, Figure (VI-14). Tetenbaum[7] has observed an analogous decrease in BrCN in going to the $v_2 = 1$ state. Taken together these two investigations appear to constitute the only observations to-date of this effect.

It is reasonable to suppose that, in a linear molecule forced to vibrate with ever increasing amplitude in the degenerate bending mode, the gradient of the molecular electric field along the internuclear axis must undergo some kind of change. The molecule is no longer linear, in the strict sense, but slightly asymmetric, and the degree of asymmetry increases as v_2 increases. Quantitatively the effect does not appear to lend itself to ready evaluation. So far as the writer is aware no theory of such an effect appears to have been published.

iii) In comparing the results in Table IX with the work of others one very important aspect of the analysis must be kept in mind, viz. how many intervals did other investigators have at their disposal in the evaluation of (eqQ)? Another question, the answer of which may only be surmised, is: how many did they use? For the work of Townes et al.[13] the maximum possible number of intervals, with their data, is ten. For the group at Duke[15] it was six. In the present case seven h.f.s. lines are observed in the (000) state and therefore twenty-one intervals exist. For (35-12-14), (000), nineteen out of the twenty-one intervals were used; for (37-12-14), (000), eighteen were used.

With the most probable value of (eqQ) evaluated, a series of hypothetical intervals were calculated. Then, expressing ν_o as an unknown interval, y, from some standard harmonic, as many equations for y could be solved as there were lines. In this way a weighted average of ν_o was obtained. For example, theoretically the $F_1' \leftarrow F_1'' = 5/2 \leftarrow 3/2$; $3/2 \leftarrow 3/2$ line in the 02^20 h.f.s. group is <u>exactly</u> at the center of gravity of this h.f.s. In arriving at the best value for ν_o, however, information from <u>all</u> lines is used (above method). The observed and calculated values agree, in $Cl^{37}C^{12}N^{14}$, to within $\pm$ 0.01 mc/s.

iv) The designations X^{35}, β^{35} and X^{37}, β^{37} refer to two groups of lines observed in the (35-12-14) and (37-12-14) species of ClCN. They have not been positively identified. Refer to Figure (III-2), then except for the somewhat added complication of hyperfine structure, the (10^00) and (02^00) lines should be observed at some perturbed position. The magnitude of the perturbation is not known. However, since $\ell = 0$ for both "lines", (hyperfine groups), the expected h.f.s. patterns can be calculated, and the intensities predicted from near infra-red data. After all "known" lines are accounted for, (000), (01^10), (02^20), etc., the unknowns are examined.

X^{35} consists of two lines of the correct relative amplitude and approximate spacing to be classed as belonging to an $\ell = 0$ state and $Cl^{35}C^{12}N^{14}$. These lines are observed only at relatively high electric fields, therefore they are quadratic Stark lines, (that is, $\ell = 0$ is apparently proved). They do not shift position with the magnitude of the modulating (Stark) voltage, and therefore are true lines, not Stark-components or "forbidden" lines. In every respect they behave as ordinary lines. As the pressure is reduced the intensity falls and

ultimately the lines disappear when the liquid nitrogen has condensed all gas out of the cell. It is interesting to examine the shape of these lines at fairly low pressures. Refer to Figure (VI-10c). This photograph indicates quite clearly that the major component is asymmetric, and the minor component is peaked. This of course is very nearly the theoretical contour for these lines when the effect of the nitrogen quadrupole is considered, Figure (VI-4). We therefore conclude that these lines, in all probability, belong to a system in which $\ell = 0$.

An $\ell = 0$ group can arise from: a) the (000) state; b) the $02^{0}0$ state; c) the $10^{0}0$ state. Intensity considerations rule out the $04^{0}0$ state.

a) All isotopic species of any consequence, ($\geq 0.05\%$), have been located. In any case their positions can be calculated, that is whether they had been observed or not, and shown not to fit X^{35}.

b), c) Assume the line X^{35} to be $02^{0}0$ or $10^{0}0$. Examination of Figure (VI-10a), (photograph), shows X^{35}, center, and the $F_1' \leftarrow F_1'' = 3/2 \leftarrow 3/2$ (000) line, left, under very low resolution. The Klystron power transmitted through the cell, as measured at the detector end, is shown in the upper curve. The "mode" is just about cut-off on the left. An absorption in the waveguide cell or arising from some other microwave frequency-sensitive component is superimposed on the power. An estimate of the intensity of the strongest X^{35} line relative to the single line from the (000) state, would suggest that it is possibly one-third or more, (keeping the power loss immediately above X^{35} in mind). The calculated ratio for the $10^{0}0$ line is about one half or less.

Therefore a tentative designation of $X^{35} = (10^{0}0)$ is made.

v) Repeating this experiment for X^{37} yields a surprising result. The absolute intensity of X^{37} appears far below what it should be. Indeed it is not an easy line to work with. A multiple exposure photograph, to integrate signal over noise, is shown in Figure (VI-13a). In all other respects X^{37} acts like X^{35}.

vi) β^{35} and β^{37} appear in analogous positions just below the $0l_1^1 0$ doublet in $Cl^{35}C^{12}N^{14}$ and $Cl^{37}C^{12}N^{14}$ respectively, Figure (VI-11a) and Figure (VI-12b). In. Fig. (VI-11a) the X^{35} group appears to the left.

β^{35} is single, but the strong suggestion of a shoulder on the $F_1' \leftarrow F_1'' = 7/2 \leftarrow 7/2$ $(0l_1^1 0)$ line, Figures (VI-11a, b), indicates that possibly the "missing", or strong, component to β^{35} is unresolved, and masked by the ℓ-doublet line. For the frequency standard adjusted to set a marker opposite the position where the "missing" component should be, the marker coincides almost exactly with the right edge of the ℓ-doublet line. If the "bulge" is taken as an unresolved line then this line lies approximately 1.2 mc/s or less above the ℓ-doublet line. The amount of gas required to raise the intensity of the higher vibrational state lines so that they can be properly observed is already too much for good observation on the ℓ-doublet. Therefore broadening occurs and resolution goes down. β^{35} appears only at high fields, indicative of $\ell = 0$. When the voltage is reduced to the linear Stark region β^{35} and the "bulge" disappear, Figure (VI-12c). (This photograph includes two ℓ-doublet lines.) The $0l_2^1 0$ doublet does not exhibit an analogue of β^{35}. Figure (VI-11c), taken under high electric-field conditions for the $F_1' \leftarrow F'' = 7/2 \leftarrow 7/2$ line in $(0l_2^1 0)$, shows complete absence of such components.

Again, the intensity appears too low by a factor of possibly five times or more.

vii) β^{37} is a much "cleaner" line than β^{35}. No corresponding bulge on the ℓ-doublet line is seen. Quadrupole coupling considerations, however, would require less separation in the β^{37} group (of two lines). Calculation shows that the "missing" component in this case would be expected to lie almost in the center of the ℓ-line, Figure (VI-12b), at the position of the frequency standard marker.

The intensity here is somewhat better, relatively, but still low by about five times or less.

viii) The possibility that the β lines might arise from the $03^{1}0$ state has been considered. The intensity is about right. This state can be expected to give rise to a quasi-quadratic Stark effect because of the large separation of the doublets. The observed voltage at which the β and X lines begin to appear, however, suggests a true quadratic effect as would be expected only if $\ell = 0$.

ix) Assume, for the moment, that the X and β lines are the $10^{0}0$ and $02^{0}0$ Fermi perturbed lines. Then for $Cl^{35}C^{12}N^{14}$ the mixing constant, b^2, can be evaluated. Therefore:

$$b^2 = \frac{133.06 \text{ mc/s}}{281.56 \text{ mc/s}} = 0.473$$

This result may be compared with the very recent infra-red work of Freitag and Nixon[49]. They observe:

$$\nu_1 = 714 \text{ cm}^{-1}$$

$$2\nu_2^{0} = 784 \text{ cm}^{-1}$$

from which ϵ, the perturbed separation, is 70 cm^{-1}. From their anharmonic constants δ, the unperturbed separation, is found to be 30.8 cm^{-1}. This gives $b^2 = 0.280$ which is in strong disagreement with the above interpretation for X^{35} and β^{35}.

x) The infra-red work of the above investigators may be compared with the microwave work of Tetenbaum[7] in the matter of cyanogen bromide:

$$b^2 \text{ (infra-red)} = 0.033$$

$$b^2 \text{ (microwave)} = 0.1069$$

(The numerical evaluation is by the writer in both cases, taking α_2 from the 02^20 state in the microwave spectrum.) In this case, too, therefore there is an even larger disagreement.

xi) Freitag and Nixon have apparently observed the unusual result that, in both ClCN and BrCN, the hypothetical unperturbed $2\nu_2^o$ level, ($G_o(02^o0)$ level), is <u>greater</u> than twice ν_2. In other cases for which the constants have been determined, according to these authors, the difference is slightly <u>less</u> than twice ν_2. For example, for CO_2 this difference is 6 cm^{-1}; for SCO it is 7.1 cm^{-1}.

The value for δ has been determined in the infra-red work, above, by a method of integrated intensities, while ϵ has been observed as the frequency difference between two measured energy levels.

In the microwave method b^2 is calculated very simply from observed intervals. Unless actual line misidentification occurs it is difficult to understand where any serious error could come into this method.

Simple calculation shows that, if Tetenbaum's analysis is correct, then for BrCN δ should be 91.2 cm^{-1}, rather than 109.4 cm^{-1} which follows from Freitag's and Nixon's work.

A similar calculation for ClCN indicates that the unperturbed level separation, δ, would be not more than 10 cm^{-1}, possibly less. Taking δ = 8 cm^{-1} gives b^2 = 0.443. This value is not too far from the tentative value b^2 = 0.473 determined from the X^{35} and β^{35} lines in the present work.

On the strength of the ClCN data alone there is not sufficient evidence to question the work of Freitag and Nixon. The work of Tetenbaum with BrCN, however, raises the entire question anew.

In conclusion, therefore, the X and ζ lines are tentatively assigned as the $(10^{o}0)$ and $(02^{o}0)$ lines, respectively, in each main isotopic species of ClCN. This leads to the tentative α_1 values listed in Table VIII. It is the question of intensities above all else which is difficult to understand, A wide and detailed search has failed to show any other lines.

TABLE III

J = 3 ← 2 Ground Vibrational State Transitions in Cyanogen Chloride

Isotopic Species ClCN	Absolute Isotopic Abundance*	Frequency (center-of-gravity of h.f.s.) ν_o in mc/s
35-12-14	74.3%	35,824.83 ± 0.06
37-12-14	24.2	35,083.29 ± 0.07
35-13-14	0.832	35,638.49 ± 0.03
37-13-14	0.272	34,888.10 ± 0.02
35-12-15	0.272	34,488.32 ± 0.02
37-12-15	0.089	33,818.57 ± 0.04

* Relative abundances from Hollander, Perlman and Seaborg[82]:

Cl^{35} = 75.4%, C^{12} = 98.892%, N^{14} = 99.635%

Cl^{37} = 24.6 C^{13} = 1.108 N^{15} = 0.365

TABLE IV

The Observed Spectrum of $Cl^{35}C^{13}N^{14}$
$J = 3 \leftarrow 2$ transition; $\nu_o = 35,824.83 \pm 0.06$ mc/s

Transition $F_1' \leftarrow F_1''$	Abs. Intensity (calc.) at 300°K. in 10^{-6} cm^{-1}	Absolute Frequency observed mc/s	calculated mc/s
(000)			
7/2 ← 7/2	16.8 x 10^{-6} cm^{-1}	35,805.15	35,805.01
5/2 ← 7/2	0.84	814.82	814.73
3/2 ← 1/2; 5/2 ← 3/2	107.0	820.49	820.67
7/2 ← 5/2; 9/2 ← 7/2	248.0	825.76	825.82
5/2 ← 5/2	21.5	835.55	835.53
3/2 ← 3/2	16.5	841.46	841.48
3/2 ← 5/2	1.2	856.35	856.35
$(01^1_1 0)$			
7/2 ← 7/2	2.25	35,887.35	35,887.40
5/2 ← 3/2; 7/2 ← 5/2‡	22.3	897.67	897.61
3/2 ← 1/2; 9/2 ← 7/2‡	25.2	902.70	902.77
5/2 ← 5/2	3.06	904.98	904.86
3/2 ← 3/2	2.21	912.94	912.92
$(01^1_2 0)$			
7/2 ← 7/2	2.25	35,932.11	35,932.14
5/2 ← 3/2; 7/2 ← 5/2‡	22.3	942.47	942.38
3/2 ← 1/2; 9/2 ← 7/2‡	25.2	947.61	947.56
5/2 ← 5/2	3.06	949.63	949.65
3/2 ← 3/2	2.21	957.69	957.73
$(02^2 0)$			
7/2 ← 5/2; 5/2 ← 5/2; 3/2 ← 5/2	3.08	36,006.01	36,005.98
5/2 ← 3/2; 3/2 ← 3/2	2.06	020.55	020.56
5/2 ← 7/2; 7/2 ← 7/2; 9/2 ← 7/2	4.12	026.12	026.39
3/2 ← 1/2	1.03	041.21	040.97
$X^{35}(10^0 0)$ tentative			
3/2 ← 1/2; 5/2 ← 3/2	3.0	35,868.06 ± 0.07	
7/2 ← 5/2; 9/2 ← 7/2	6.9	35,872.98 ± 0.06	
$\beta^{35}(02^0 0)$ tentative			
3/2 ← 1/2; 5/2 ← 3/2	2.6	35,883.45 ± 0.08	

‡ = very close structure, not degenerate.

TABLE V

The observed spectrum of $Cl^{35}C^{12}N^{14}$
$J = 3 \leftarrow 2$ transition, (000) group

Nitrogen h.f.s. in $F_1' \leftarrow F_1'' = 3/2 \leftarrow 3/2$ transition

$\nu_o = 35{,}841.467 \pm 0.001$ mc/s; $(eqQ)_N 14 = -3.32 \pm 0.07$ mc/s

Transition $F_2' \leftarrow F_2''$	Abs. Intensity 300°K; in 10^{-6} cm^{-1} (calc.)	Absolute Frequency observed mc/s	calculated mc/s
3/2←3/2; 3/2←5/2; 3/2←1/2	5.50	35,840.937	35,840.935
5/2←5/2; 5/2←3/2	8.25	841.600	841.600
1/2←1/2; 1/2←3/2	2.75	842.132	842.131

TABLE VI

The Observed Spectrum of $Cl^{37}C^{12}N^{14}$

$J = 3 \leftarrow 2$ transition; $\nu_0 = 35{,}083.29 \pm 0.07$ mc/s

Transition $F_1' \leftarrow F_1''$	Abs. Intensity (calc.) at 300°K in 10^{-6} cm^{-1}	Absolute Frequency observed mc/s	Absolute Frequency calculated mc/s
(000)			
7/2←7/2	5.2×10^{-6}	35,067.98	35,067.78
5/2←7/2	0.25	075.54	075.39
3/2←1/2; 5/2←3/2	33.0	079.90	080.03
7/2←5/2; 9/2←7/2	76.0	084.03	084.07
5/2←5/2	6.7	091.74	091.66
3/2←3/2	5.1	096.40	096.31
3/2←5/2	0.37	108.25	107.96
$(01^1_1 0)$			
7/2←7/2	0.68	35,147.38	35,147.36
5/2←3/2; 7/2←5/2*	6.8	155.34	155.47
3/2←1/2; 9/2←7/2*	7.7	159.42	159.57
5/2←5/2	0.89	161.39	161.23
3/2←3/2	0.67	167.71	167.64
$(01^1_2 0)$			
7/2←7/2	0.68	35,190.77	35,190.91
5/2←3/2; 7/2←5/2*	6.8	198.95	198.81
3/2←1/2; 9/2←7/2*	7.7	202.88	202.81
5/2←5/2	0.89	204.45	204.42
3/2←3/2	0.67	210.68	210.67
$(02^2 0)$			
7/2←5/2; 5/2←5/2; 3/2←5/2	0.95	35,264.23	35,264.24
5/2←3/2; 3/2←3/2	0.61	275.51	275.50
5/2←7/2; 7/2←7/2; 9/2←7/2	1.28	280.09	280.00
3/2←1/2	0.31	291.15	291.25
X^{37}			
3/2←1/2; 5/2←3/2**	1.0	35,128.0 ± 0.25	
7/2←5/2; 9/2←7/2	2.3	35,132.02 ± 0.08	
β^{37}			
3/2←1/2; 5/2←3/2	0.8	35,143.78 ± 0.09	

* See note Table IV;

** estimated from photograph

TABLE VII

The Observed Spectra of the Lesser Abundant Isotopes

J = 3 ← 2 transition Cyanogen Chloride

(000) state

Transition $F_1' \leftarrow F_1''$	Abs. Intensity (calc.) at 300°K in 10^{-6} cm^{-1}	Absolute Frequency observed mc/s
$Cl^{35}C^{13}N^{14}$	ν_o = 35,638.49 ± 0.03 mc/s $(eqQ)_{Cl^{35}}$ = -86.1 ± 0.94 mc/s	
3/2 ← 1/2; 5/2 ← 7/2	1.2 x 10^{-6}	35,634.18
7/2 ← 5/2; 9/2 ← 7/2	2.8	35,639.51
$Cl^{37}C^{13}N^{14}$	ν_o = 34,888.10 ± 0.02 mc/s $(eqQ)_{Cl^{37}}$ = -65.75 ± 0.58 mc/s	
3/2 ← 1/2; 5/2 ← 7/2	0.36 x 10^{-6}	34,884.71
7/2 ← 5/2; 9/2 ← 7/2	0.83	34,888.78
$Cl^{35}C^{12}N^{15}$	ν_o = 34,488.32 ± 0.02 mc/s $(eqQ)_{Cl^{35}}$ = -82.1 ± 0.65 mc/s	
3/2 ← 1/2; 5/2 ← 7/2	0.31 x 10^{-6}	34,484.13
7/2 ← 5/2; 9/2 ← 7/2	0.71	34,489.31
$Cl^{37}C^{12}N^{15}$	ν_o = 33,818.57 ± 0.04 mc/s $(eqQ)_{Cl^{37}}$ = -67.2 ± 1.1 mc/s	
3/2 ← 1/2; 5/2 ← 7/2	0.10 x 10^{-6}	33,815.21
7/2 ← 5/2; 9/2 ← 7/2	0.23	33,819.37

TABLE VIII

Molecular Constants for Cyanogen Chloride

The first entry, underlined, is the value obtained in the present work

Isotopic Species	B_{000}* mc/s		α_2 mc/s		$q_\ell = 2q_o$ mc/s		α_1 mc/s
35-12-14	5970.835 ± 0.010		-16.36 ± 0.01 ($v_2 = 1$)		7.465 ± 0.01		(14.30 ± 0.1)
	5970.820 ± 0.02	13	-16.31 ± 0.02 ($v_2 = 2$)		7.500 ± 0.015	13	tentative
	5970.853 **	15	-16.39 ± 0.02 ($v_2 = 1$)	13	7.459	83	
	5970.831	83					
37-12-14	5847.243 ± 0.012		-16.03 ± 0.02 ($v_2 = 1$)		7.21 ± 0.01		(13.43 ± 0.1)
	5847.260 ± 0.02	13	-16.02 ± 0.01 ($v_2 = 2$)		7.166	83	tentative
	5847.275 **	15					
	5847.243	83					
35-13-14	5939.778 ± 0.005						
	5939.775 ± 0.03	13					
	5939.825 **	15					
37-13-14	5814.712 ± 0.003						
	5814.705 ± 0.03	13					
	5814.739 **	15					
35-12-15	5748.083 ± 0.003						
37-12-15	5636.457 ± 0.007						

* Assuming[83] D = 1.66×10^{-3} mc/s for all Cl^{35} species of molecule
D = 1.61×10^{-3} mc/s for all Cl^{37} species of molecule

** Frequencies are given in reference 15. These B-values calculated by writer using above D-values.

TABLE IX

Variation of Quadrupole Coupling Constant with excited vibrational state in ClCN

Vibration state	$(eqQ)_{Cl}$	
	this work	other
$Cl^{35}C^{12}N^{14}$		
000	-83.24 ± 0.50 mc/s	(-83.50);[15] (-82.2 ± 0.5)[13]
$01^{1}0$	-82.26 ± 0.54	
$02^{2}0$	-81.64 ± 0.54	
$X^{35} = (10^{0}0)$ tentative	-79.50 ± 1.12	
$Cl^{37}C^{12}N^{14}$		
000	-65.12 ± 0.59 mc/s	(-65.0);[15] (-65.7 ± 0.5)[13]
$01^{1}0$	-64.45 ± 0.75	
$02^{2}0$	-63.02 ± 0.42	

BIBLIOGRAPHY

SECTION (I)

1. C.H. Townes and A.L. Schawlow, "Microwave Spectroscopy", (McGraw-Hill Book Co. Inc., 1955), p. 30.

2. W. Gordy, W.V. Smith and R.F. Trambarulo, "Microwave Spectroscopy", (John Wiley and Sons, Inc. 1953), p. 371.

3. W. Low and C.H. Townes, Phys. Rev. 79, 224 (A), 1950.

4. S.J. Tetenbaum, Phys. Rev. 88, 772, 1952.

5. W. Low, Phys. Rev. 97, 1664, 1955.

6. ref. 1, pp. 39-40.
7. S.J. Tetenbaum, Phys. Rev. 86, 440, 1952.

8. ref. 1, Appendix VI beginning p. 613.

9. ref. 2, Table A.4 beginning p. 346.

10. P. Kislink and C.H. Townes, "Molecular Microwave Spectra Tables", (National Bureau of Standards Circular 518, June 23, 1952.

11. M.W.P. Strandberg, T. Wentink, Jr. and R.L. Kyhl, Phys. Rev. 75, 270, 1949.

12. J. Bardeen and C.H. Townes, Phys. Rev. 73, 97, 1948.

13. C.H. Townes, A.N. Holden and F.R. Merritt, Phys. Rev. 74, 1113, 1948.

14. G. Herzberg and L. Herzberg, J. Chem. Phys. 18, 1551, 1950.

15. A.G. Smith, H. Ring, W.V. Smith and W. Gordy, Phys. Rev. 74, 370, 1948.

16. A.G. Smith, H. Ring, W.V. Smith and W. Gordy, Phys. Rev. 73, 633(L), 1948.

SECTION II

none

SECTION III

17. C.H. Townes, American Scientist 40, 270, 1952.

18. ref. 1, p. 33, Eqn. (2-14), except that (Townes) $q_\ell = 2q_o$ (Nielsen).

19. G. Geschwind, G.R. Gunther-Mohr and C.H. Townes, Rev. Mod. Phys. 26, 444, 1954.

20. H.H. Nielsen, Phys. Rev. 78, 296(L), 1950.

21. G. Herzberg, "Infrared and Raman Spectra of Polyatomic Molecules", (D. Van Nostrand Co. Inc., New York, 1945), p. 371.

22. G. Herzberg, Rev. Mod. Phys. 14, 219, 1942.

23. ref. 21, p. 378, (A question is raised concerning ref. 24).

24. H.H. Nielsen and W. Schaffer, J. Chem. Phys. 11, 140, 1943.

25. H.H. Nielsen, Phys. Rev. 77, 130, 1950. (Nielsen uncovers an earlier error concerning the question raised in ref. 23).

26. E. Teller, Hand -und Jahrbuch d. Chem. Physik 9/II, 1934.

27. ref. 1, p. 33.

28. ref. 21, p. 215.

29. E. Fermi, Z. Physik 71, 250, 1931.

30. G. Herzberg, "Spectra of Diatomic Molecules", second edition, (D. Van Nostrand Co. Inc., New York, 1950) p. 13; p. 282.

31. Ta-You Wu, "Vibrational Spectra and Structure of Polyatomic Molecules", National University of Peking, Kun-Ming, China, 1939. p. 140.

32. ref. 21, Chapter II, section 5.

33. ref. 21, Equation (II-287), p. 211.

34. ref. 21, Equation (II-290), p. 216.

35. ref. 21, Equation (II-289), p. 215.

36. ref. 30, Equation (V-75), p. 282.

37. ref. 30, Equation (V-76), p. 283;
ref. 21, Equation (II-291), p. 216.

38. ref. 21, Equation (II-293), p. 216.

39. A. Adel and D.M. Dennison, Phys. Rev. 43, 716, 1933.

40. ref. 21, pp. 376-377.

41. ref. 1, p. 29.

42. ref. 21, p. 273.

43. ref. 31, p. 88.

44. ref. 21, Equation (II-296), p. 218.

45. ref. 5, Equation (5), except that we use α_{122} in the place of K_{122}. This may be seen from ref. 21, Equation (II-296), p. 218, for the special case $v_1 = 1$, $v_2 = 2$, $\ell = 0$. The use of α_{122} is retained in conformity with the usage in reference 21.

46. ref. 21, Table 56, p. 274.

47. A. Adel and D.M. Dennison, Phys. Rev. 43, 716, 1933.

48. A. Adel and D.M. Dennison, Phys. Rev. 44, 99, 1933.

49. a) E.B. Wilson, Jr. and A.J. Wells, Jour. Chem. Phys. 14, 578, 1946.
b) E.R. Nixon and P.C.Cross , Jour. Chem. Phys. 18, 1316, 1950.
c) W.O. Freitag and E.R. Nixon , Jour. Chem. Phys. 24, 109, 1956.

SECTION IV

50. R.H. Hughes and E.B. Wilson, Jr. Phys. Rev. 71, 526(L), 1947.

51. R. Karplus, Phys. Rev. 73, 1027, 1948.

52. W. Gordy, Rev. Mod. Phys. 20, 668, 1948.

53. R.R. Unterberger and W.V. Smith, Rev. Sci. Instr. 19, 550, 1948.

54. K.B. McAfee, Jr., R.H. Hughes and E.B. Wilson, Jr., Rev. Sci. Instr. 20, 821, 1949.

55. A.H. Sharbaugh, Rev. Sci. Instr. 21, 120, 1950.

56. ref. 2, Chapter I.

57. F. Butler, Wireless Engineer, pp 521-526, Nov. 1944.

58. G. Goldberg and E.L. Crosley, Jr., Proc. Nat. Elec. Conf. 3, 240, 1947.

59. The writer is indebted to Mr. Langdon C. Hedrick for bringing this idea to his attention.

60. W.E. Good, Westinghouse Research Laboratories, Scientific Paper No. 1538.

61. M.I.T. Radiation Laboratory Series, Vol. 11, "Technique of Microwave Measurements", McGraw-Hill Book Co. Inc., 1947, p. 502.

SECTION V

62. C.M. Johnson, R. Trambarulo and W. Gordy, Phys. Rev. 84, 1178, 1951.

63. W.C. King and W. Gordy, Phys. Rev. 93, 407, 1954.

64. C.H. Townes and S. Geschwind, Phys. Rev. 74, 626, 1948.

65. ref. 1, p. 24.

66. ref. 21, p. 501 and following.

67. H.J. Callomon, D.C. McKean and H.W. Thompson, Proc. Roy. Soc. (London), A208, 341, 1951.

68. E.B. Wilson, Jr., J.C. Decius and P.C. Cross, "Molecular Vibrations", (McGraw-Hill Book Co. Inc., 1955), p. 151.

69. ref. 1, p. 77.

70. P. Bartunek and E.F. Barker, Phys. Rev. 48, 516, 1935.

71. W. West and M. Farnsworth, Jour. Chem. Phys. 1, 402, 1933.

SECTION VI

72. W.E. Good, Phys. Rev. 70, 213, 1946.

73. H.B.G. Casimir, "On the Interaction Between Atomic Nuclei and Electrons", (De Erven F. Bohn, Haarlem, 1936).

74. J.H. Van Vleck, Phys. Rev. 71, 468, 1947.

75. ref. 1, Appendix I, p. 499.

76. ref. 1, p. 165 and following

77. G. Racah, Phys. Rev. 61, 186, 1942.
Phys. Rev. 62, 438, 1942.
Phys. Rev. 63, 367, 1943.

78. A. Simon, J.H. Vander Sluis, L.C. Biedenharn, "Tables of Racah Coefficients" (ORNL-1679-Special), 1954.
Oak Ridge National Laboratory, Oak Ridge, Tenn.

79. J. Bardeen and C.H. Townes, Phys. Rev. 73, 627; 1204, 1948.

80. ref. 1, Appendix II, p. 517.

81. H.E. White, "Introduction to Atomic Spectra", (McGraw-Hill Book Co. Inc., 1934), p. 441.

82. J.M. Hollander, I. Perlman and G.T. Seaborg, Rev. Mod. Phys. 25, 469, 1953.

83. C.A. Burrus and W. Gordy, Phys. Rev. 101, 599, 1956.

Upper Picture

Frequency Standard, left center

Klystron Power Supply, center

Microwave Components

Absorption Cell in long wooden box

Interpolation Receiver, with remote tuning rod

BC-221-AK Frequency Meter

Lower Picture

Gas Handling Systems

Square Wave Modulator, 100 Kc/s, extreme left

Remote Tuning Knob, (above modulator)

Double Beam Oscilloscope, extreme right

Figure 1 - General View of Microwave Spectroscope

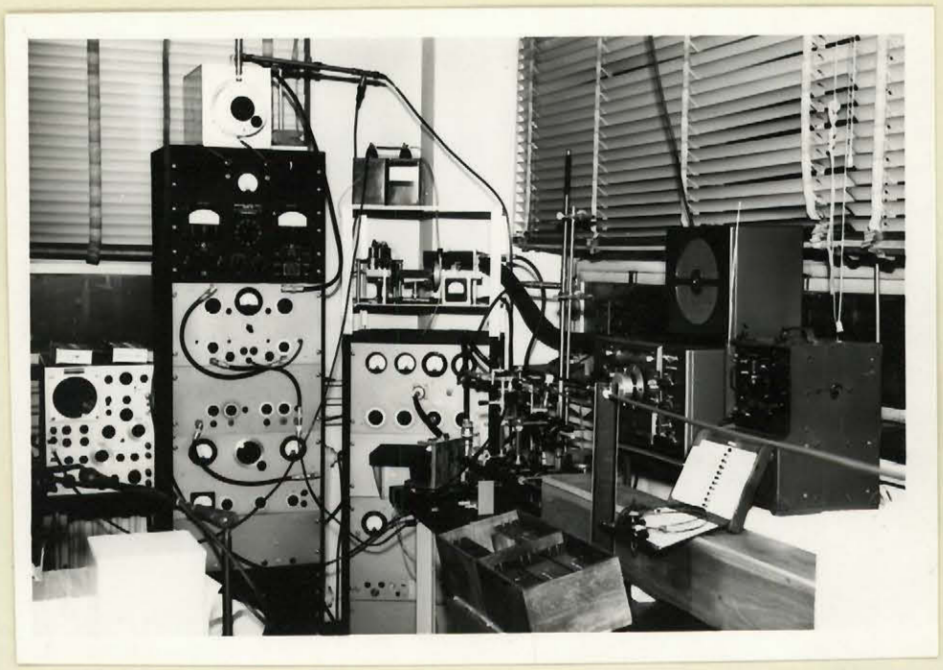

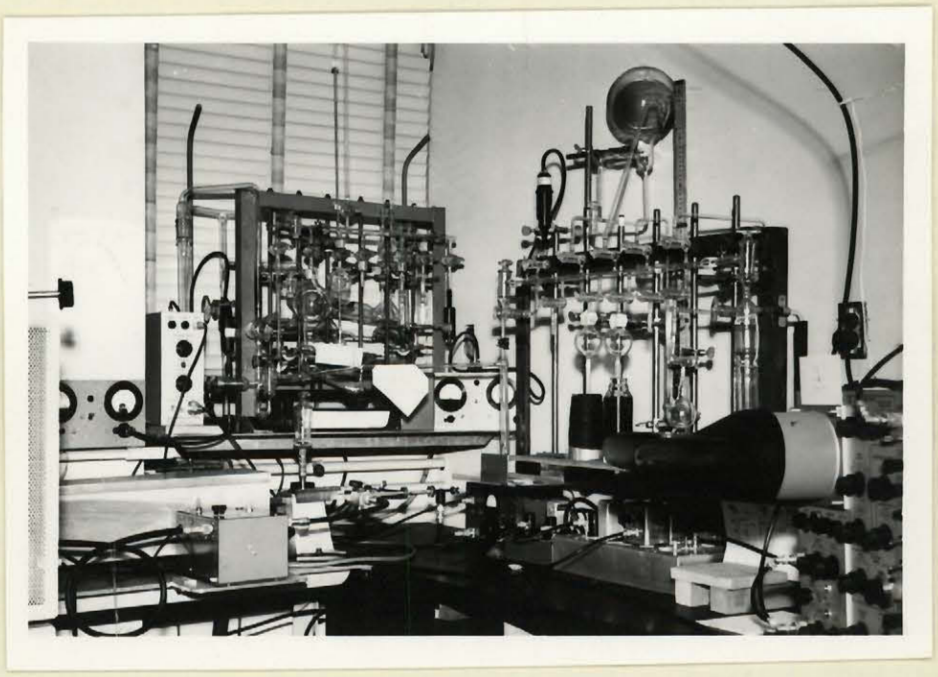

FIG. 1.

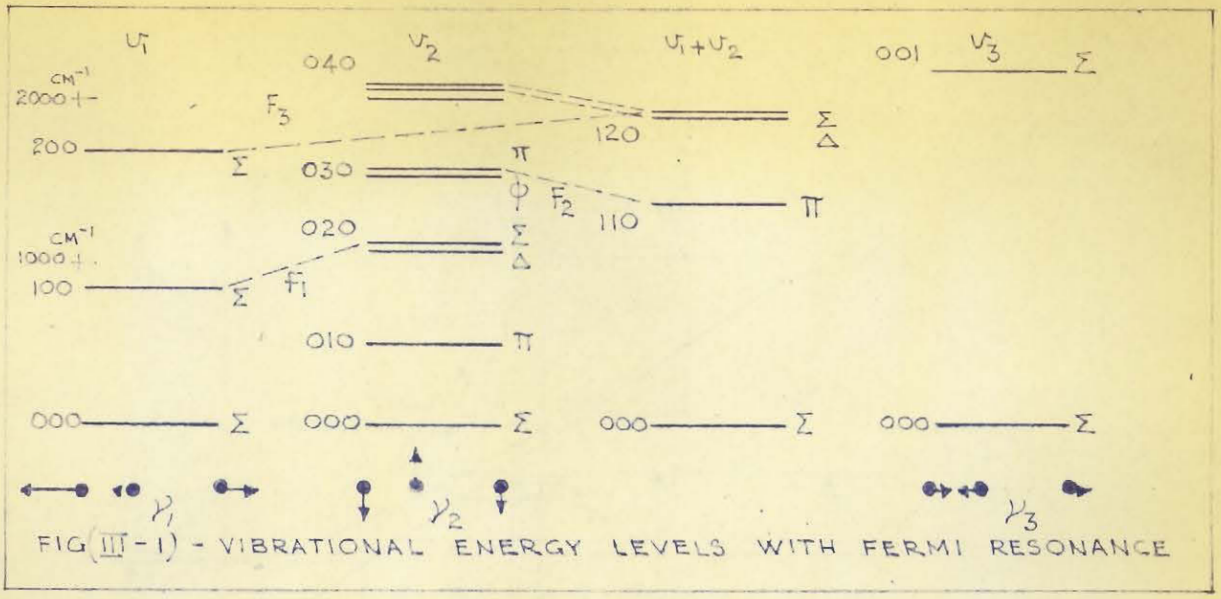

FIG (III-1) - VIBRATIONAL ENERGY LEVELS WITH FERMI RESONANCE

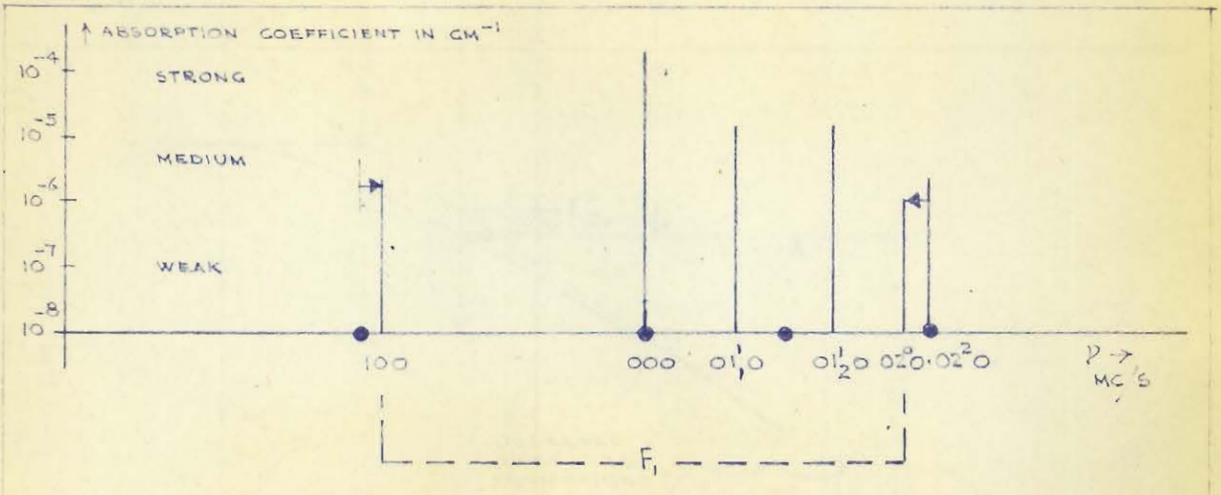

FIG (III-2) - FIRST FERMI RESONANCE, J = 3 ← 2 TRANSITION FOR SCO

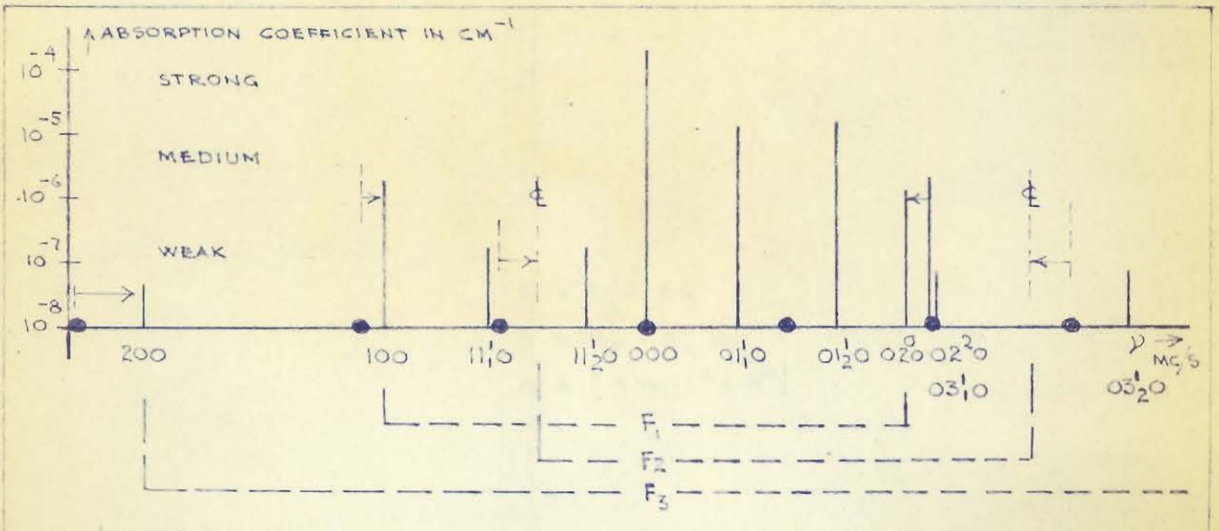

FIG (III-3) - FERMI RESONANCE, J = 3 ← 2 TRANSITION FOR SCO

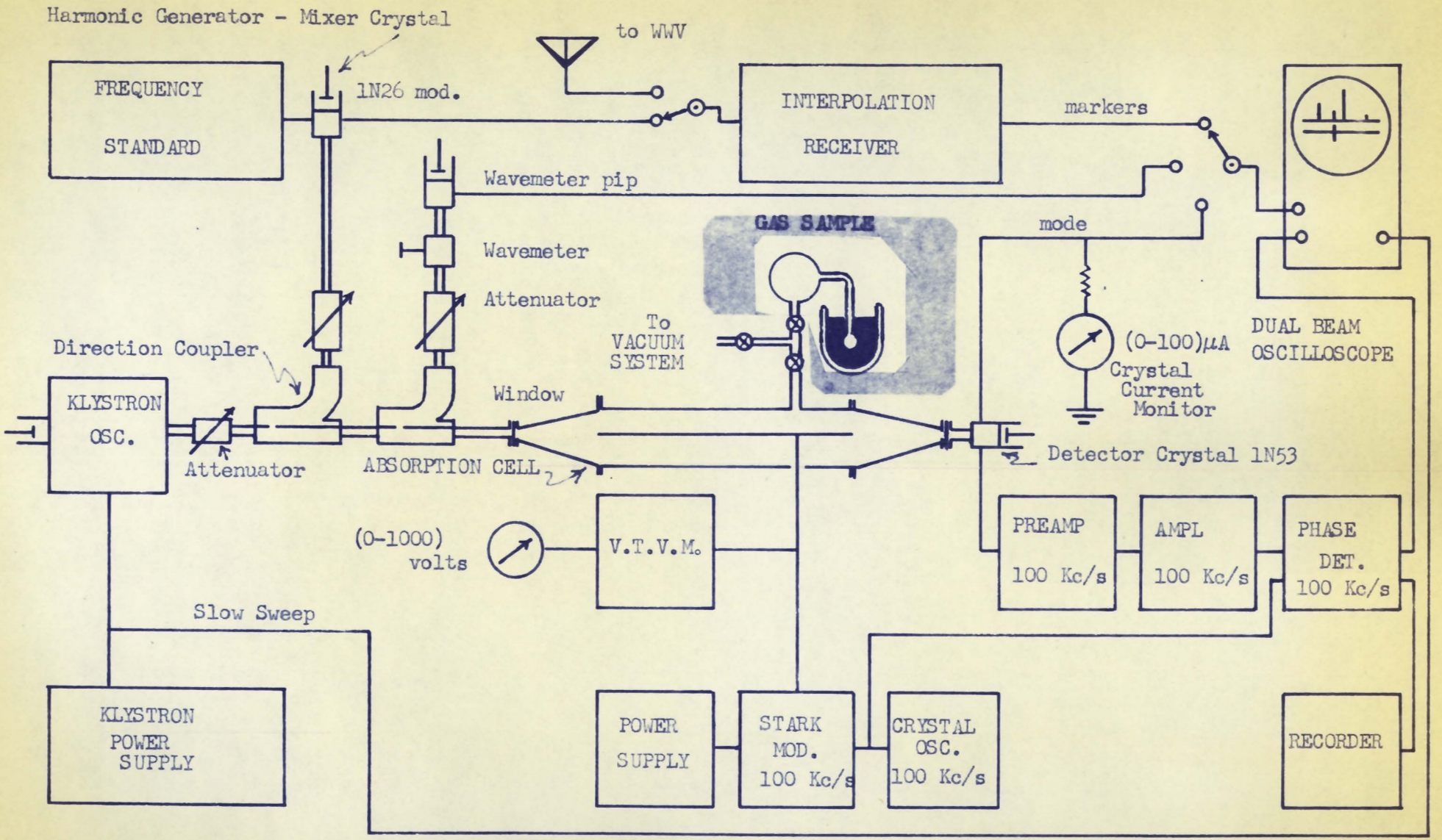

FIGURE (IV-1) - SCHEMATIC DIAGRAM STARK MODULATED MICROWAVE SPECTROSCOPE

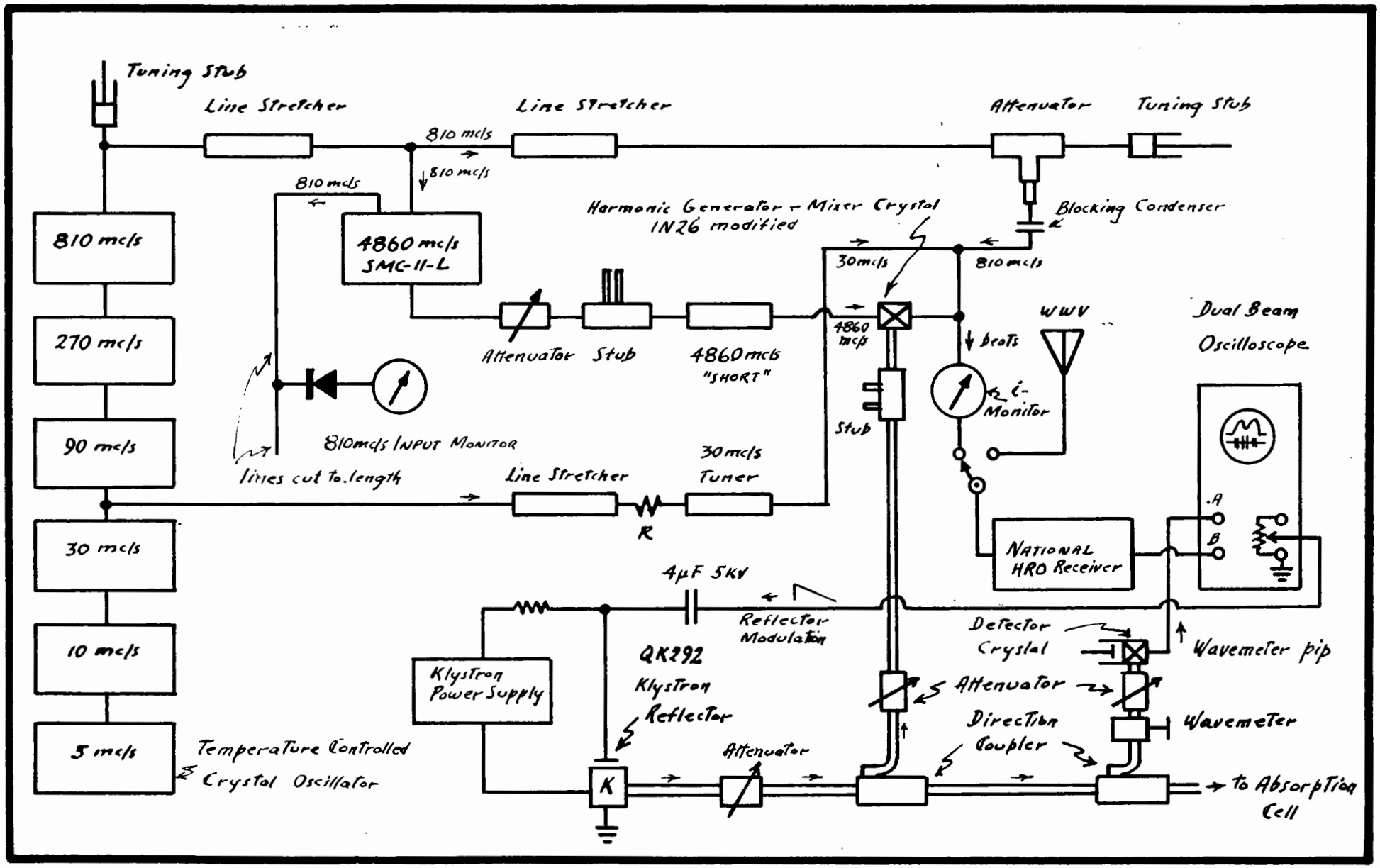

FIG. IV-2 : MICROWAVE FREQUENCY STANDARD - (33 - 40) Kmc/s. - block - diagram

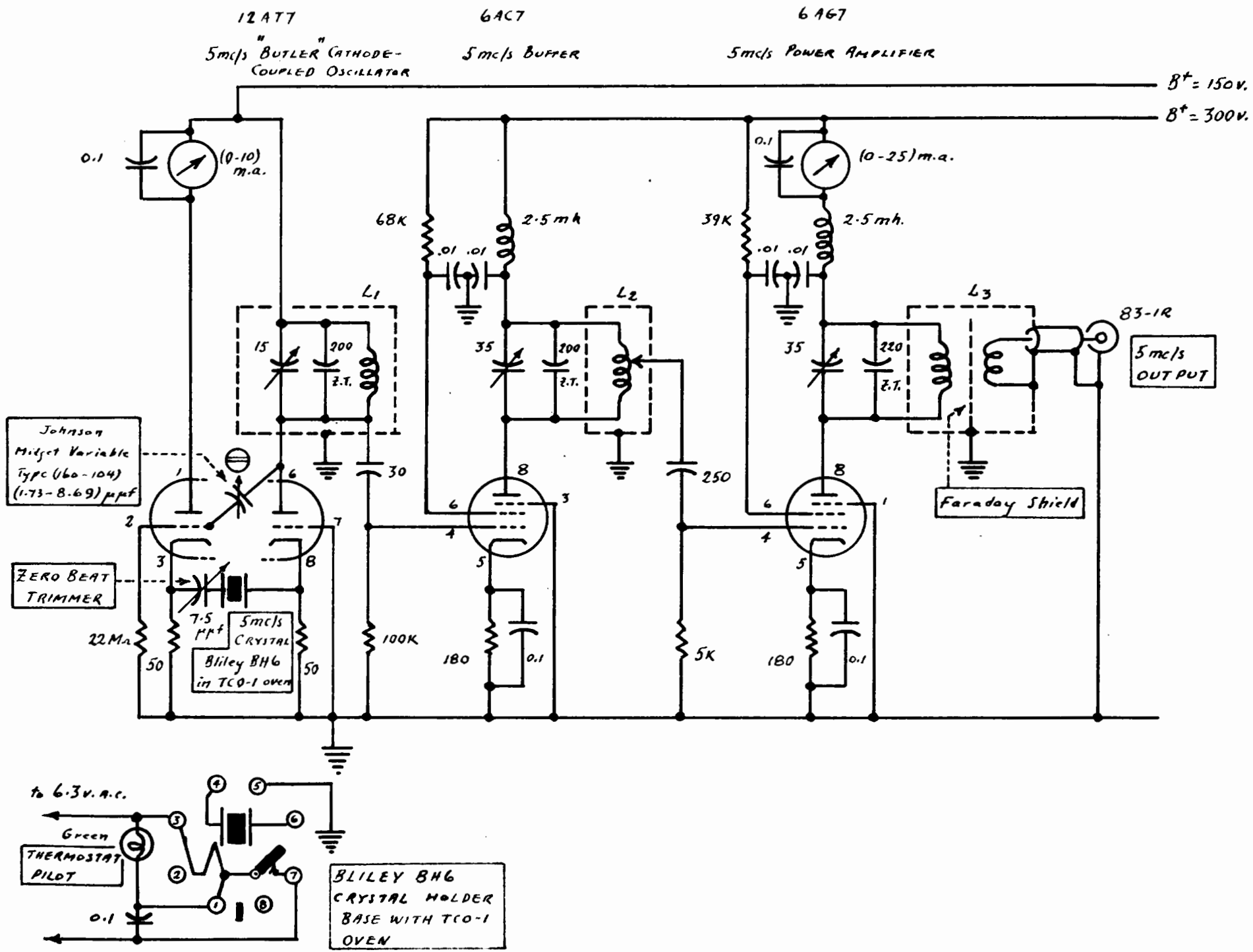

FIG. IV-3 : FREQUENCY STANDARD - 5mc/s Oscillator, Buffer, Power Amplifier

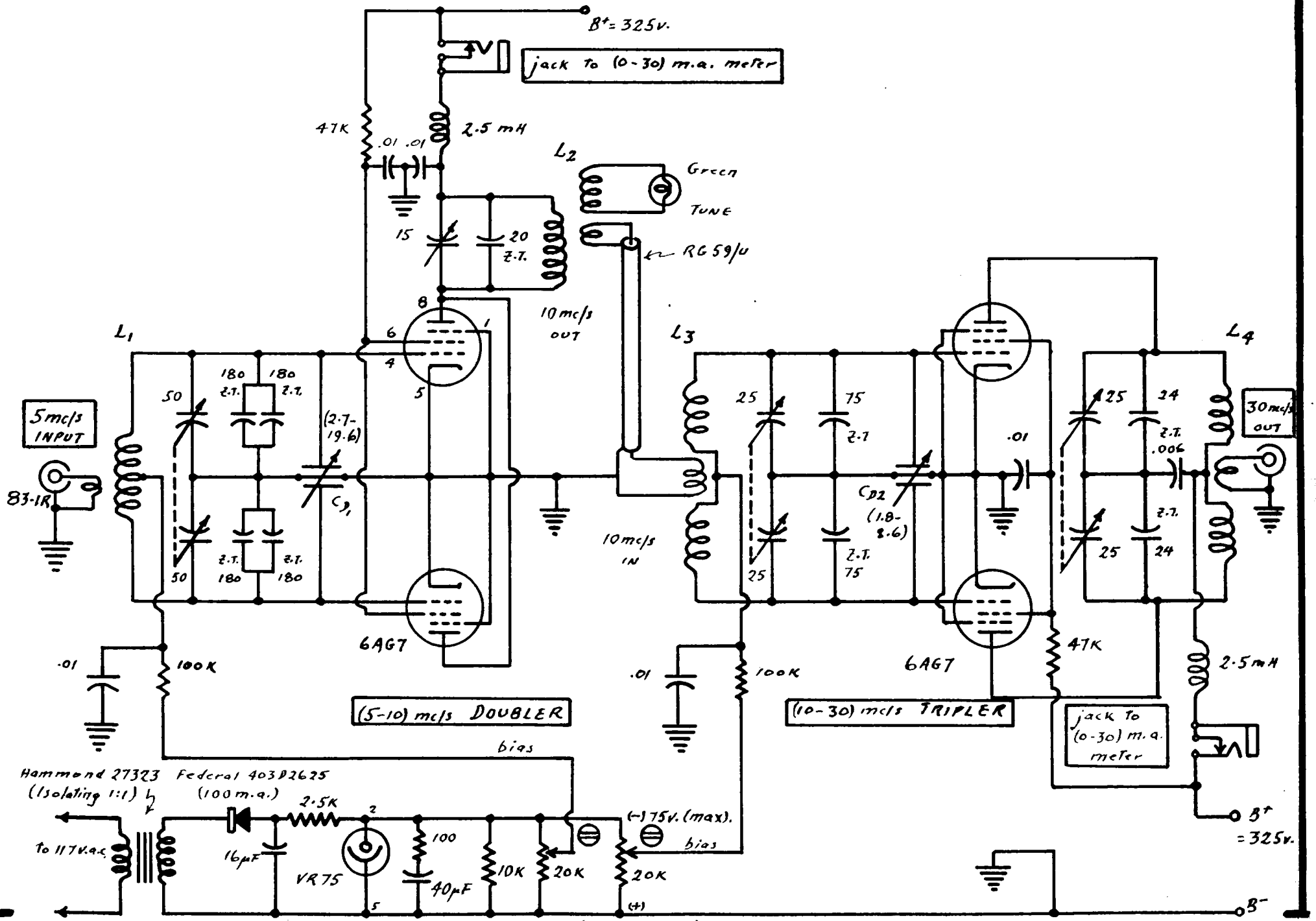

FIG. IV-4 : FREQUENCY STANDARD - (5-10-30) mc/s multipliers

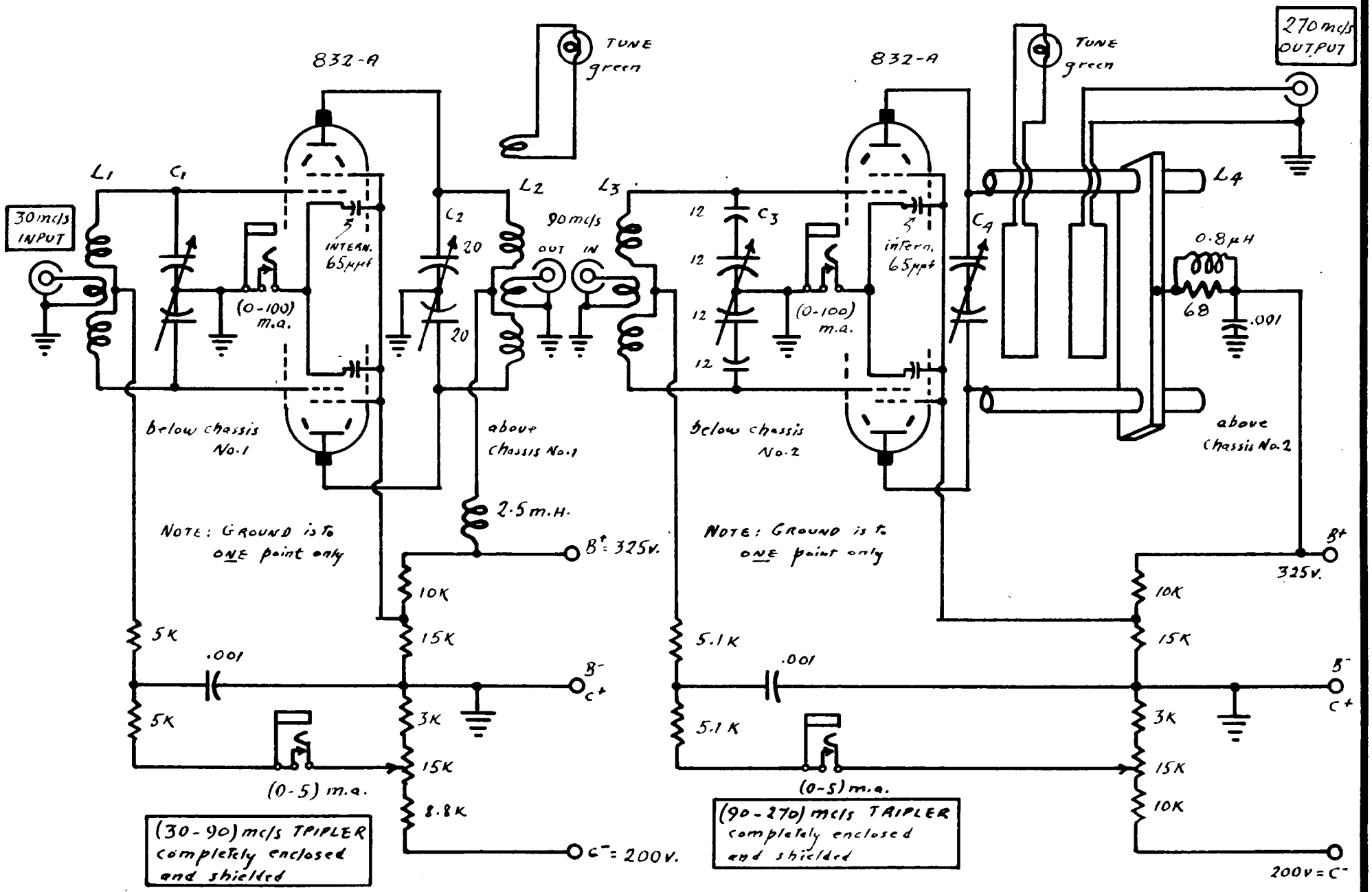

FIG. IV-5 : FREQUENCY STANDARD - (30-90-270) mc/s multipliers.

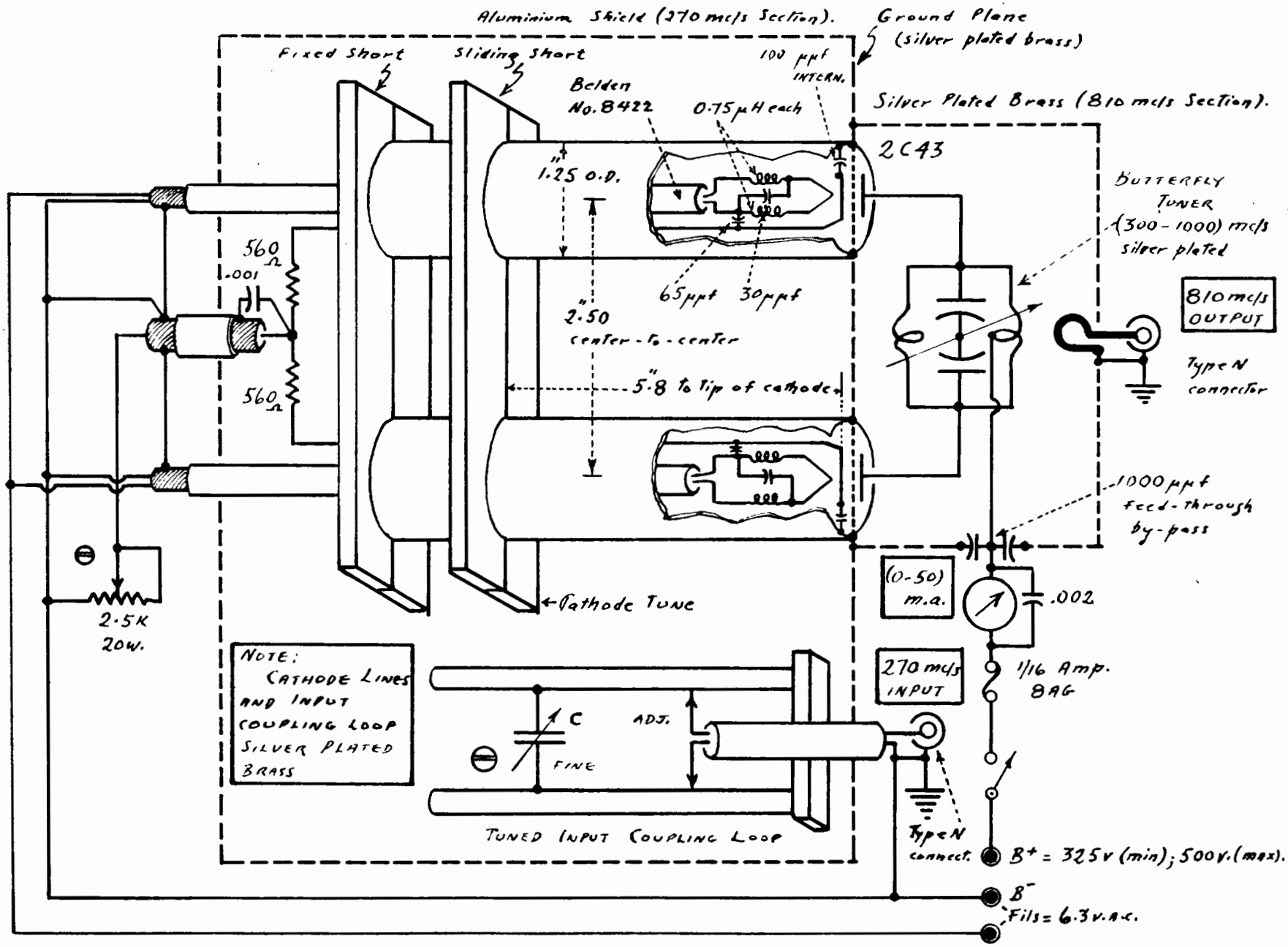

FIG. IV-6 : FREQUENCY STANDARD -(270 - 810) mc/s multiplier

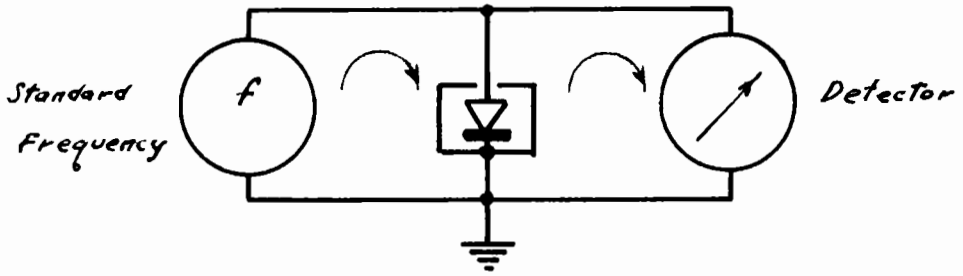

a) Principle of Harmonic Generation

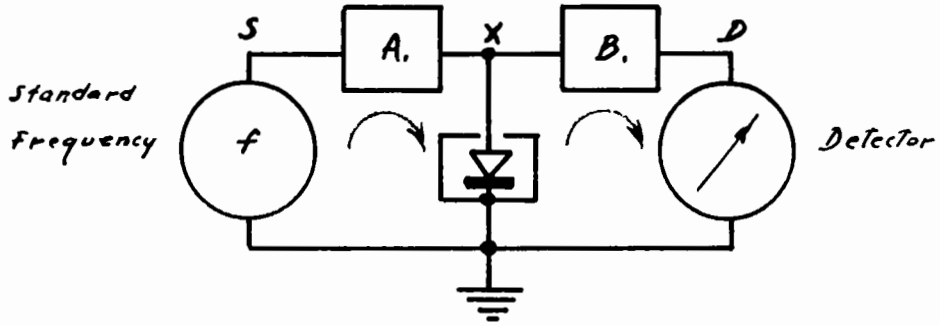

b) Practical Circuit - Single Exciter

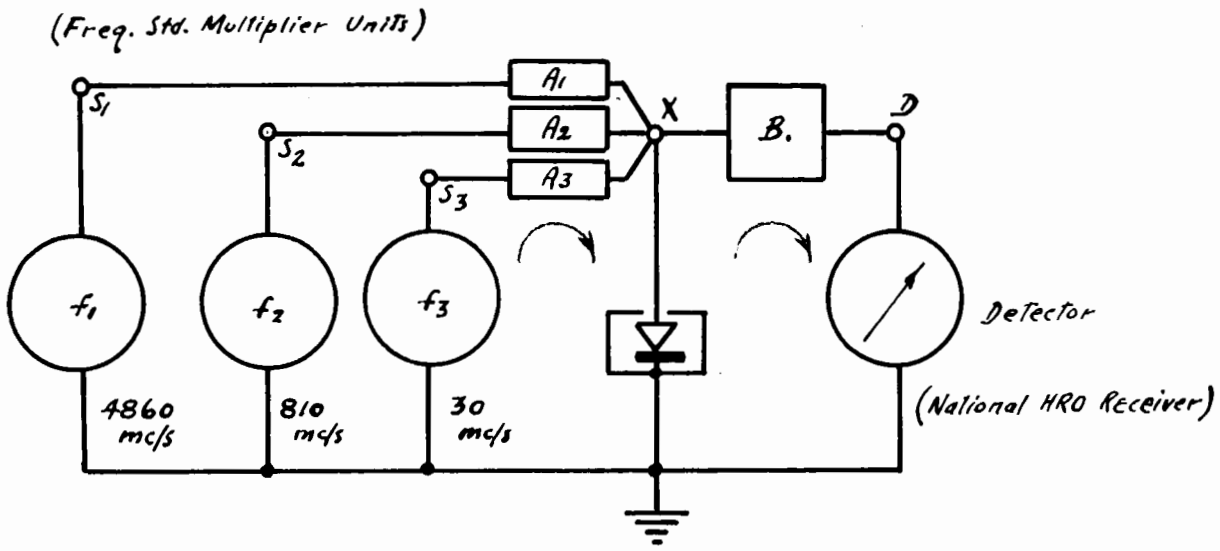

c) Practical Circuit - Several Exciters

FIG. IV-7 : Circuits for Generation of Harmonic Spectrum

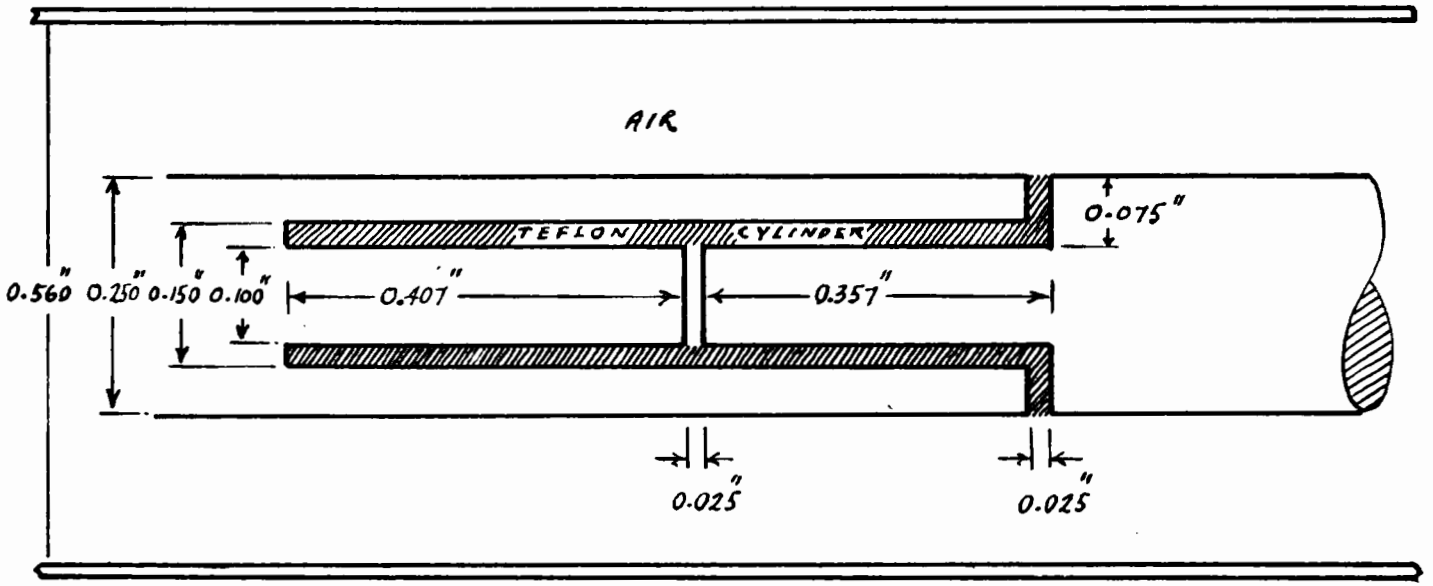

Outer Conductor : Silver-plated brass

Inner Conductor : Silver

Slot to be filled with press-fit TEFLON insert

$\frac{\lambda}{2}$ for 4860 mc/s (AIR) = 1.214"

(TEFLON) = $\frac{1.214}{\sqrt{2.1}}$ = 0.839" = median length of slot

$Z_0 = 138 \log_{10}\left(\frac{D}{d}\right)$ = 50 ohms (nominal)

FIG. IV-8 : 4860 mc/s Co-axial Line Series Resonant Circuit, ("short-circuit").

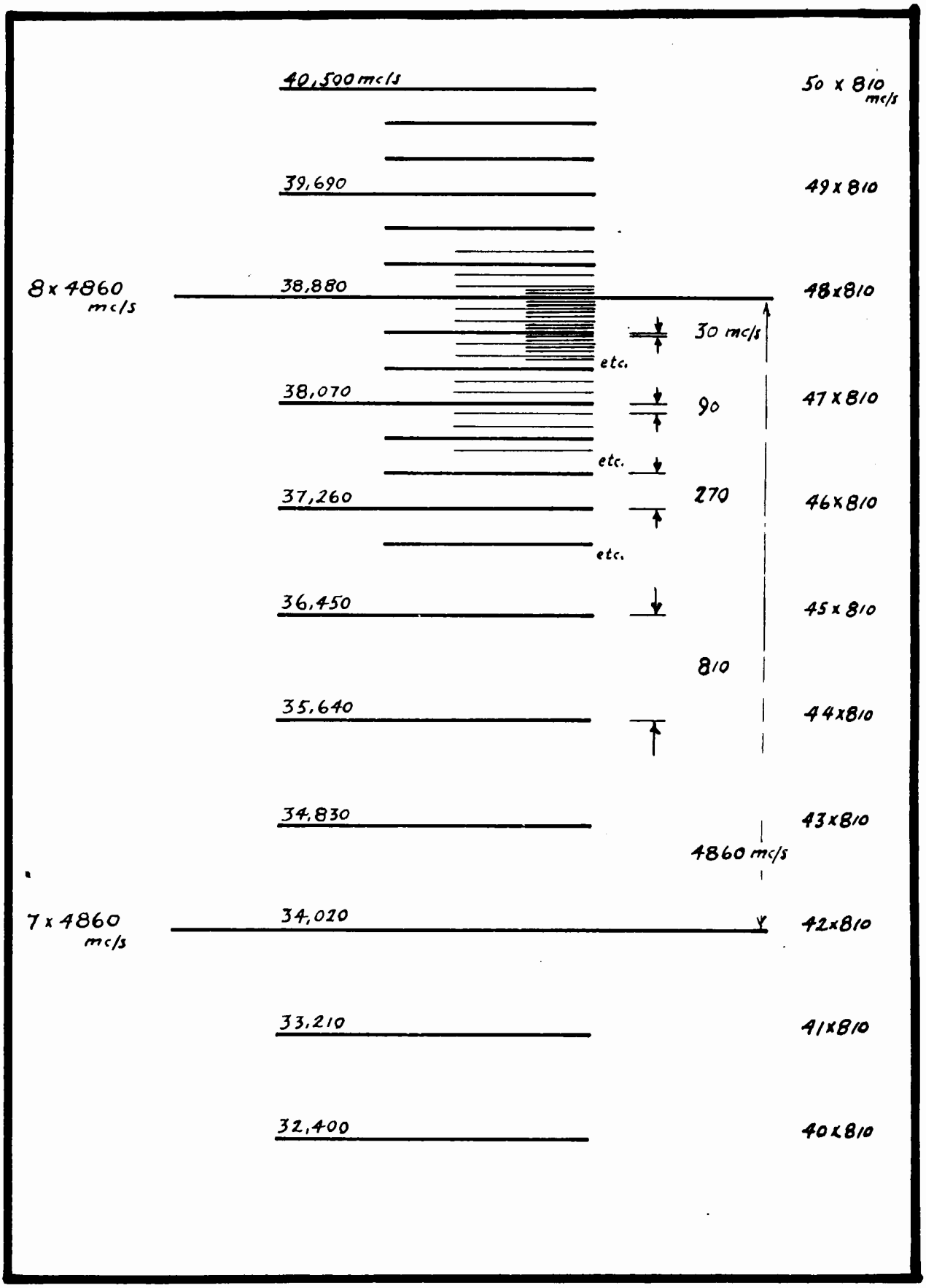

Fig. IV-9 : The Harmonic Spectrum

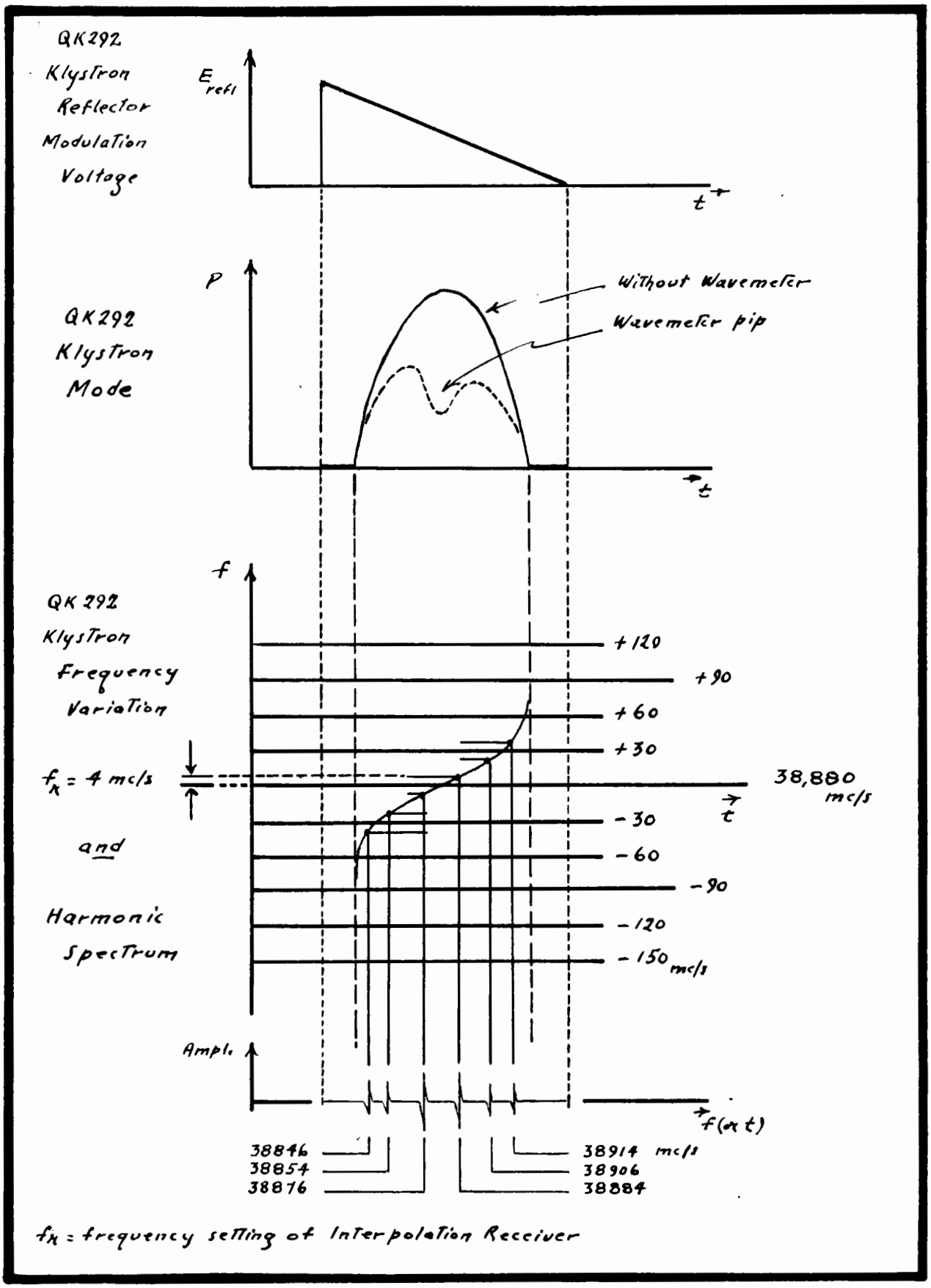

FIG. IV-10 : Generation of Frequency Markers from the Harmonic Spectrum

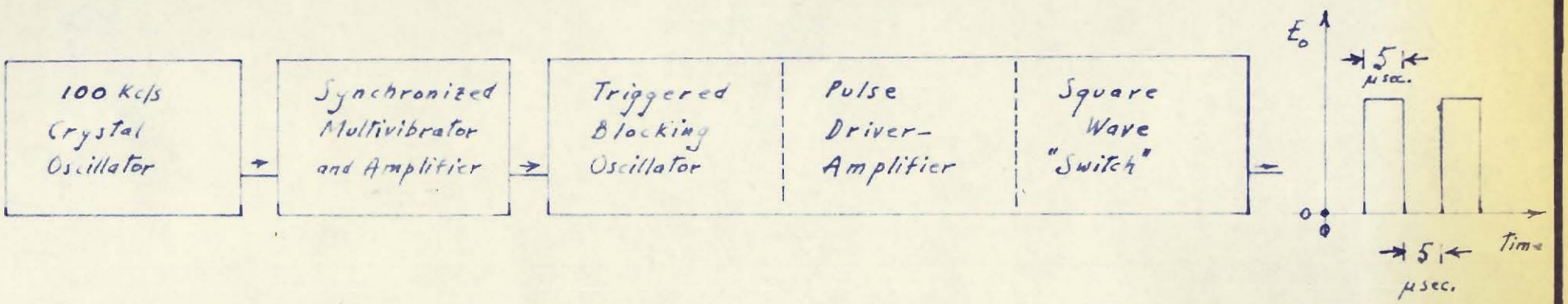

FIG. IV-11 : STARK CELL MODULATOR - block diagram

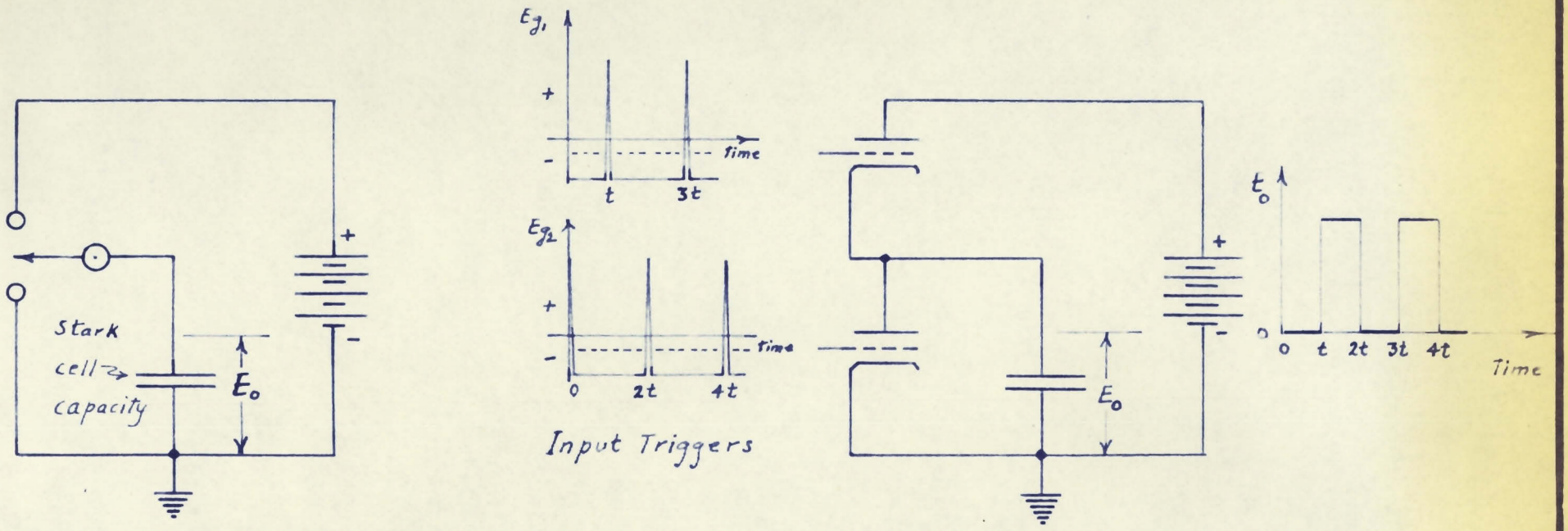

FIG. IV-12: STARK CELL MODULATOR - principle

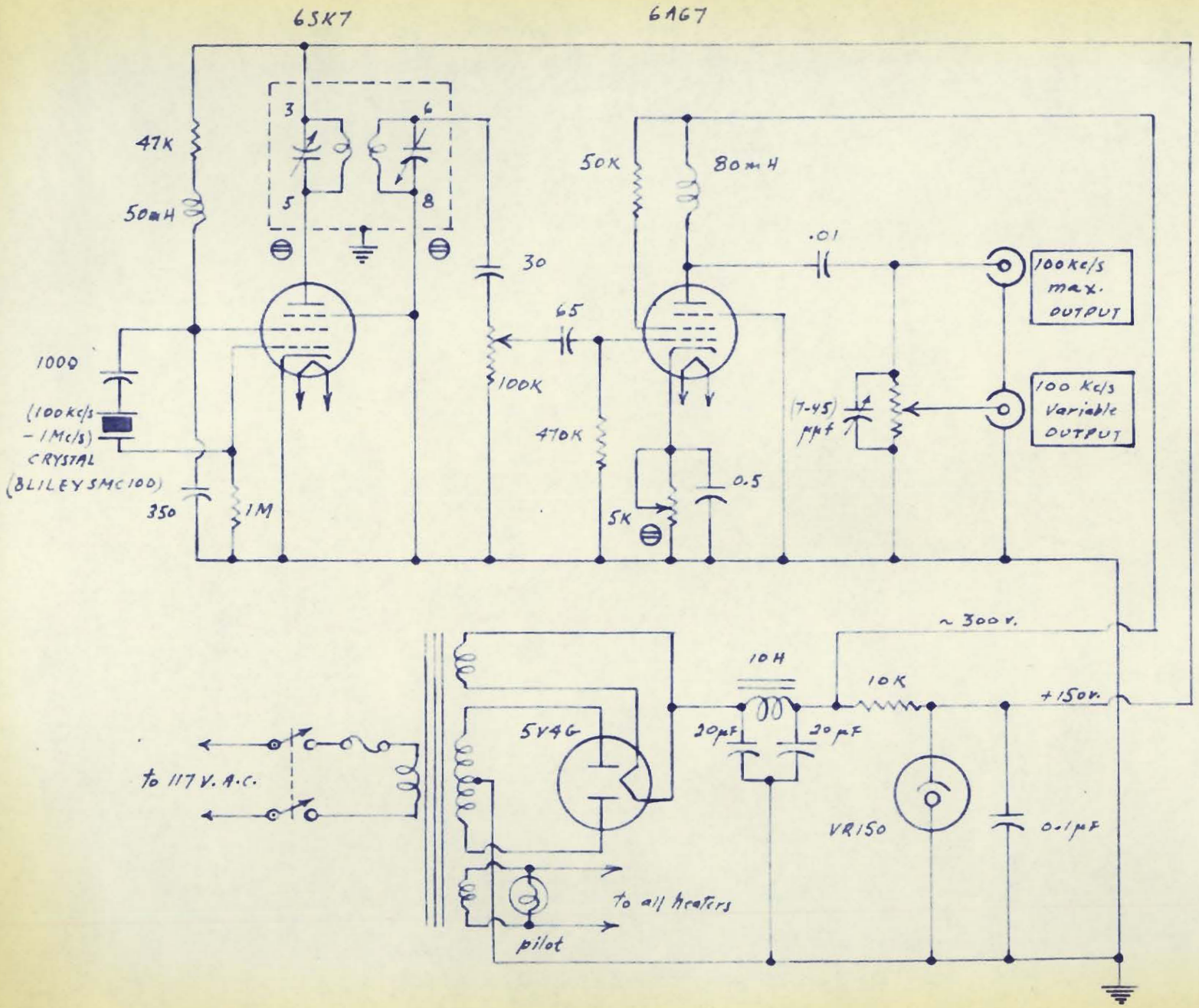

FIG. IV-13 : STARK CELL MODULATOR - 100 kc/s Crystal Oscillator

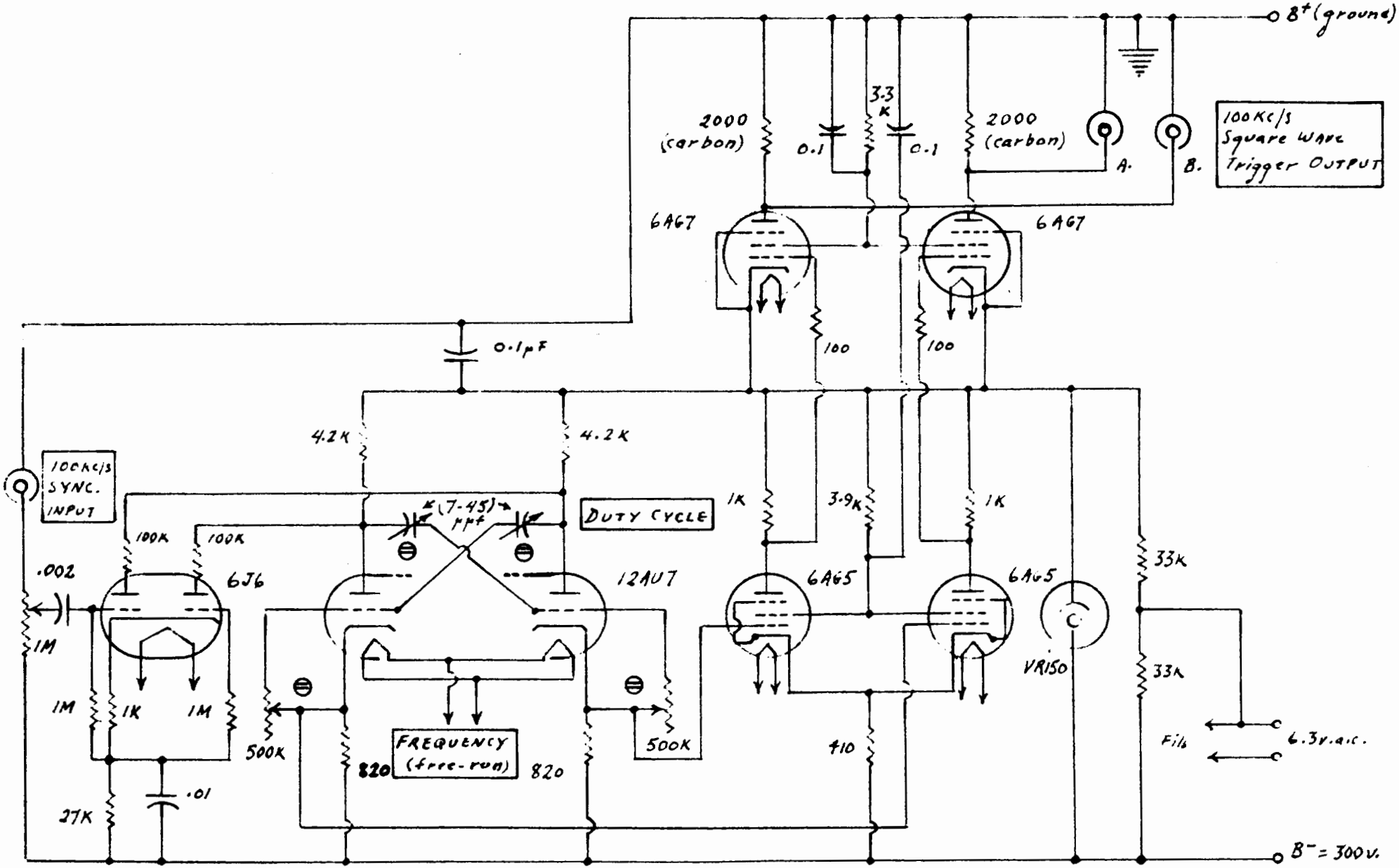

FIG. IV-14: STARK CELL MODULATOR - 100 kc/s Synchronized Multivibrator and Amplifiers

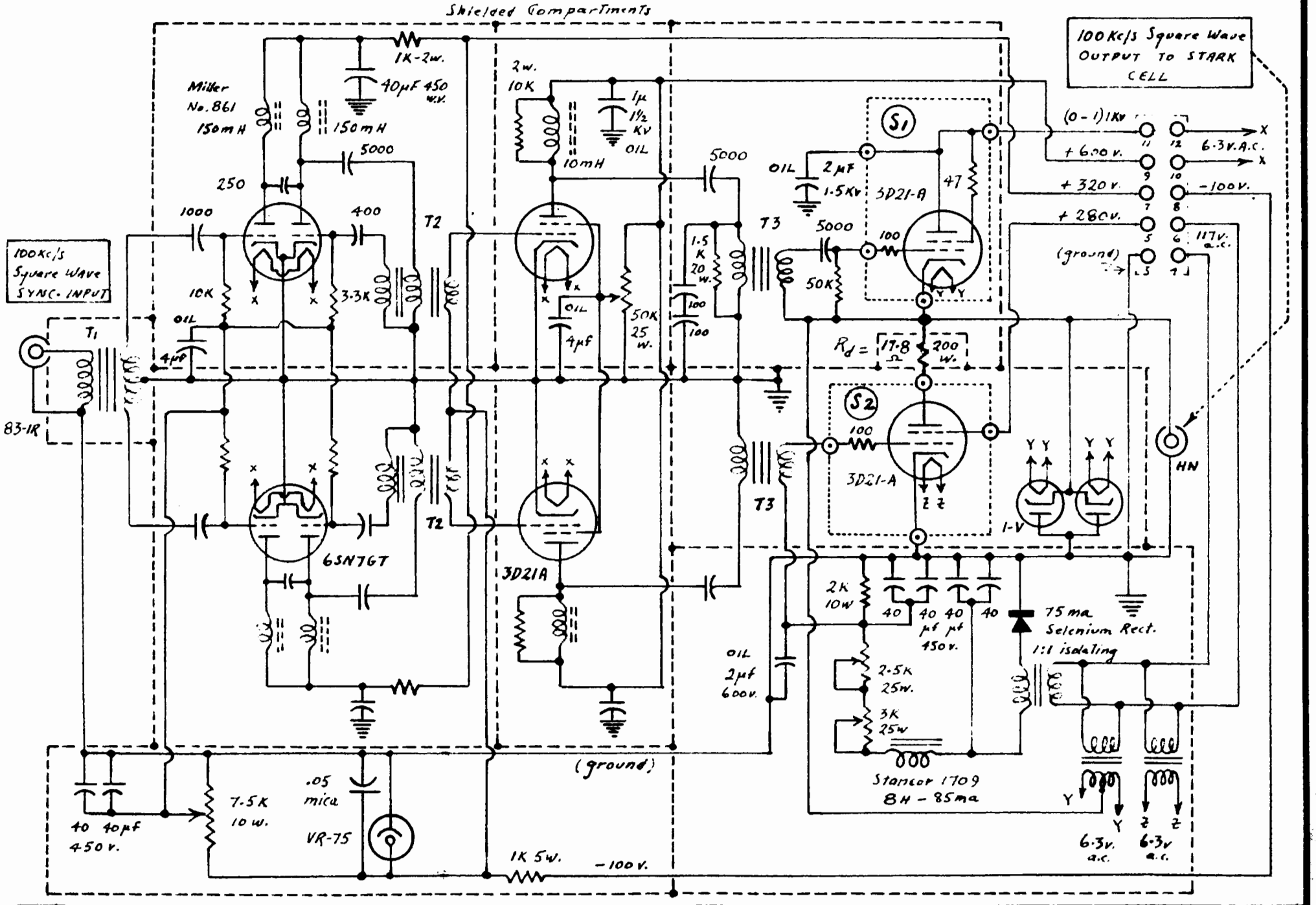

Fig. IV-15 : STARK CELL MODULATOR - 100 kc/s Blocking Oscillators, Pulse-Drivers and Square-Wave "Switch"

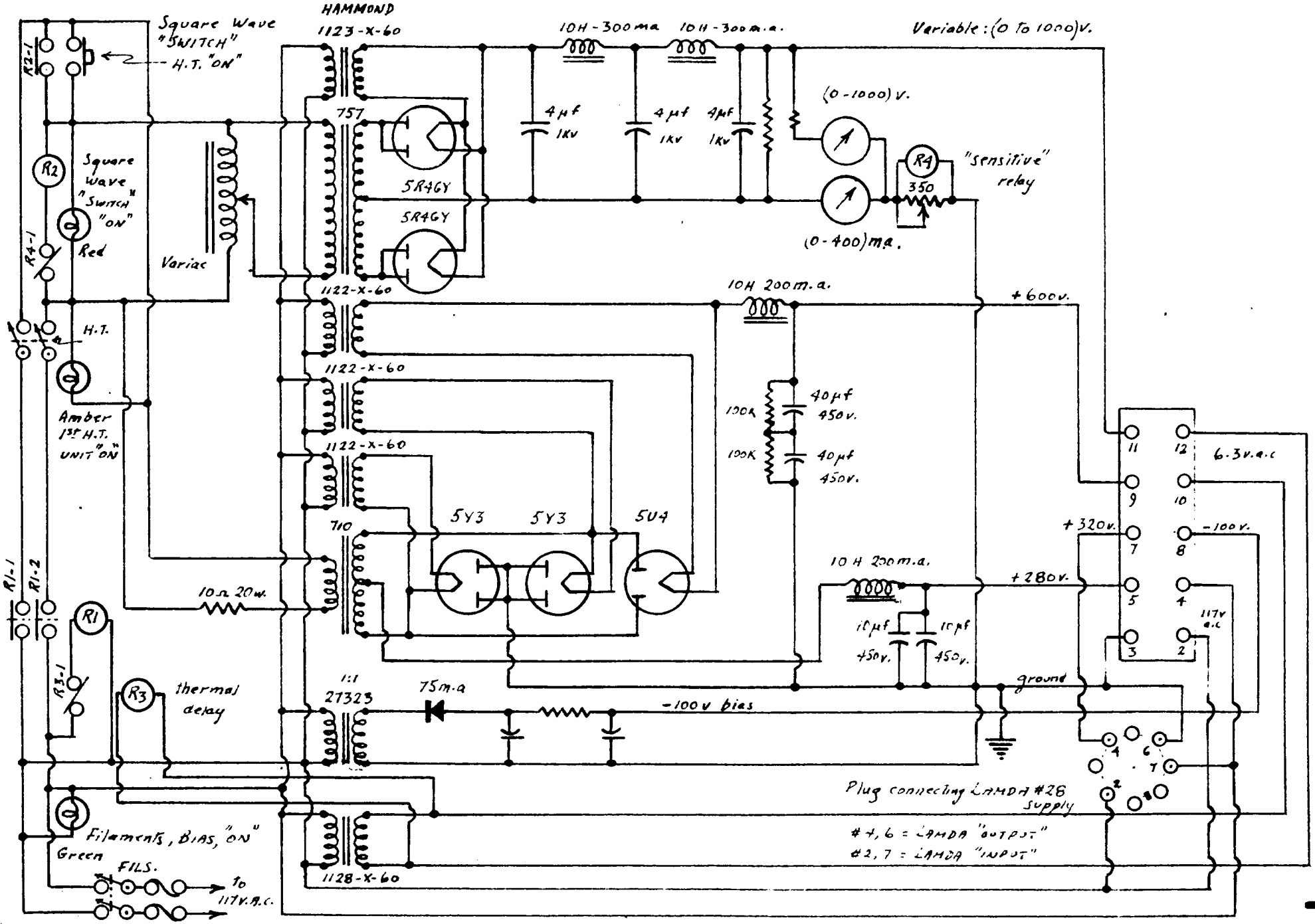

FIG. IV-16 : STARK CELL MODULATOR - power supply

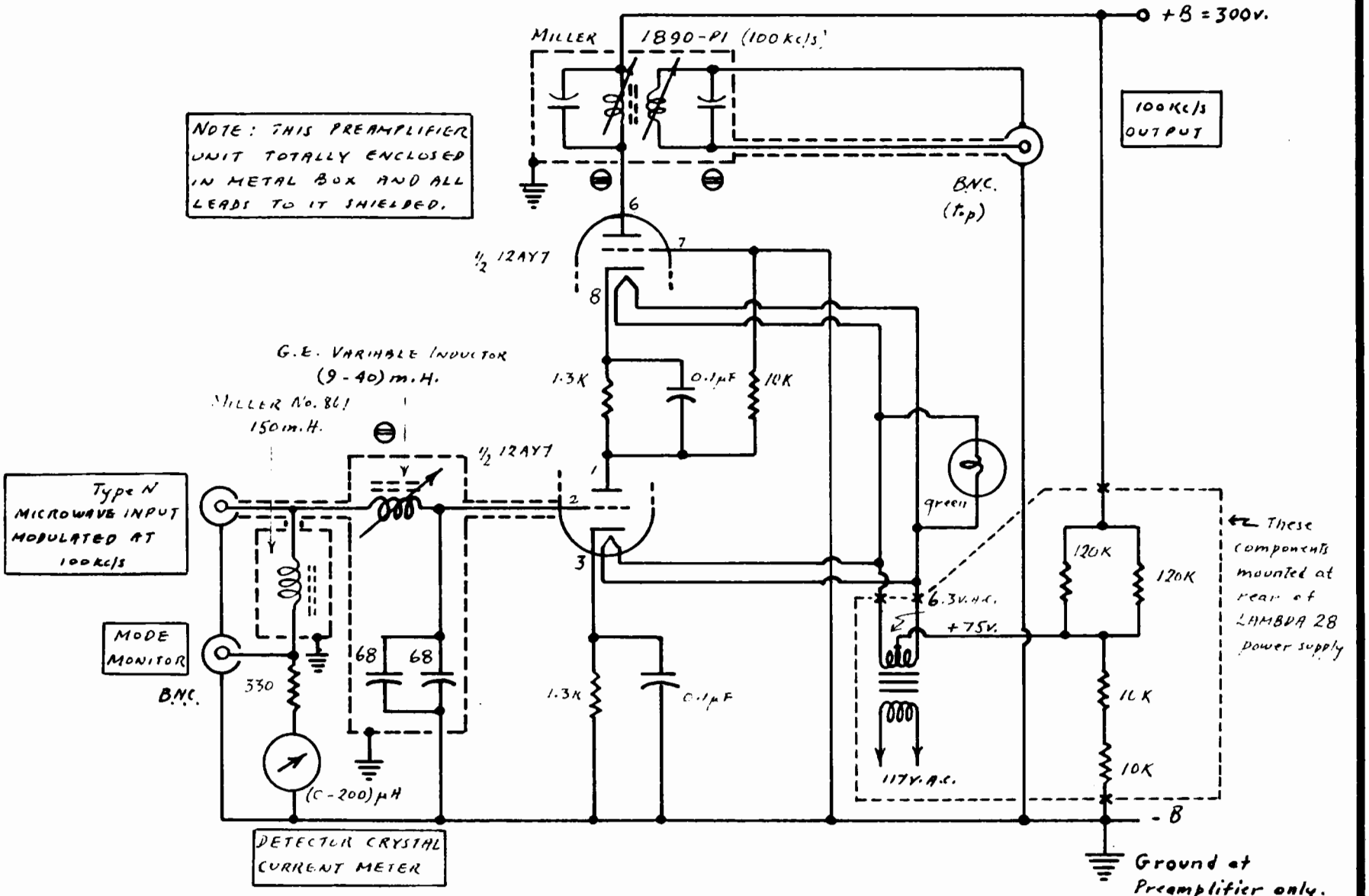

FIG. IV-17: MICROWAVE DETECTOR - 100 Kc/s Cascode Preamplifier

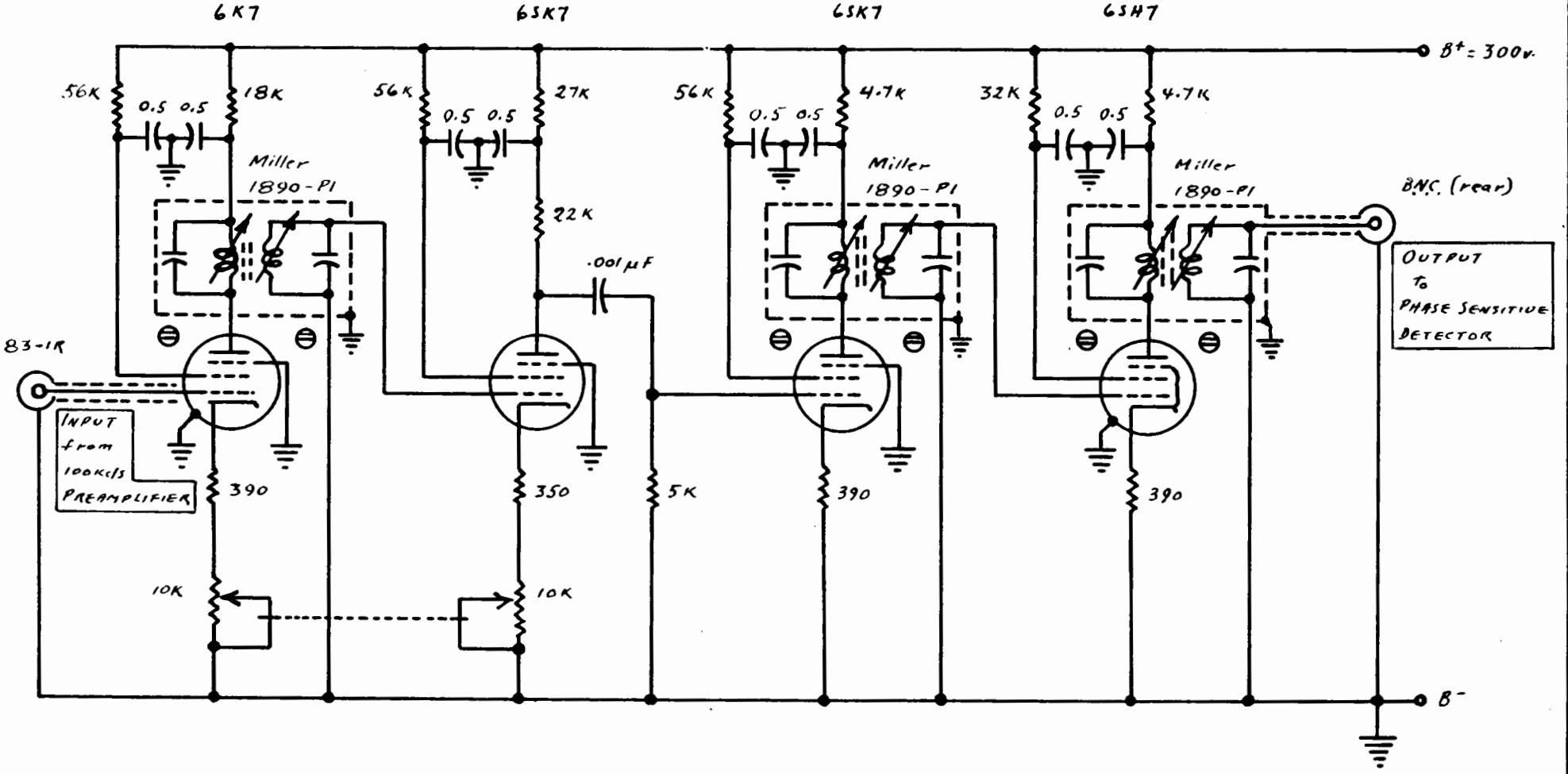

Fig. IV-18 : MICROWAVE DETECTOR - 100 Kc/s Tuned Amplifier

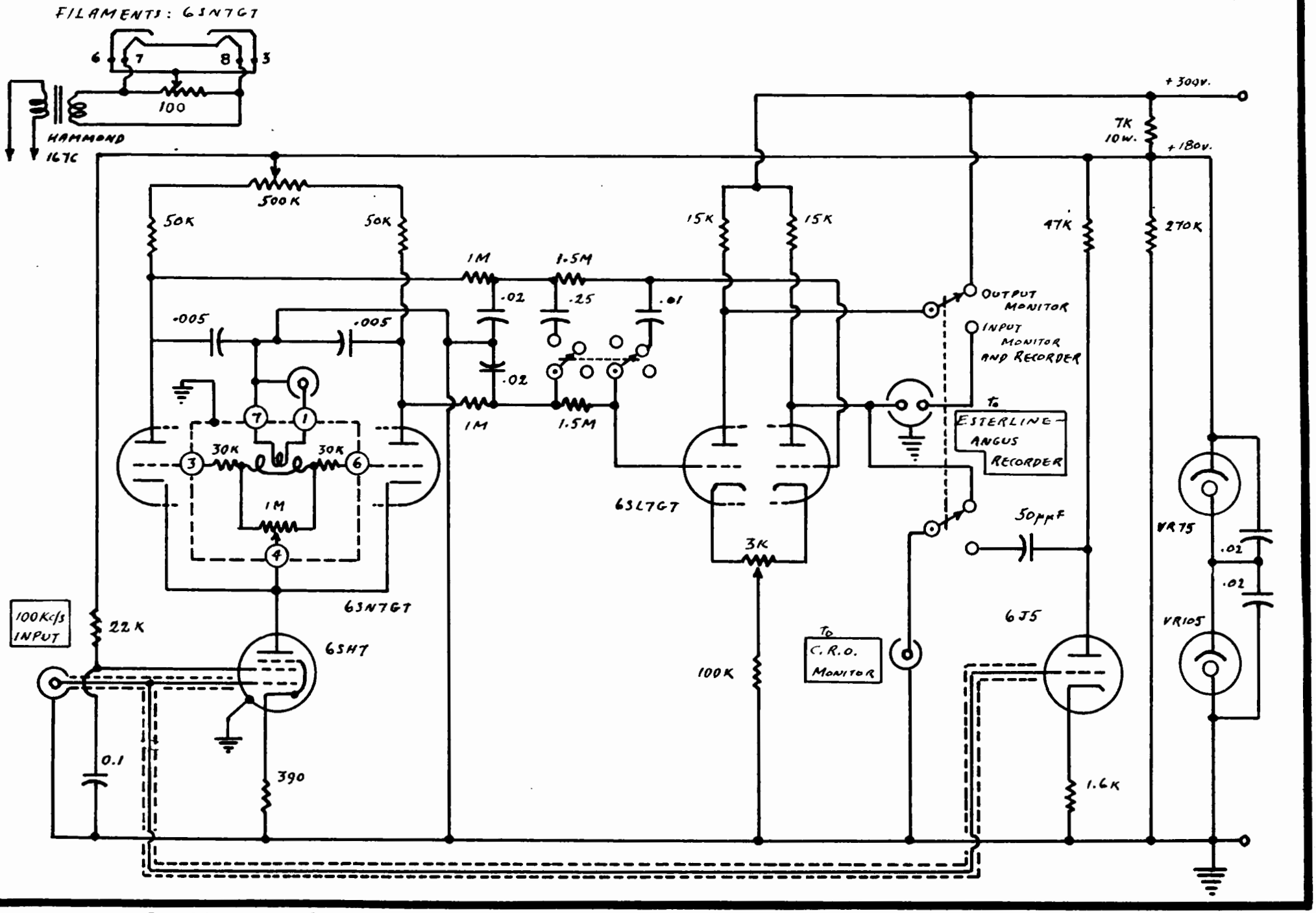

FIG. IV-19 : MICROWAVE DETECTOR - 100 kc/s Phase Sensitive Detector

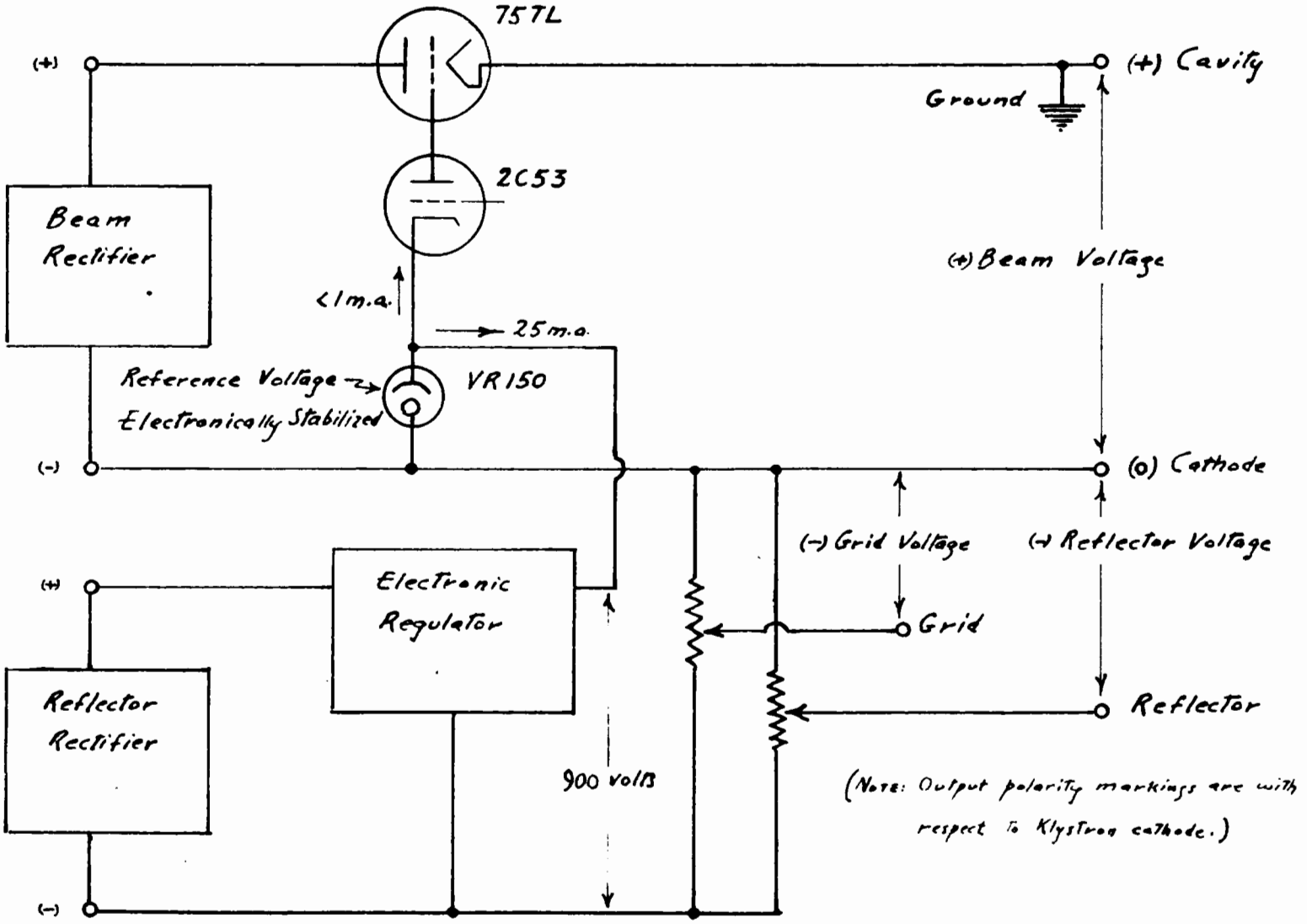

Fig. IV-20 = KLYSTRON POWER SUPPLY - principle, (the beam-regulator)

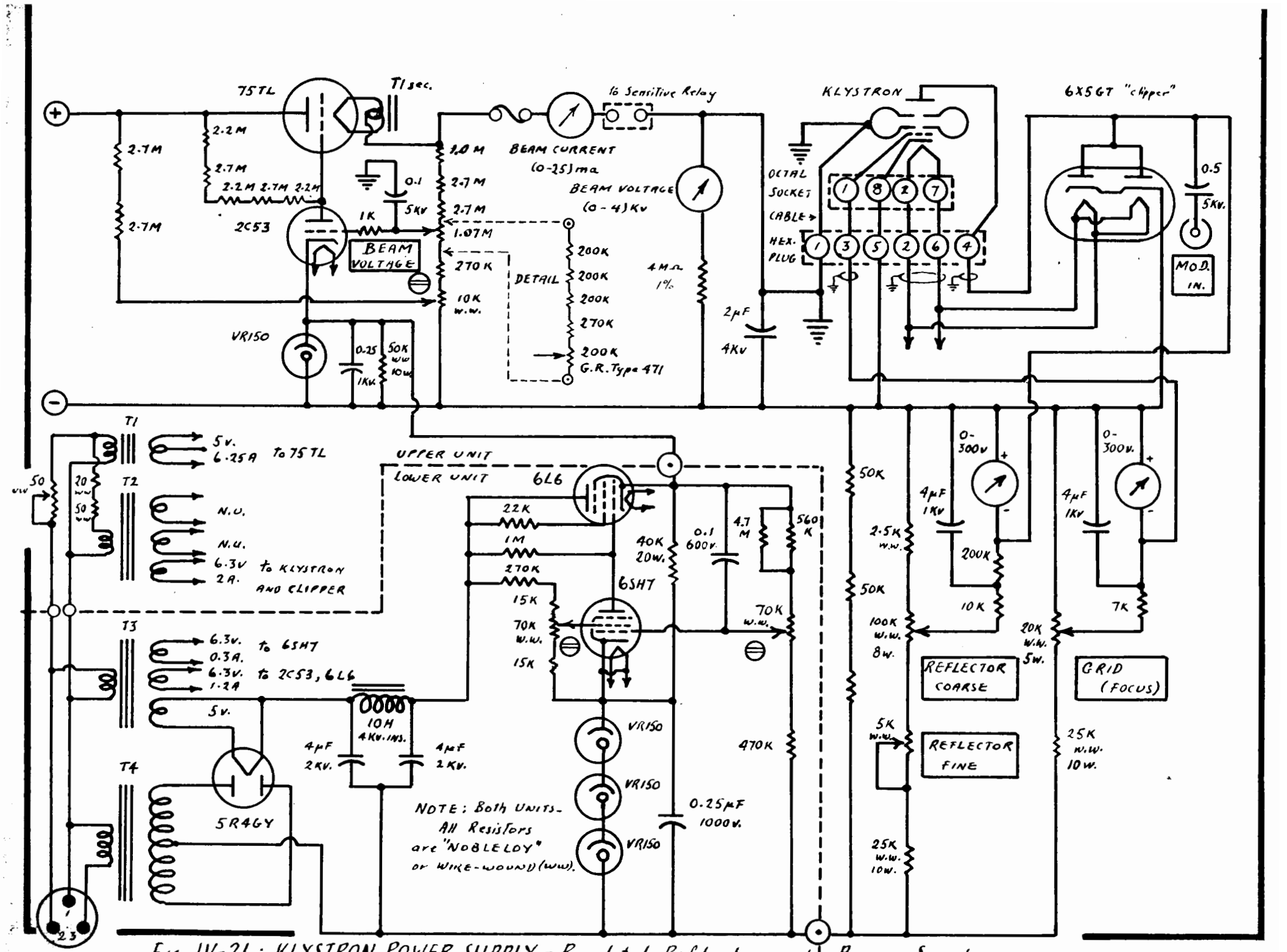

FIG. IV-21 : KLYSTRON POWER SUPPLY - Regulated Reflector and Beam Supply

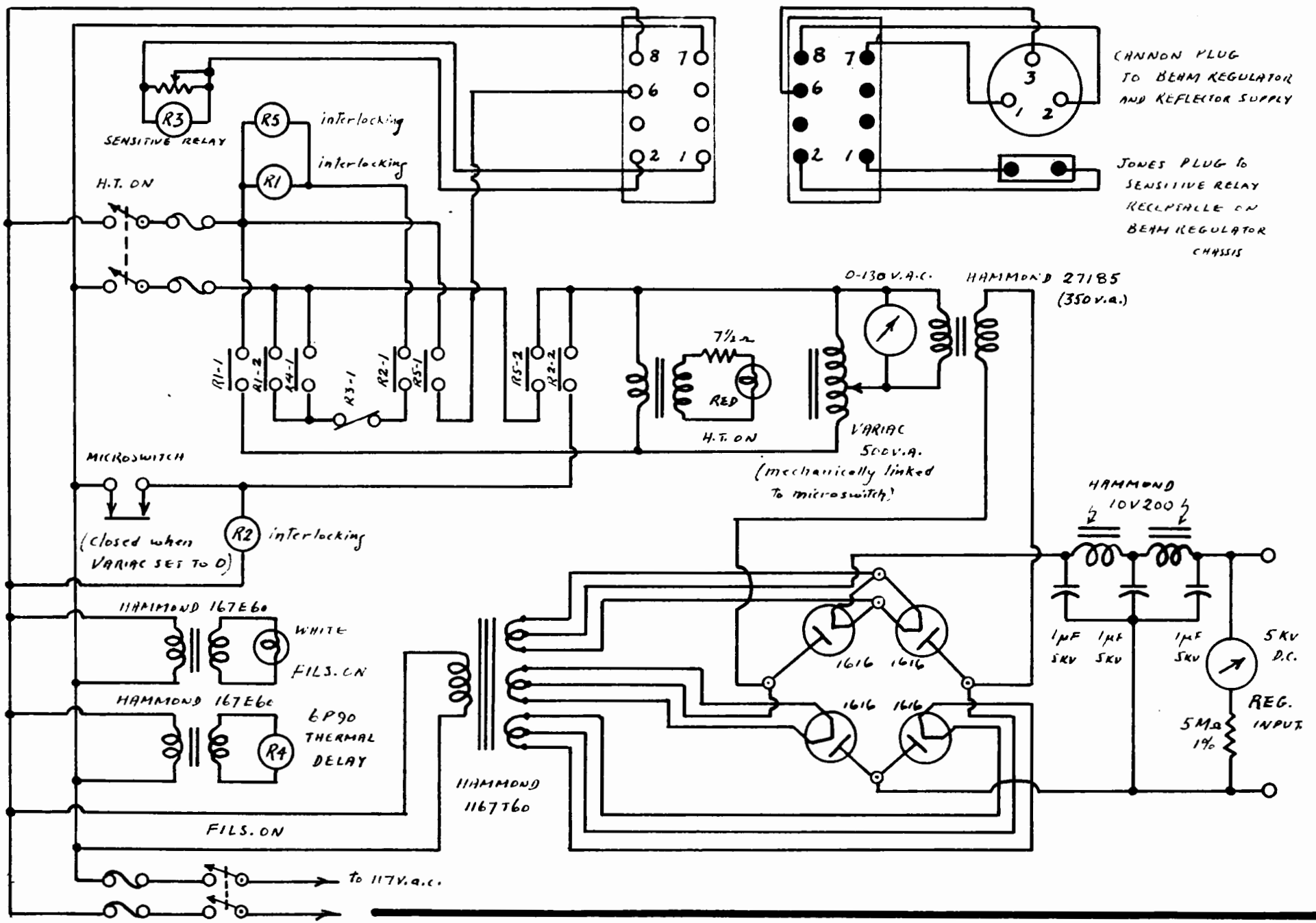

FIG. IV-22 : KLYSTRON POWER SUPPLY - Unregulated Beam Supply

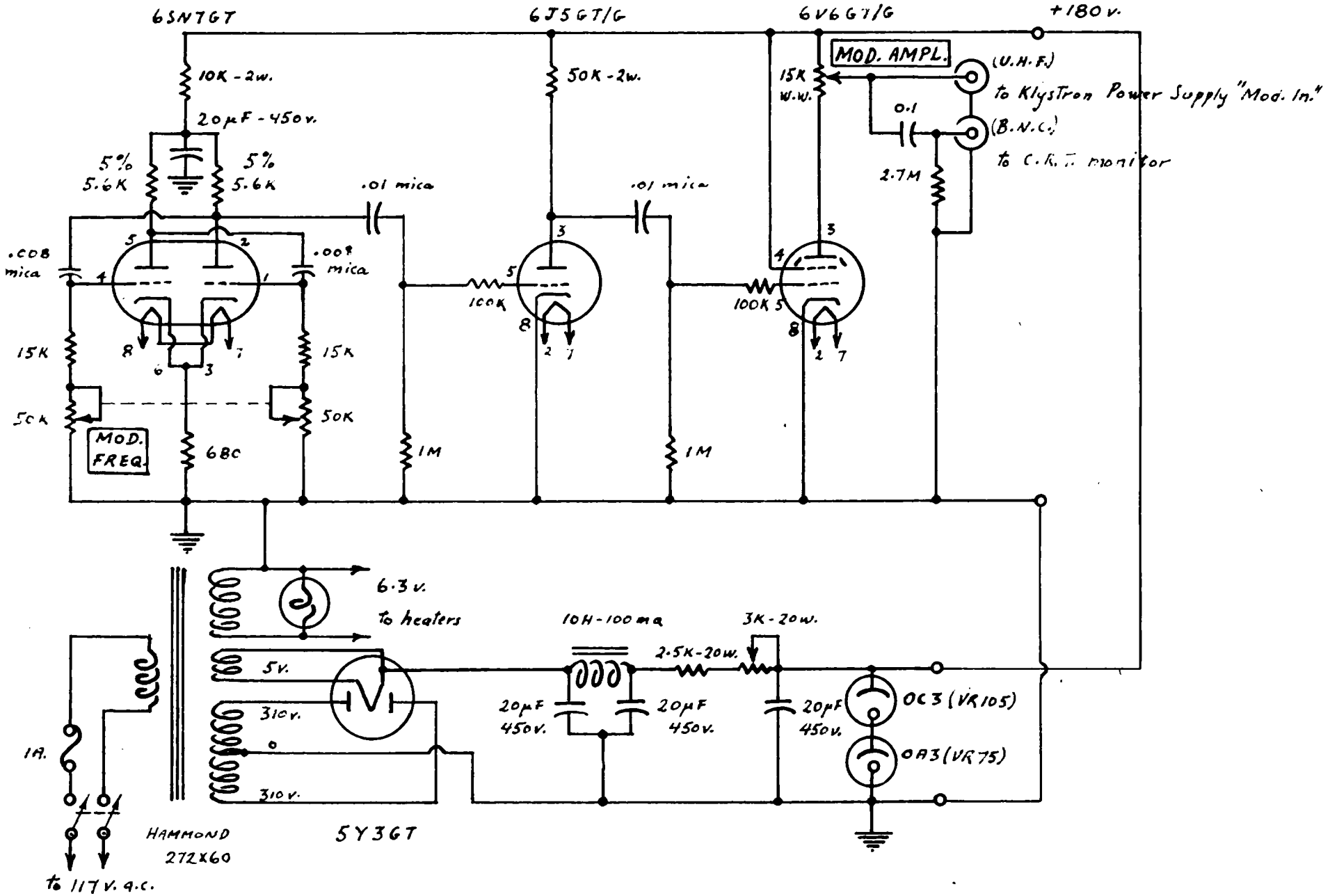

Fig. IV-23 : V.S.W.R. Modulator

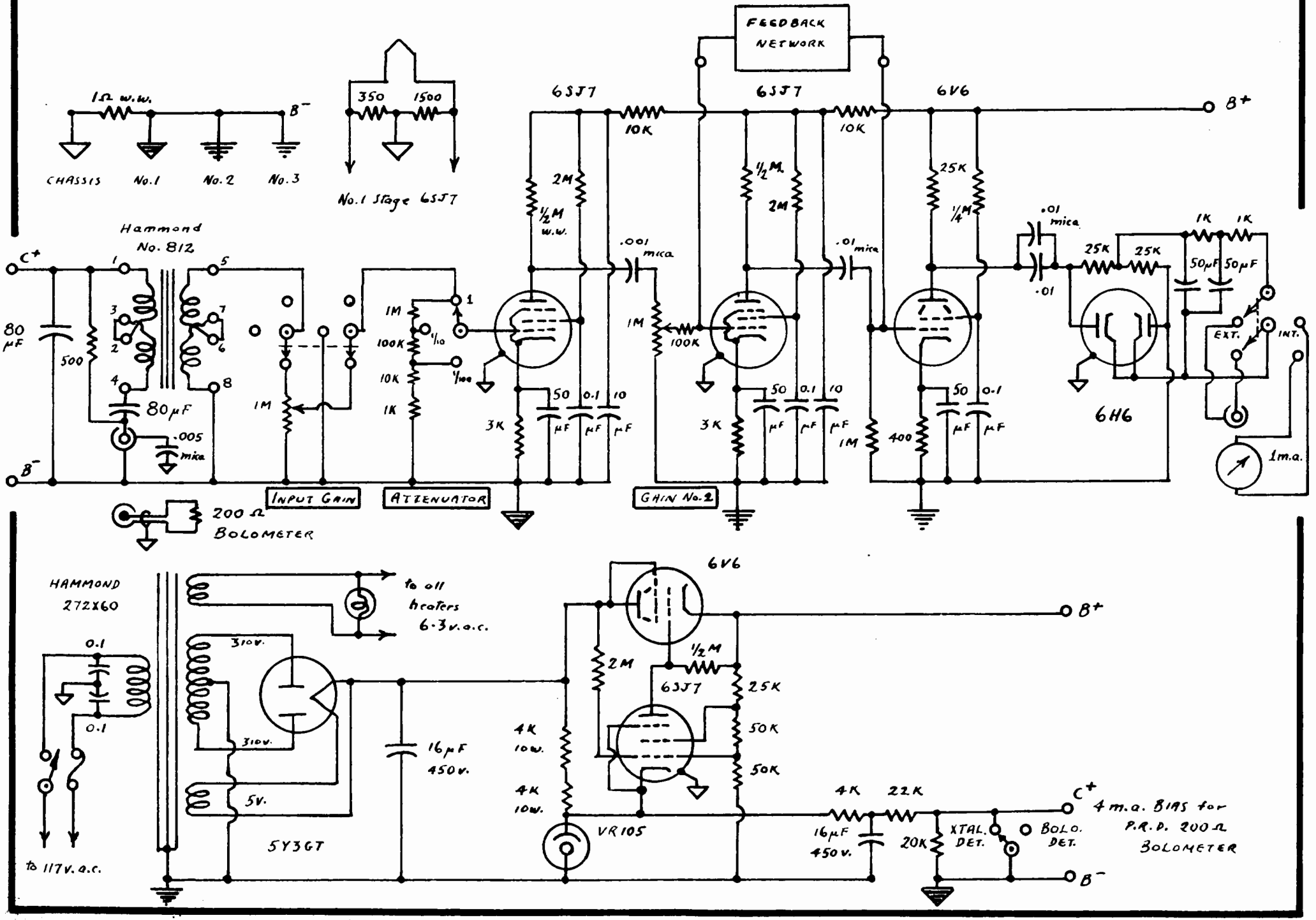

Fig. IV-24: V.S.W.R. Detector and Amplifier.

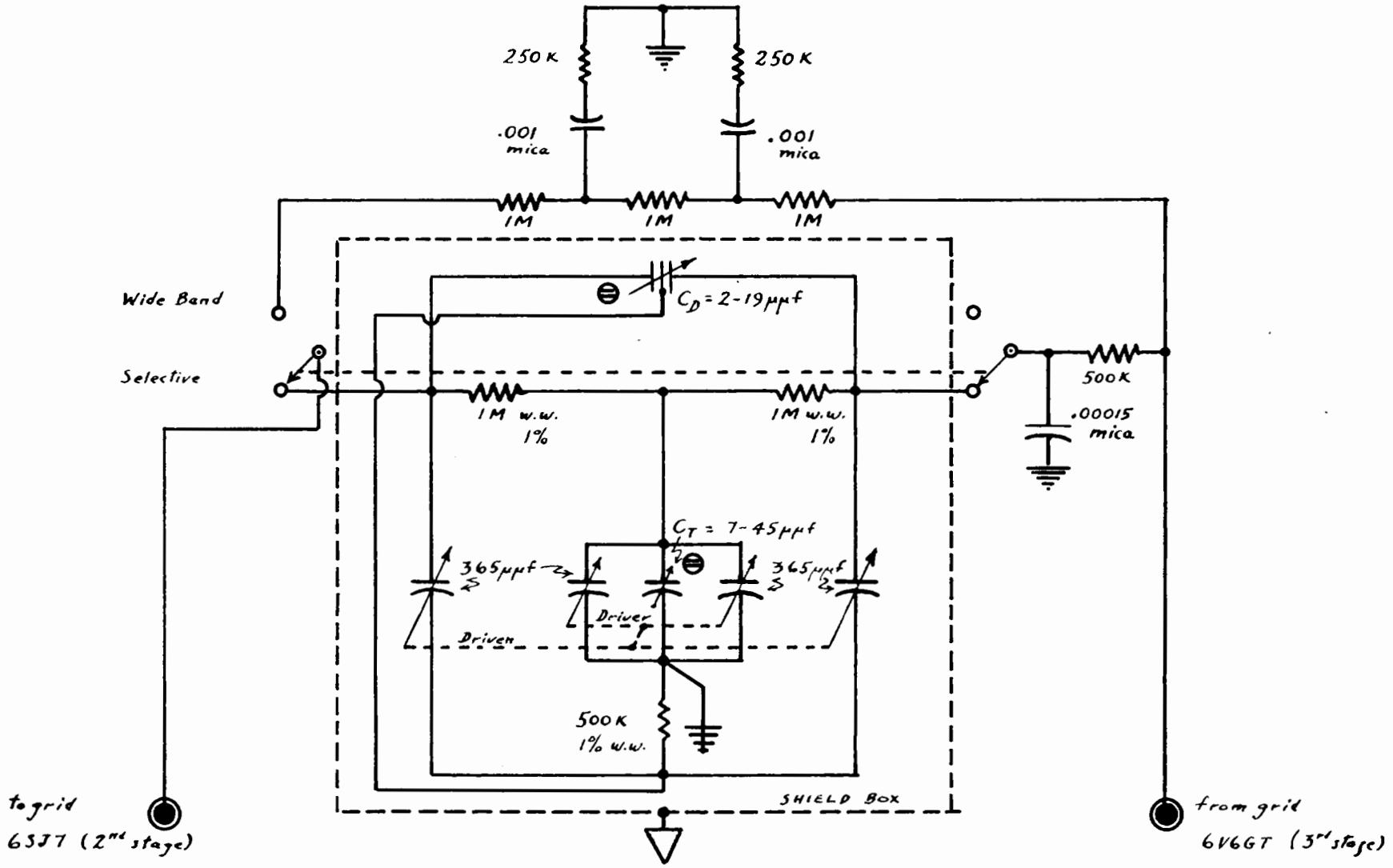

FIG. IV-25 : V.S.W.R. Amplifier - "Twin-T" and Wide Band Feedback Network.

$S^{32}C^{12}O^{16}$ $(01^{1}0)$

showing strong Stark components at low field

a)

$S^{32}C^{12}O^{16}$ (100), right

$S^{32}C^{13}O^{16}$ (000), left

b)

$S^{33}C^{12}O^{16}$ (000)

$$F' \leftarrow F'' = \begin{pmatrix} 3/2 & 1/2 \\ 5/2 & 3/2 \end{pmatrix} \quad \begin{pmatrix} 7/2 & 5/2 \\ 9/2 & 7/2 \end{pmatrix}$$

c)

Figure (V-1)

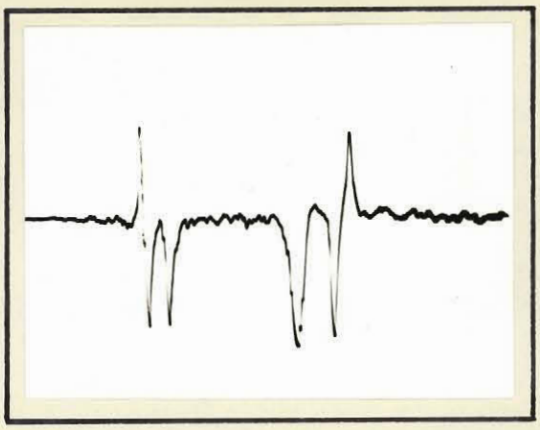

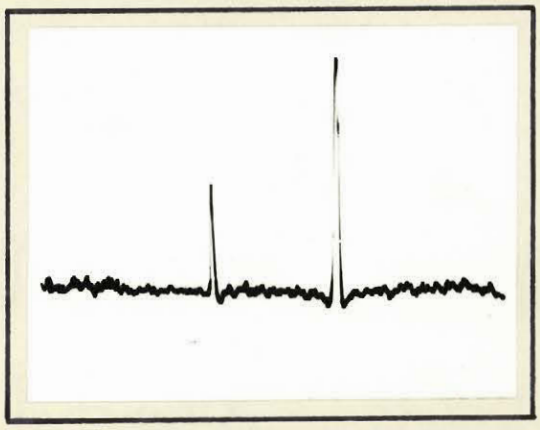

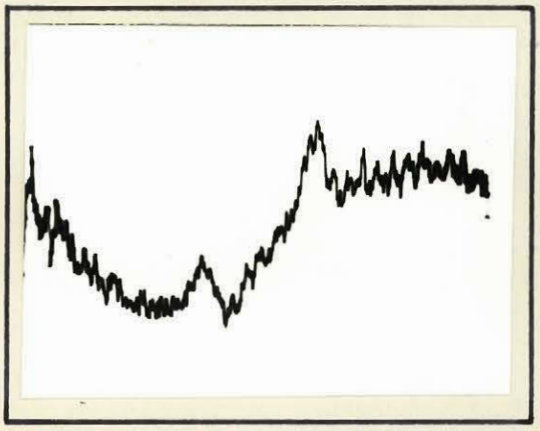

FIG. V-1

$S^{32}C^{12}O^{16}$

$02^{0}0$, left, medium field a)

$02^{2}0$, right

$S^{32}C^{12}O^{16}$

$02^{0}0$, left, higher field b)

$02^{2}0$, right

$S^{32}C^{12}O^{16}$

$02^{0}0$, left, high field c)

$02^{2}0$, right

Figure (V-2)

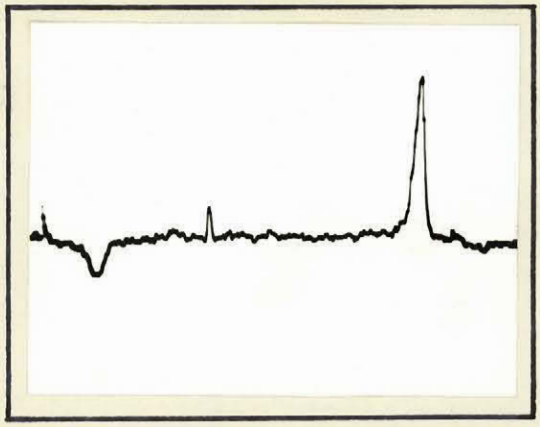

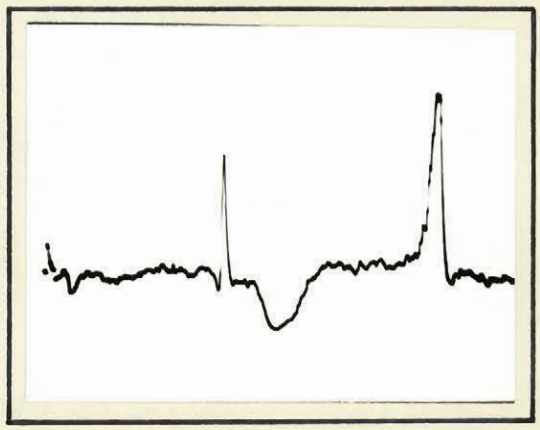

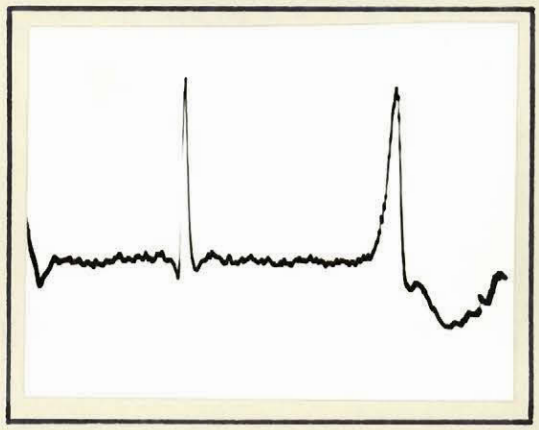

FIG. V-2

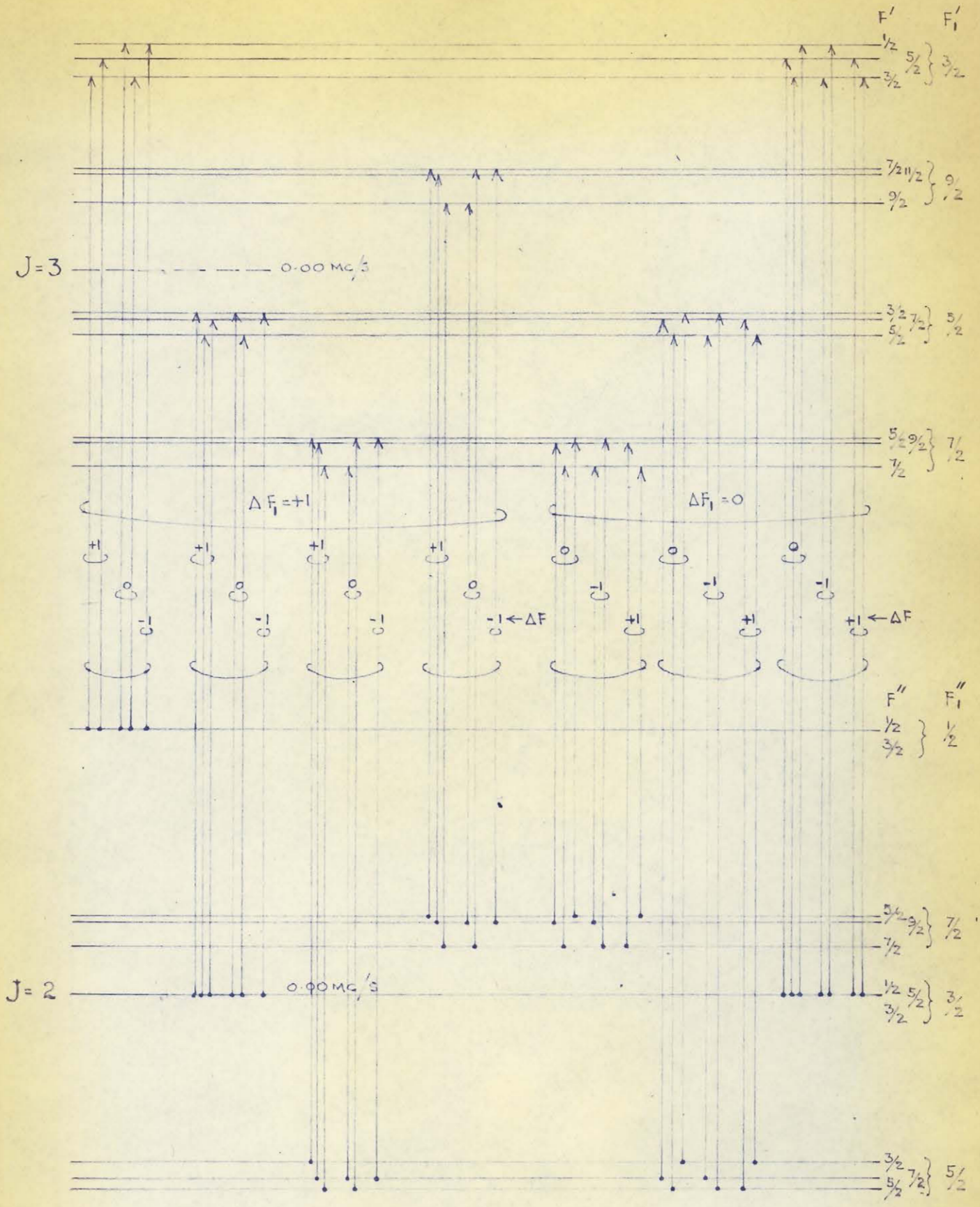

cl ON J = (3 ← 2) TRANSITION INCLUDING N^{14} SPIN

FIG (VI-1) — PURE ROTATION LEVELS ($\Delta F_1 = -1$ NOT SHOWN)

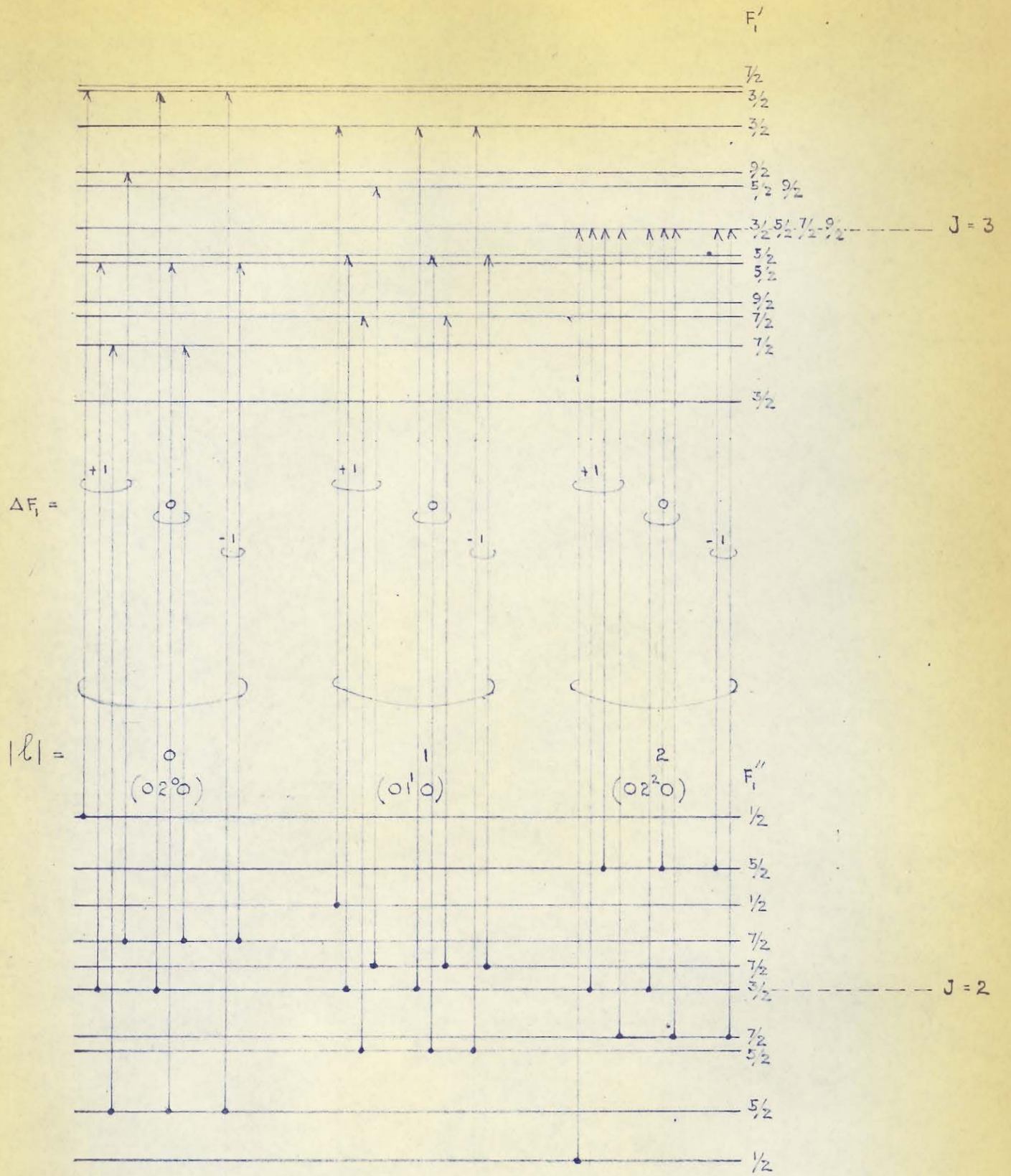

cl CN J = (3←2) TRANSITION NEGLECTING N¹⁴ SPIN

FIG (VI-2) ROTATION-VIBRATION LEVELS FOR |l| = 0, 1, 2, 3

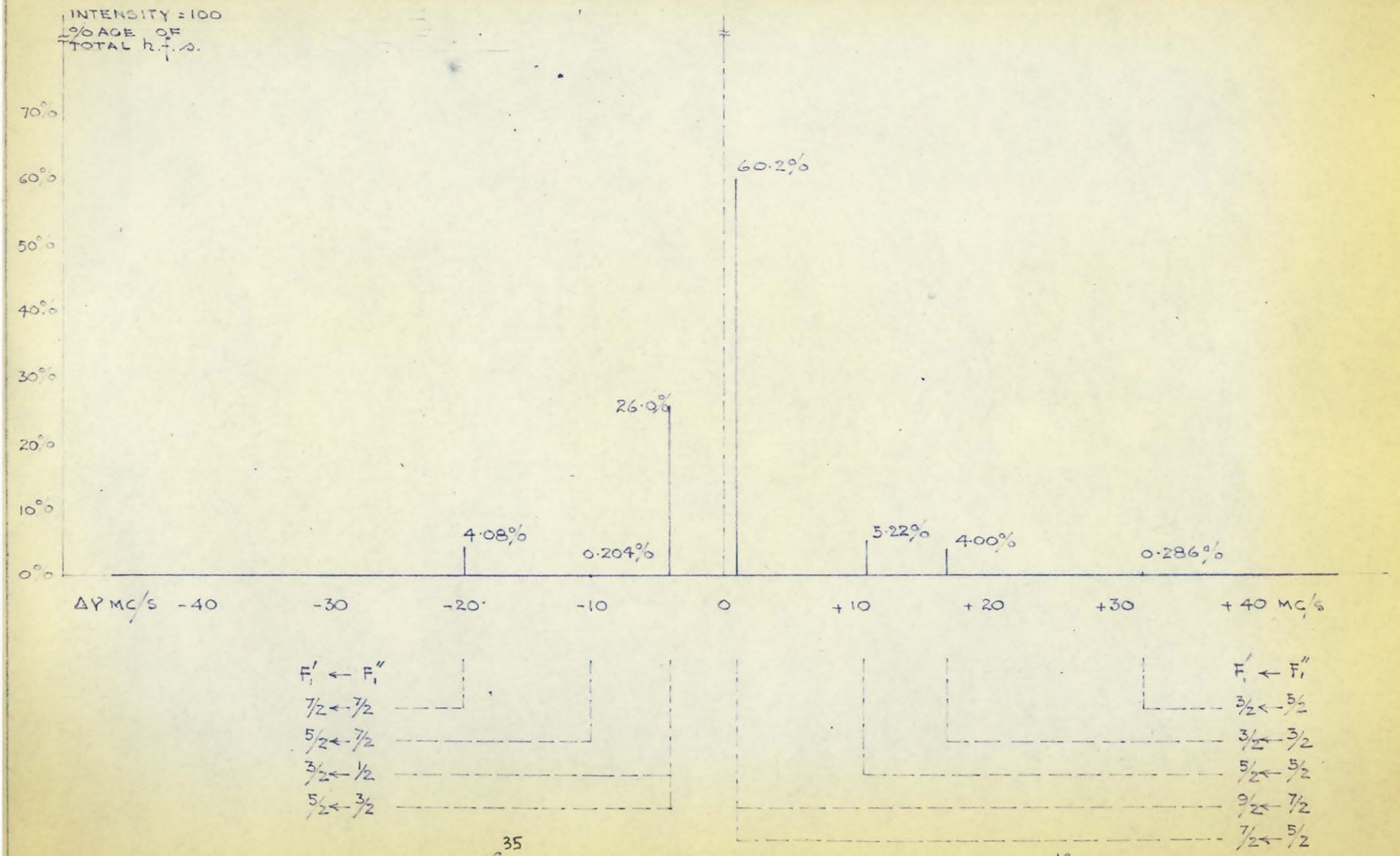

Cl^{35} CN J = (3 ← 2) TRANSITION NEGLECTING N^{14} SPIN

FIG. (VI-3) - CALCULATED SPECTRUM IN GROUND VIBRATIONAL STATE

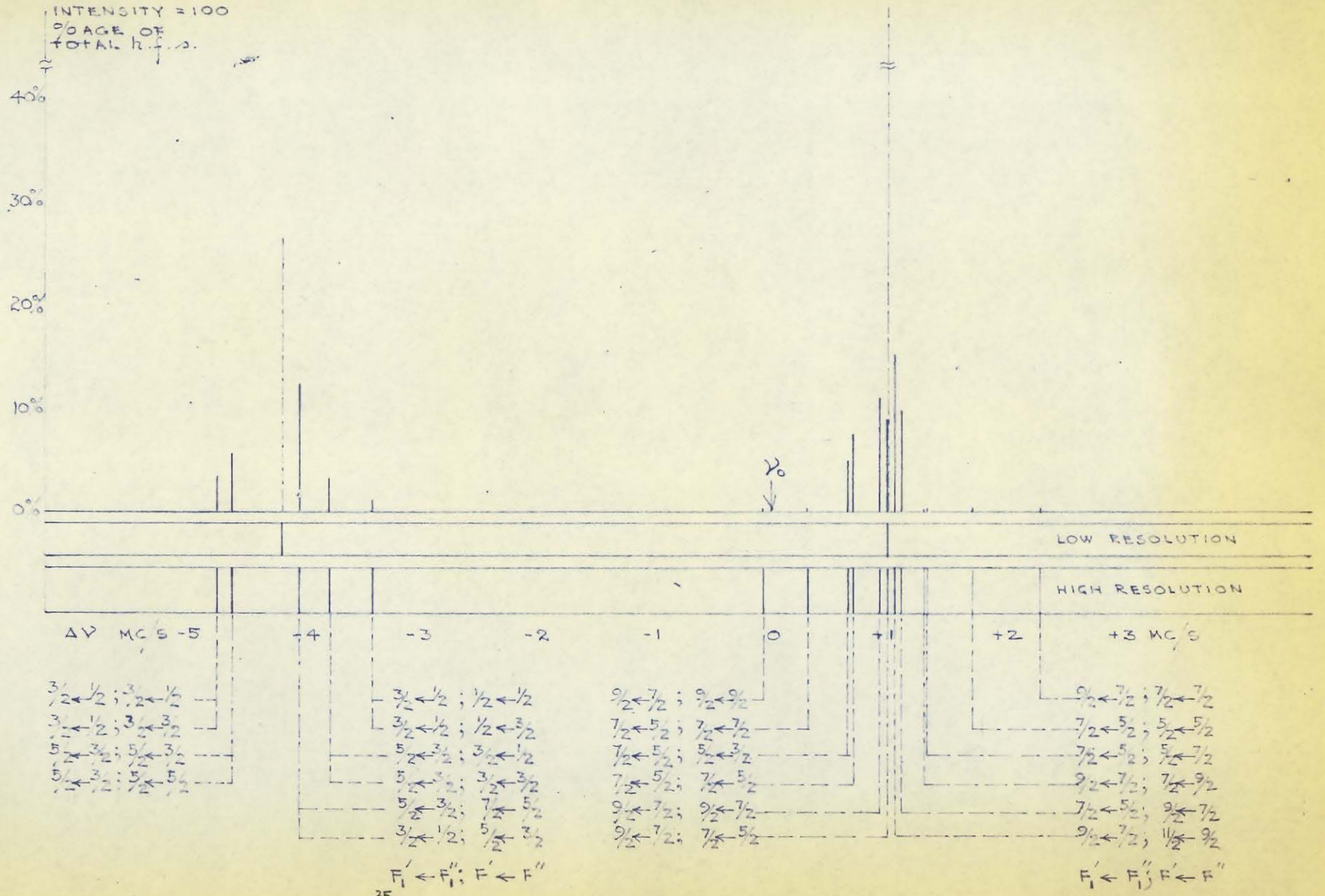

$Cl^{35}CN$ $J = (3 \leftarrow 2)$ TRANSITION $\Delta F_1 = +1$

FIG. (VI-4) – CALCULATED SPECTRUM IN GROUND VIBRATIONAL STATE

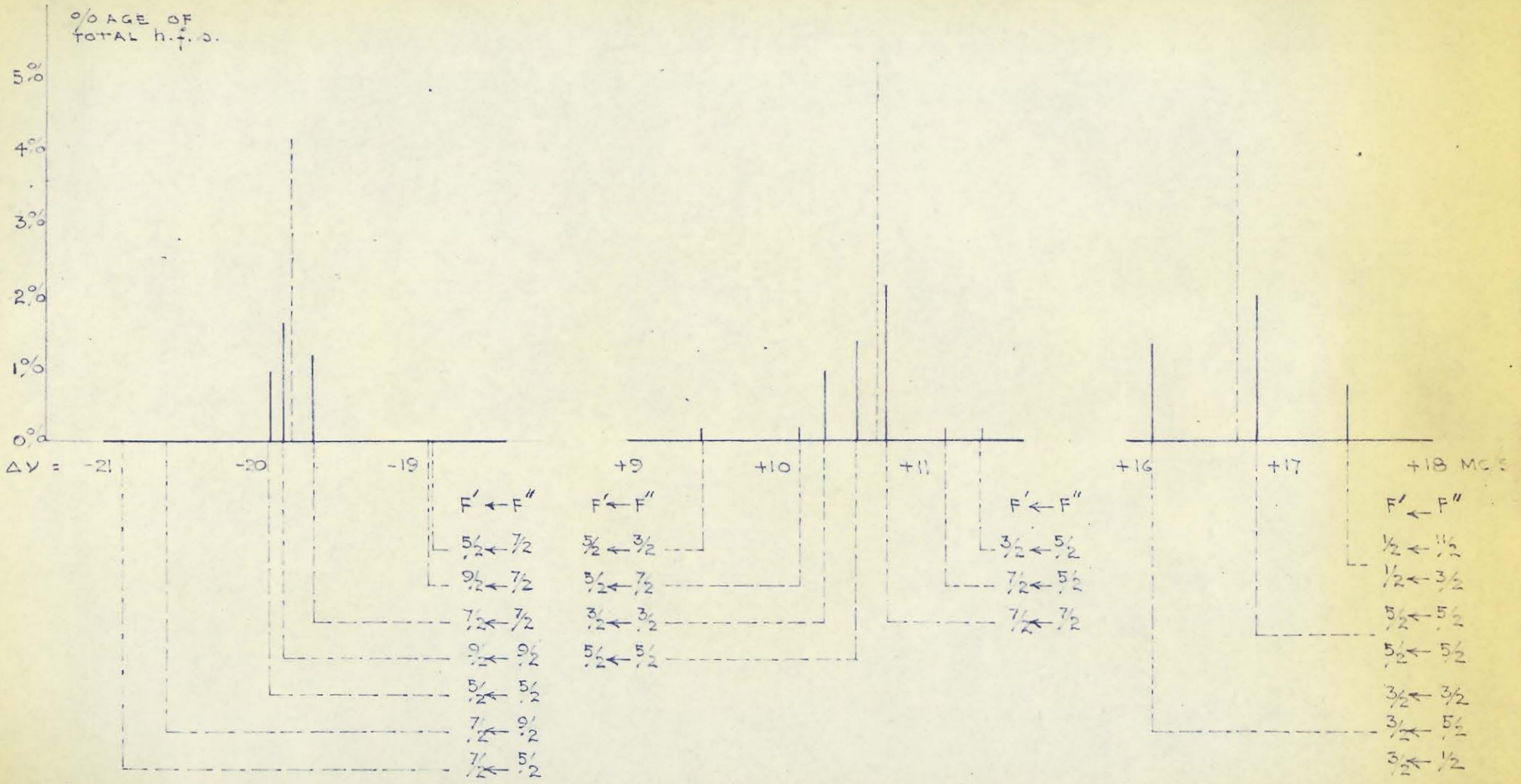

$Cl^{35}CN$ J = (3 ← 2) TRANSITION, $\Delta F_1 = 0$

FIG (VI-5) - CALCULATED SPECTRUM IN GROUND VIBRATIONAL STATE

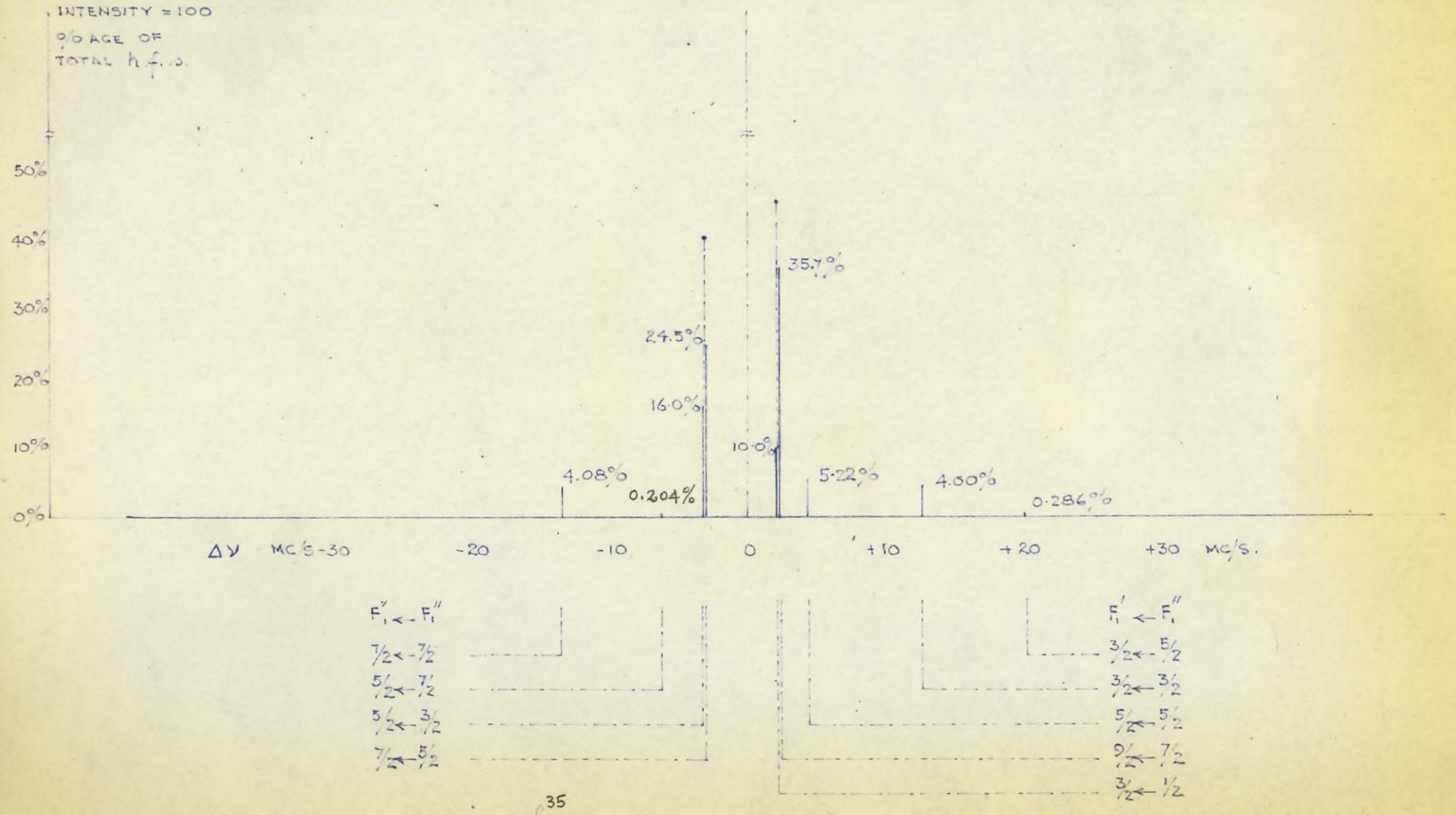

Cl^{35} CN J = (3 ← 2) TRANSITION NEGLECTING N^{14} SPIN

FIG (VI-6) - CALCULATED SPECTRUM IN FIRST EXCITED STATE. $V_2 = 1$
(ONLY ONE l - DOUBLET COMPONENT IS SHOWN)

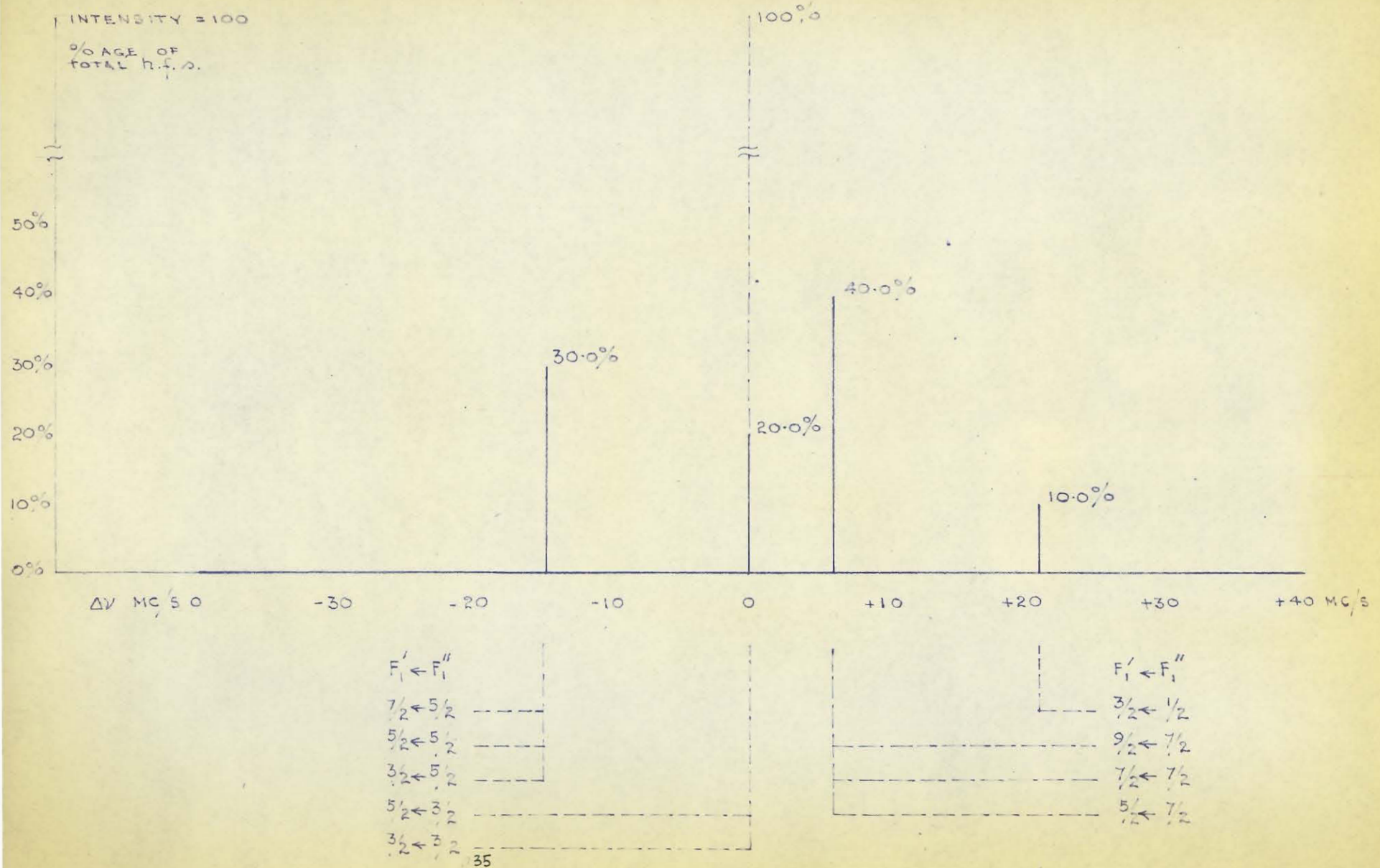

$C^{35}N$ $J = (3 \leftarrow 2)$ TRANSITION NEGLECTING N^{14} SPIN

FIG (VI-7) - CALCULATED SPECTRUM IN SECOND EXCITED STATE, $V_2 = 2$

(ONLY THE UNPERTURBED GROUP IS SHOWN)

$Cl^{35}C^{12}N^{14}$ (000) a)

$Cl^{35}C^{12}N^{14}$ ($01^{1}_{2}0$) b)

$Cl^{35}C^{12}N^{14}$ ($02^{2}0$) c)

Figure (VI-8)

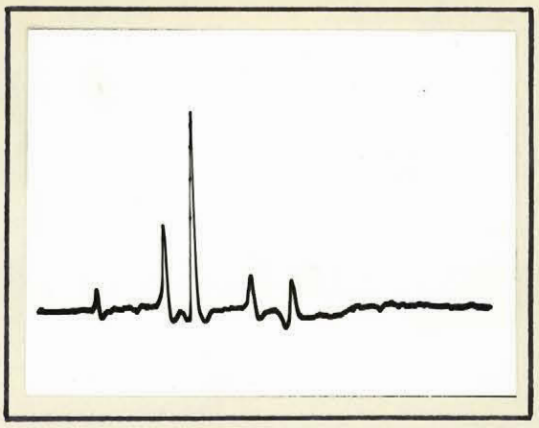

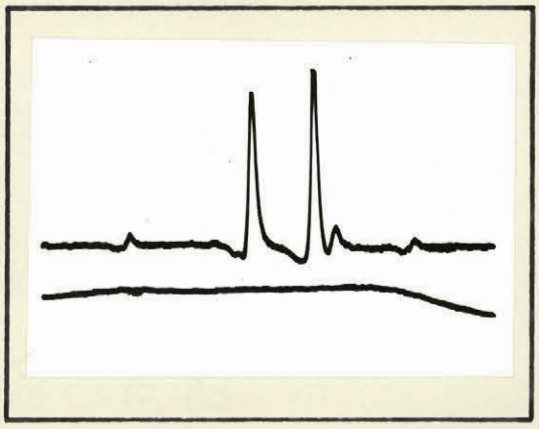

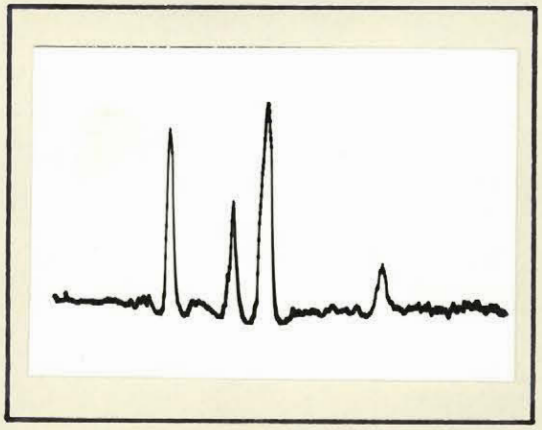

Fig. VI-8

$Cl^{35}C^{12}N^{14}$ (000)

$F_{-1}' \leftarrow F_1'' = 3/2 \leftarrow 3/2$ a)

showing N^{14} h.f.s.

$Cl^{37}C^{13}N^{14}$ (000) b)

$Cl^{37}C^{12}N^{15}$ (000) c)

—Figure (VI-9)

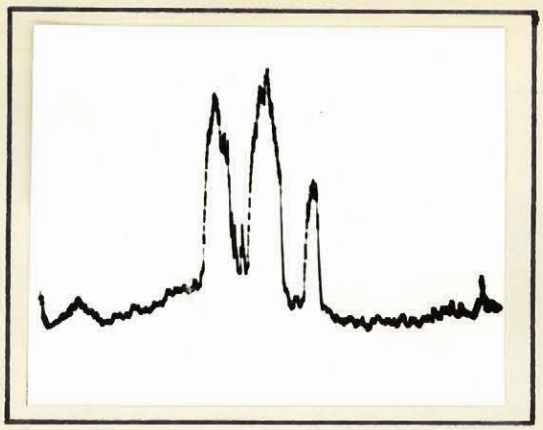

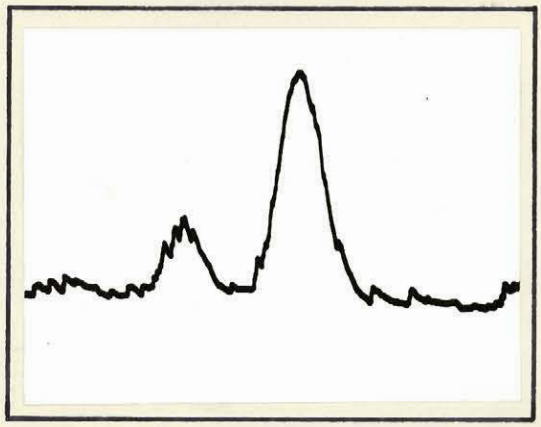

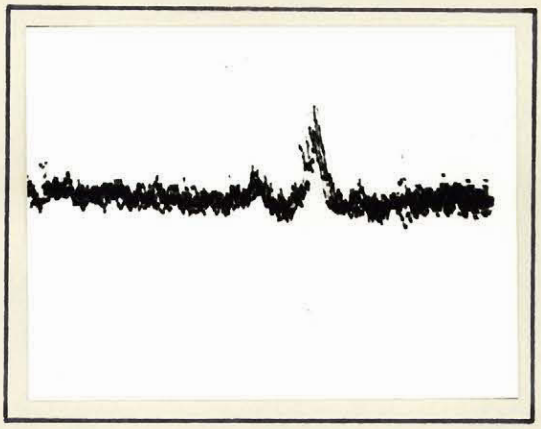

FIG. VI-9

$Cl^{35}C^{12}N^{14}$

X^{35}, centre a)

very low resolution

$Cl^{35}C^{12}N^{14}$

X^{35}, centre b)

$Cl^{35}C^{12}N^{14}$

X^{35}, detail c)

to show contour

Figure (VI-10)

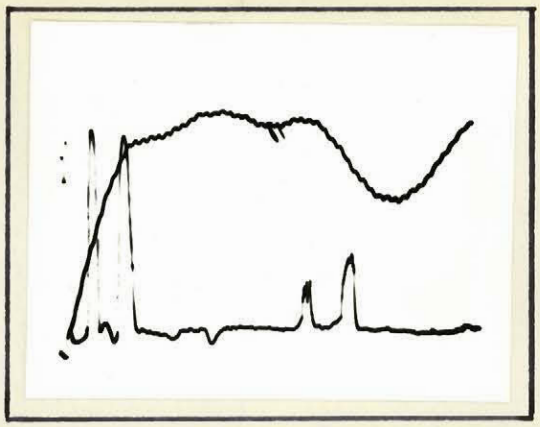

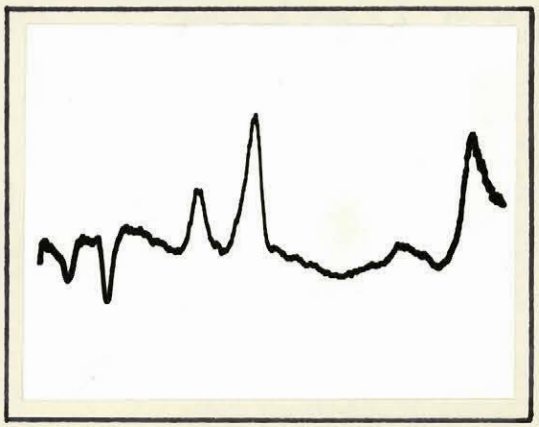

FIG. VI-10

~~Cl~~$^{35}C^{12}N^{14}$

X^{35}, centre left

β^{35}, center, at foot of

$F_1' \leftarrow F_1'' = 7/2 \leftarrow 7/2 \quad (0l_1^1 0)$

a)

$Cl^{35}C^{12}N^{14}$

β^{35}, centre

Bulge on right base

of $7/2 \leftarrow 7/2 \quad (0l_1^1 0)$ line

b)

$Cl^{35}C^{12}N^{14}$

$7/2 \leftarrow 7/2 \quad (0l_2^1 0)$ line

c)

Figure (VI-11)

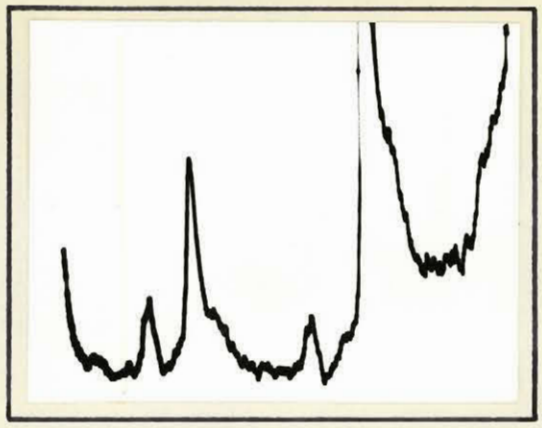

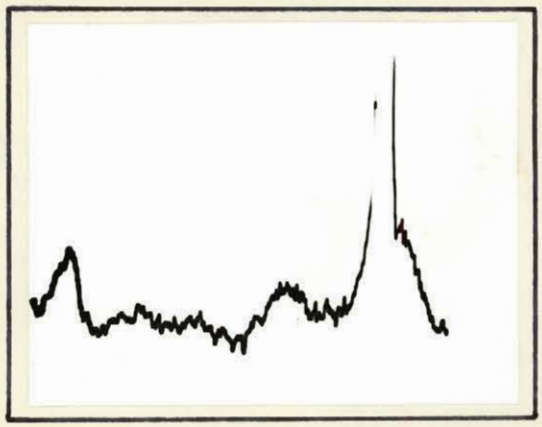

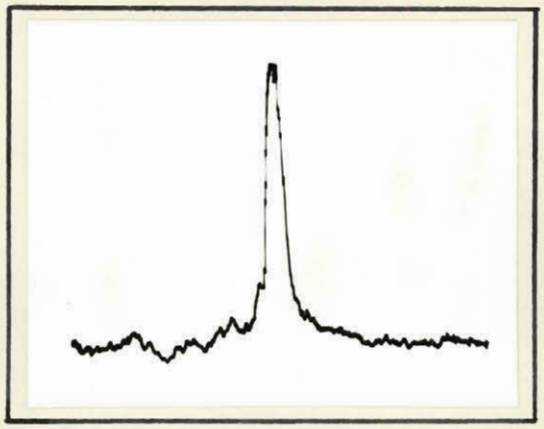

FIG. VI-11

$Cl^{37}C^{12}N^{14}$

β^{37} left a)

$7/2 \leftarrow 7/2$ $(01^{1}_{1}0)$ line, right

$Cl^{37}C^{12}N^{14}$

β^{37} left b)

$Cl^{35}C^{12}N^{14}$

$7/2 \leftarrow 7/2$ $(01^{1}_{1}0)$, left c)

$5/2 \leftarrow 3/2$; $7/2 \leftarrow 5/2$ $(01^{1}_{1}0)$ right

low field

Figure (VI-12)

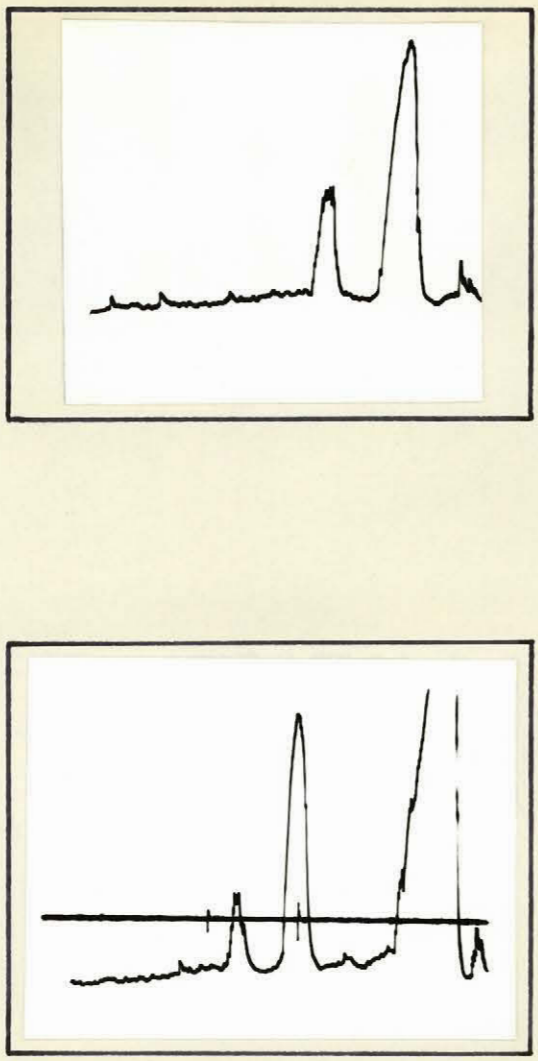

Fig. VI-12

$Cl^{37}C^{12}N^{14}$

X^{37} a)

(integrated exposures)

$Cl^{37}C^{12}N^{14}$ (02^20)

(the $F_1' \leftarrow F_1''$ = 3/2 ← 1/2 b)

line is not included at

this resolution.)

Figure (VI-13)

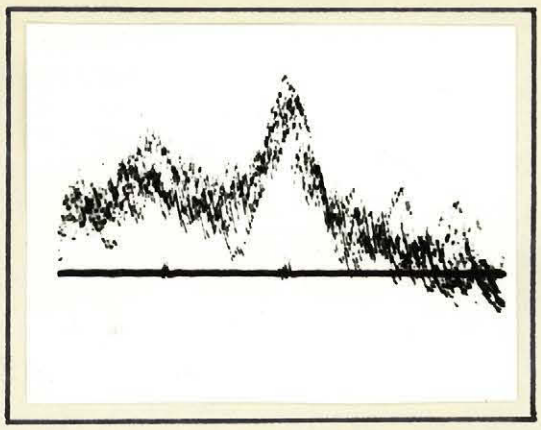

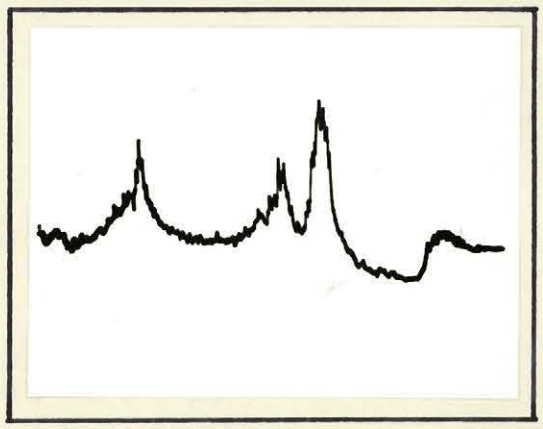

Fig. VI-13

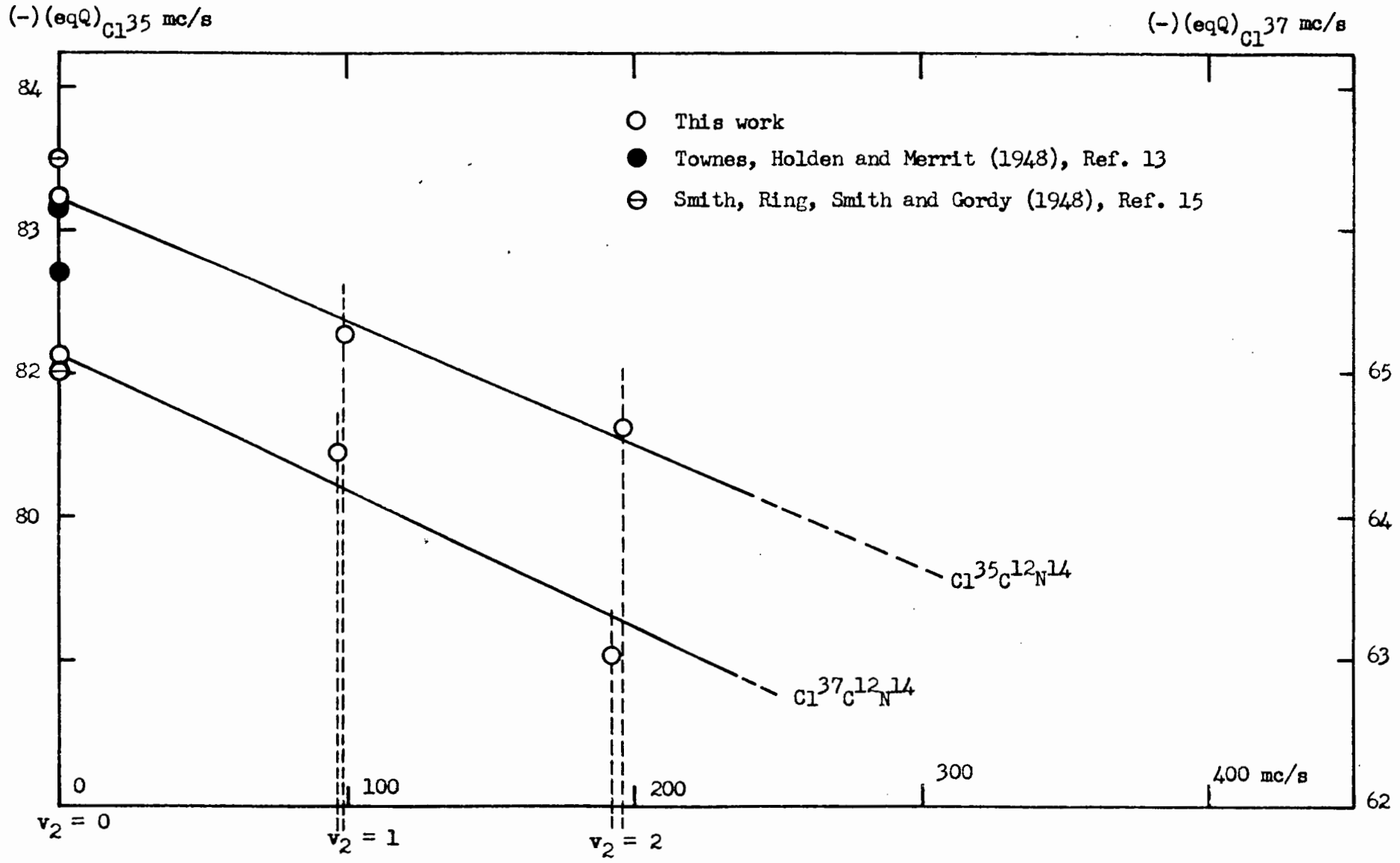

FIGURE (VI-14) - Variation of $(eqQ)_1$ With Excited Vibration State, v_2